



Welsh School of Architecture

Cardiff University

# Investigating the Performance of Drainage Stack of High Rise Buildings in Hong Kong

Thesis for the degree of Doctor of Philosophy

PhD Candidate: Wong Siu Wing

Student No.: 0535831

Supervisors: Prof. Phillip J. Jones

Submission Date: April, 2013

## **TABLE OF CONTENT**

<b>Declaration .....</b>	<b>ii</b>
<b>Abstract .....</b>	<b>iii</b>
<b>List of Publications .....</b>	<b>iv</b>
<b>Acknowledgements .....</b>	<b>v</b>
<b>Contents .....</b>	<b>vi</b>
<b>List of Figures .....</b>	<b>x</b>
<b>List of Tables.....</b>	<b>xiv</b>

## **Abstract**

The design and proper operation on the above-ground drainage systems can be challenging in a densely populated city like Hong Kong.

Discharge loading imposed to a single vertical stack can be large enough that those systems without a proper design, installation or maintenance would suffer problems such as backflow of foul water, contaminated foul air, or even soil waste to the sanitary fittings at lower floors. Any of these nuisances can be regarded as failure because the soil and waste water cannot be properly disposed away from a building. The risk of such a failure would be higher in densely occupied tall buildings. SARS outbreak in 2003 revealed that the consequence of failing to properly manage the drainage system can be as serious as a fatal disaster. The contaminated aerosols, with water droplets with the microorganisms are fatal to human like the SARS virus since it will flow back to the living environment.

This research aims at proposing advanced design and monitoring practices upon the drainage system and its components, to minimize the risk of failure and nuisances occurrence. A brief review on several types of failure will be gone through. Besides, a simulation model has been established to predict the air pressure in drainage system. The result will be compared with those from real 1:1 test-rig experiments. This assists the development of innovative inventions of system components such as 8S twin drainage stack which is designed to self-balance air pressure generated by falling water discharge in drainage stack. It ensures better protection of water seal in traps. Smart trap is available to enlarge retention time of water seal due to evaporation. Regarding the management of existing installed drainage system, a protocol has been proposed to troubleshoot the nuisances. It includes remote-control air pressure monitoring and statistical analysis with the development of probability density functions to decide future remedial engineering measures. All of these are integrated as a risk management model aimed to reduce the risk of occurrence of the nuisances.

## List of Publications

Eric S.W.Wong, Yinglin Li, and Zuojin Zhu, 2013, “*Predicting air pressure in a drainage stack of high-rise building*”, Applied Mathematics and Mechanics (English Edition), vol. 34, no. 3, pp. 1-14 (ISSN: 0253-4827) **DOI: 10.1007/s10483-013-1675-7.**

Eric S.W.Wong, Daniel W.T. Chan and Zuojin Zhu, 2011, “*Air Pressure Fluctuation Behaviors in a High-Rise Building Drainage System*”, Journal of Architectural Engineering, vol. 17, no. 2, pp. 82-84 (ISSN: 1076-0431) **DOI: 10.1061/(ASCE)AE.1943-5568.0000029.**

S.W.Wong, W.M. Lau and W.T. Chan, 2008, “*Positive Pressure Profiles in Drainage Stacks – Full Scale Tests*”, Proceedings from the CIB W062 34th International Symposium on Water Supply and Drainage for Buildings, Hong Kong, China, 8-10 September 2008.(ISBN: 2070-1373)

Eric S. W. Wong, Daniel W. T. Chan, Phil Jones and Leo K. C. Law, 2008, “*Assessment of Air Pressure inside a Drainage Stack*”, Proceedings of the International Multi-conference of Engineers and Computer Scientists 2008 Vol. II IMECS 2008, Hong Kong, China, 19-21 March 2008, page 1534-1539 (ISBN: 978-988-17012-1-3)

Henry C.K. Hung, Daniel W.T. Chan, Leo K.C. Law, Edwin H.W. Chan and Eric S.W. Wong, 2006, “*Industrial experience and research into the causes of SARS virus transmission in a high-rise residential housing estate in Hong Kong*”. Building Services Engineering Research and Technology, vol. 27, no. 2, pp. 91–102 (ISSN: 1477-0849) **DOI: 10.1191/0143624406bt145oa**

## List of Patent

Inventor of Twin Drainage Stack System (8S) –Patent number: IP-594A China, held by the Hong Kong Polytechnic University

## **Acknowledgements**

I would like to express my deepest gratitude to my supervisor Prof. Phil Jones, who has been very supportive to my research. I would give my heartfelt thanks to Prof. Daniel W.T. Chan, who has given me helpful comments and suggestions on different occasions during my study. I also want to appreciate Ms. Zhang Lei who is very helpful with my research.

Last but not the least; I also want to express my sincere gratitude to the following teams which have supported the Building Drainage System research: Department of Building Services Engineering, Facilities Management Office and Industrial Centre (Building Services Engineering Unit and Automation Unit) at The Hong Kong Polytechnic University.

# Contents

<b>Chapter 1 _ Introduction .....</b>	<b>1</b>
1.1 SARS OUTBREAK: DRAINAGE SYSTEM CAN KILL THE OCCUPANTS? .....	1
1.2 RESEARCH QUESTIONS .....	3
1.3 RESEARCH OBJECTIVES .....	5
1.4 REVIEW OF MAIN BACKGROUND LITERATURE .....	6
1.4.1 SEWAGE DISPOSAL SYSTEM, PUBLIC HEALTH, AND SARS OUTBREAK .....	6
1.4.2 A CLOSER LOOK TO THE BUILDING DRAINAGE PART .....	9
1.4.3 PLUMBING RISK MANAGEMENT GUIDE FROM WORLD HEALTH ORGANIZATION .....	11
1.5 RISK MANAGEMENT MODEL OF THIS RESEARCH .....	12
1.6 RESEARACH MEHTODOLOGY .....	12
1.6.1 RISK RECOGNITION .....	12
1.6.2 MODELLING THE DRAINAGE SYSTEM FLOW MECHANISM .....	14
1.6.3 RISK ABATMENT (I) .....	15
1.6.4 RISK ABATMENT (II) .....	16
1.6.5 RISK MONITORING BY REMOTE COMMUNICATION SYSTEM .....	18
1.7 THEISS STRUCTURE .....	20
<b>Chapter 2 _ Risks Recognition .....</b>	<b>24</b>
2.1 HIGH DISCHARGE LOADING TO THE VERTICAL STACK AND ITS RISKS .....	24
2.2 RISK DUE TO FAILURE IN RETAINING WATER SEAL IN TRAPS .....	27
2.2.1 TRAP SEAL LOSS DUE TO AIR PRESSURE TRANSIENTS AT THE STACK NEARBY .....	27
2.2.2 CAUSES OF EXCESSIVE STACK AIR PRESSURE NEAR THE TRAPS .....	29
2.2.3 IMPORTANCE OF WATER TRAP SEAL RETENTION .....	29
2.3 RISKS FORMATION INVESTIGATION .....	30
2.3.1 FORMATION OF HYDRAULIC JUMP AND THE ASSOCIATED RISKS .....	30
2.3.2 MALFUNCTION OF TRAP .....	35
2.3.3 A CASE OF EXCESS AIR PRESSIUR IN DRAIANGE STACK .....	38
2.3.4 HAZARDS CASUED BY DRAINAGE STACK .....	46

### **Chapter 3 \_ Primary Investigation on the Performance of Drainage Stack ..... 48**

3.1	REVIEW ASSESSMENT METHODOLOGIES FOR DRAINAGE STACK .....	48
3.1.1	DISCHARGE UNITS .....	48
3.1.2	FORMATION OF FALLING WATER VOLUME .....	51
3.1.3	VISUAL INSPECTION ON FALLING WATER VOLUME .....	54
3.1.4	AIR PRESSURE INSIDE DRAINAGE STACK .....	60
3.2	DRAINAGE RESEARCH PLATFORMS .....	62
3.2.1	DISCHARGE TEST IN A 3 STOREYS DRAINAGE RESEARCH RIG .....	63
3.2.2	DISCHARGE TEST IN A 17 STOREYS DRAINAGE RESEARCH PLATFORM .....	66
3.2.3	THE FIRST DRAINAGE RESEARCH TOWER IN CHINA .....	68

### **Chapter 4 \_ Estimation of Air Pressure Inside Drainage Stack ..... 71**

4.1	COMPUTER FLUID DYNAMIC (CFD) ESTIMATION .....	71
4.1.1	NAVIER-STOKES EQUATIONS USED IN CFD .....	71
4.1.2	AIR MOVEMENT IN DRAINAGE STACK .....	74
4.2	ASSESSMENT ON DRAINAGE STACK BY CFD SIMULATION AND EXPERIMENTS .....	75
4.2.1	PRINCIPLE AND CFD ASSESSMENT FOR AIR MOVEMENT INSIDE THE STACK .....	75
4.2.2	DATA VERIFICATION FOR CFD SIMULATION IN DRAINAGE RESEARCH RIG .....	87
4.3	NUMERICAL ASSESSMENT –MATHEMATICAL MODEL OF AIR PRESSURE IN DRAINAGE STACK .....	91
4.3.1	ST VENANT EQUATION .....	91
4.3.2	ONE-DIMENSIONAL CHARACTERISTIC LINES .....	94
4.3.3	MATHEMATICAL MODEL – CHARACTERISTIC LINE METHOD (CLM) .....	96
4.3.4	GOVERNING EQUATIONS AND APPLICATION IN BUILDING DRAINAGE SYSTEM (BDS) .....	97
4.3.5	NUMERICAL METHOD .....	104
4.3.6	SENSITIVITY FACTORS TO $\sigma_s$ and $\beta$ .....	114
4.3.7	EVOLUTIONS OF VELOCITY AND PRESSURE .....	116
4.4	COMPARISON BETWEEN CFD AND MATHEMATICAL MODEL .....	121

### **Chapter 5 \_ Control of Air Pressure Inside Drainage Stack ..... 125**

5.1	SMART PIPE CONNECTION .....	126
5.1.1	USAGE OF VENTILATION PIPE .....	126
5.1.2	PRINCIPLE OF SMART CROSS VENTILATION PIPE CONNECTION .....	127
5.1.2.1	CASE 1 – INSTALL VENTILATION PIPE ONLY .....	128

5.1.2.2	CASE 2 – INSTALL CROSS VENTILATION PIPE TO ONE PIPE SYSTEM .....	130
5.1.2.3	CASE 3 – INSTALL CROSS VENTILATION PIPES FOR ONE PIPE SYSTEM .....	132
5.1.2	DATA VERIFICATION .....	135
5.2	INNOVATION OF A TWIN-DRAINAGE STACK SYSTEM (8S) .....	140
5.2.1	IDEA OF 8S TWIN STACK .....	140
5.2.2	CFD SIMULATION FOR 8S .....	143
5.2.3	COMPARISON BETWEEN 8S AND OTHER CONNECTION CFD SIMULATION .....	152
5.2.4	VALIDATION IN DRAINAGE RESEARCH RIG AND BUILDING .....	155
5.2.4.1	COMPARISON WITH DRAINAGE RESEARCH RIG OF THE HONG KONG POLYU .....	155
5.2.4.2	COMPARISON WITH A NEW BUILDING .....	158
5.3	SMART FLOOR TRAPS .....	163
5.3.1	SMART WATER SEAL REIFIED FLOOR TRAP CONNECTIONS .....	164
5.3.2	SMART FLOOR TRAP .....	165
5.3.3	VERIFICATION – EVALUATION OF EVAPORATION RATE OF SMART TRAP .....	168
5.3.3.1	EVAPORATION MODEL .....	169
5.3.3.2	TEST IN AN AIR CHAMBER – EVAORATION TEST .....	171
5.3.3.3	FINDING IN THE TEST .....	174
5.4	SOME SUGGESTIONS ON FUTURE WORKS: IDENTIFYING EMPTIED TRAPS ALONG A STACK .....	175

## **Chapter 6 \_ Drainage Monitoring and Communication Research..... 179**

6.1	DATA COLLECTION OF AIR PRESSURE INSIDE THE DRAINAGE STACK .....	179
6.1.1	DATA COLLECTION IN A REAL BUILDING - LI KA SHING BUILDING .....	180
6.1.2	AIR FLUCTUATION IN A DRAINAGE SYSTEM IN LKS .....	182
6.1.2.1	DATA COLLECTION AT M/F OF LKS .....	182
6.1.2.2	DATA COLLECTION AT 6/F OF LKS .....	183
6.1.2.3	DATA COLLECTION AT 12/F OF LKS .....	183
6.2	REMOTE MONITORING IN DRAINAGE SYSTEM .....	185
6.2.1	COMMUNICATION WITH DRAINAGE SYSTEM .....	185
6.3	AIR PRESSURE FLUCTUATION DRAINAGE STACK .....	189
6.3.1	AIR FLUCTUATION BEHAVIOR IN LKS DRAINAGE SYSTEM .....	190
6.3.2	PROBABILITY DENSITY FUNCTION (PDF) IN AIR PRESSURE FLUCTUATION BEHAVIOR STUDY .....	195
6.3.3	VISUAL INSPECTION INSIDE THE STACK .....	200



<b>Chapter 7 _Conclusion .....</b>	<b>204</b>
7.1 RISK MODEL IN DRAINAGE STACK .....	204
7.2 LIMITATON .....	208
7.3 FUTURE DEVELOPMENT .....	210
7.3.1 IMPROVEMENT IN RISK MODEL .....	210
7.3.2 FACILITIES MANAGEMENT IN BUILDING DRAINAGE INFORMATION SYSTEM .....	213
7.3.3 CODE SYSTM FOR ABOVE GROUND DRAINAGE STACK .....	214
7.3.4 EXPERIMENTS TESTING IN SUPER HIGH RISE BUILDING .....	214
<b>Reference .....</b>	<b>216</b>

# List of Figures

FIGURE 1-1: CONGESTED, CLOSED LIVING AND EASY FOR ILLNESS SPREADING .....	6
FIGURE 1-2: CONGESTED BUILDINGS IN MONG KOK .....	7
FIGURE 1-3: FLOW CHARTS IN RISK MANAGEMENT IN DRAINAGES TACK .....	13
FIGURE 1-4: MALFUNCTION IN DOMESTIC IN DRAINAGE SYSTEM .....	15
FIGURE 2-1: NEGATIVE AIR PRESSURE IN DRAINAGE STACK .....	28
FIGURE 2-2: POSITIVE AIR PRESSURE IN DRAINAGE STACK .....	28
FIGURE 2-3: FORMATION OF HYDRAULIC JUMP .....	31
FIGURE 2-4: PROBLEM CAUSED BY EXCESS POSITIVE AIR PRESSURE .....	34
FIGURE 2-5: EFFECT OF POSITIVE AIR PRESSURE .....	34
FIGURE 2-6: STANDARD INSTALLATION OF DRAINAGE TRAP .....	36
FIGURE 2-7: A GASKET ANTI-SIPHON VALVE DISC IN TRAP .....	37
FIGURE 2-8: SCHEMATIC DRAWING OF THE FIELD STUDY BUILDING .....	39
FIGURE 2-9: FLOW MEASUREMENT .....	42
FIGURE 2-10: DETECT AIR FLOW DIRECTION .....	42
FIGURE 2-11: VERIFICATION OF HAZARDS OF DRAINAGE SYSTEM .....	46
FIGURE 3-1: DISCHARGE GRATINGS .....	50
FIGURE 3-2: A BRANCH JET OF WATER IN A TRANSPARENT TEE .....	51
FIGURE 3-3: A BRANCH JET SKETECH .....	52
FIGURE 3-4: A FALLING WATER VOLUME .....	53
FIGURE 3-5: A TYPICAL FLOOR PLAN .....	55
FIGURE 3-6: PEARPOINT CCTV .....	55
FIGURE 3-7: CCTV OF WATER VOLUME HEAD .....	57
FIGURE 3-8: CCTV OF WATER VOLUME CENTRE .....	57
FIGURE 3-9: CCTV OF WATER VOLUME REAR .....	58
FIGURE 3-10: SECTION OF WATER RINGS .....	59
FIGURE 3-11: HYDRAULIC JUMP .....	60
FIGURE 3-12: SCHEMATIC DRAWING OF DRAINAGE RESEARCH RIG THE HK POLYU .....	64
FIGURE 3-13: WATER DISCHARGE CONDITION IN THE RIG .....	65
FIGURE 3-14: 17 STOREYS DRAINAGE RESEARCH TOWER .....	66
FIGURE 3-15: CONFIGURATION IN 17 STOREYS RESEARCH RIG .....	67
FIGURE 3-16: AIR PRESSURE PROFILE MEASURED IN THE 17 STOREYS DRAINAGE STACK .....	67
FIGURE 3-17: 123 M HEIGHT DRAINAGE RESEARCH CHINA TOWER .....	69
FIGURE 3-18: CHINA TOWER'S PRECISE EQUIPMENT .....	69

FIGURE 4-1: WATER VOLUME ESTIMATION IN DRAINAGE STACK .....	76
FIGURE 4-2: CFD SIMULATED AIR PRESSURE DISTRIBUTION IN SINGLE STACK SYSTEM .....	79
FIGURE 4-3: CFD SINGLE STACK SIMULATION CONFIGURATION .....	79
FIGURE 4-4: SINGLE STACK SIMULATION RESULTS .....	80
FIGURE 4-5: AIR PRESSURE DISTRIBUTION'S DETAILS IN SINGLE STACK SIMULATION .....	81
FIGURE 4-6: SIMULATED AIR PRESSURE PROFILE IN SINGLE STACK SYSTEM .....	83
FIGURE 4-7: REGRESSION ADJUSTMENT FOR BASE AIR PRESSURE .....	84
FIGURE 4-8 COMPLETED SIMULATED AIR PRESSURE PROFILE .....	85
FIGURE 4-9: VECTORS OF AIR FLOW IN THE SINGLE STACK SIMULATION .....	86
FIGURE 4-10: AIR PRESSURE MEASUREMENT POINTS .....	88
FIGURE 4-11: HYDRAULIC JUMP IN MEASUREMENT .....	89
FIGURE 4-12: COMPARISON BETWEEN SIMULATION AND MEASUREMENT IN SINGLE STACK DRAINAGE SYSTEM .....	90
FIGURE 4-13: SCHEMATIC FOR EQUATION OF CONTINUITY .....	92
FIGURE 4-14: SCHEMATIC FOR EQUATION OF MOMENTUM .....	93
FIGURE 4-15: AIR MOVEMENT OF AIR TRANSIENT BY CHARACTERISTIC LINE C+ & C- .....	94
FIGURE 4-16: RELATIONSHIP BETWEEN C+ & C- .....	95
FIGURE 4-17: POINTS ARE OBTAINED BY CHARACTERISTIC LINES .....	96
FIGURE 4-18: ENTRAINED AIR SPEED - SIMULATION FOR DIFFERENT SPEEDS .....	101
FIGURE 4-19(A): NUMERICAL SIMULATION FOR BRANCH DISCHARGE .....	103
FIGURE 4-19(B): NUMERICAL SIMULATION FOR DRAINAGE PARTIALLY FLOW .....	103
FIGURE 4-20: INTERPOLATION TECHNIQUE .....	107
FIGURE 4-21: COMPARISON OF AIR PRESSURES WITH EXPERIMENTAL DATA .....	113
FIGURE 4-22: NUMERICAL SIMULATION PARAMETER $\Sigma$ EFFECT .....	115
FIGURE 4-23: NUMERICAL SIMULATION PARAMETER $\beta$ EFFECT .....	116
FIGURE 4-24(A): EVOLUTION OF PRESSURE AT DIFFERENT LOCATIONS .....	118
FIGURE 4-24(B): EVOLUTION OF VELOCITY AT DIFFERENT LOCATIONS .....	118
FIGURE 4-25: SPATIOTEMPORAL EVOLUTION OF PRESSURE IN 5 SECONDS TIME RANGE .....	119
FIGURE 4-26: SPATIOTEMPORAL EVOLUTION OF VELOCITY IN 5 SECONDS TIME RANGE .....	119
FIGURE 5-1: SIMULATION IN ONE PIPE SYSTEM .....	128
FIGURE 5-2: SIMULATION IN ONE PIPE SYSTEM CASE 1 .....	129
FIGURE 5-3: SIMULATION IN ONE PIPE SYSTEM CASE 2 .....	130
FIGURE 5-4: AIR PRESSURE PROFILE IN CASE 2 .....	131
FIGURE 5-5: SIMULATION IN ONE PIPE SYSTEM CASE 3 .....	132
FIGURE 5-6: AIR PRESSURE PROFILE IN CASE 3 .....	133

FIGURE 5-7: AIR VECTOR AT TOE OF STACK .....	134
FIGURE 5-8: PRESSURE PROFILES COMPARISON .....	136
FIGURE 5-9: SPACING OF CROSS VENTILATION PIPE IN A REAL BUILDING .....	137
FIGURE 5-10: SMALLER SPACING OF CROSS VENTILATION PIPE .....	138
FIGURE 5-11: A SIMULATED CASE FOR A SHORT SPACING OF VENTILATION PIPE .....	139
FIGURE 5-12: PLAN VIEW OF 8S .....	141
FIGURE 5-13: SELF-BALANCED AIR PRESSURE IN 8S .....	142
FIGURE 5-14: SIMULATION IN 8S (2.4L/S FLOW) .....	144
FIGURE 5-15: SIMULATION IN 8S FOR DIFFERENT AIR PRESSURE ZONES (2.4L/S FLOW) .....	146
FIGURE 5-16: SIMULATION IN 8S FOR AIR VECTORS IN THE DIFFERENT PRESSURE ZONES .....	147
FIGURE 5-17: SIMULATION IN 8S FOR DIFFERENT AIR PRESSURE ZONES (5L/S @ 0.5s) .....	148
FIGURE 5-18: SIMULATION IN 8S FOR DIFFERENT AIR PRESSURE ZONES (5L/S @ 1s) .....	150
FIGURE 5-19: FALLING WATER VOLUME IN 8S FOR DIFFERENT PRESSURE ZONES .....	151
FIGURE 5-20: AIR PRESSURE PROFILE OF 8S .....	152
FIGURE 5-21: COMPARISON OF AIR PRESSURE PROFILES .....	153
FIGURE 5-22: 8S IS TESTED IN THE HK POLYU DRAINAGE RESEARCH RIG .....	156
FIGURE 5-23: 8S IS TESTED AND AIR PRESSURES AT POINTS .....	156
FIGURE 5-24: SCHEMATIC DRAWING FOR 8S IS TESTED IN 18/F BUILDING .....	158
FIGURE 5-25: 8S IS TESTED IN THE REAL BUILDING .....	159
FIGURE 5-26: 8S IS TESTED WITH AIR PRESSURE SENSOR .....	160
FIGURE 5-27 8S IS TESTED WITH DATA CAPTURE EQUIPMENT .....	160
FIGURE 5-28: 8S IS TESTED WITH FLUSHING CONTROL PANEL .....	161
FIGURE 5-29: SMART PIPE CONNECTION FOR WATER REFILL TO FLOOR TRAP .....	164
FIGURE 5-30: COMMON BELL TYPE FLOOR TRAP .....	166
FIGURE 5-31: SMART BELL TYPE FLOOR TRAP .....	166
FIGURE 5-32: SET UP FOR TRAP TEST RIG .....	172
FIGURE 5-33: AIR CHAMBER IS USED FOR TRAP TESTING .....	172
FIGURE 5-34: P TYPE FLOOR TRAP IS TESTED IN THE RIG .....	173
FIGURE 5-35: SMART BELL TYPE FLOOR TRAP IS TESTED IN THE RIG .....	173
FIGURE 5-36: SCHEMATIC DIAGRAM FOR DATA TRANSMISSION SYSTEM TESTING .....	176
FIGURE 5-37: SCHEMATIC DIAGRAM RIG FOR EMPTY TRAP DETECTION .....	176
FIGURE 6-1: LOCATION OF AIR PRESSURE MONITORING STATION IN LKS BUILDING .....	181
FIGURE 6-2: MONITORING STATION AT 6/F, LKS BUILDING .....	181
FIGURE 6-3: MONITORING STATION AT M/F LKS BUILDING .....	181
FIGURE 6-4: AIR PRESSURE PROFILE INSIDE 150 STACK AT M/F, LKS BUILDING .....	182
FIGURE 6-5: AIR PRESSURE PROFILE INSIDE 150 STACK AT 6/F, LKS BUILDING .....	183

FIGURE 6-6: AIR PRESSURE PROFILE INSIDE 150 STACK AT 12/F, LKS BUILDING .....	184
FIGURE 6-7: SCHEMATIC DIAGRAM FOR DATA TRANSMISSION SYSTEM .....	186
FIGURE 6-8: A TYPICAL AIR PRESSURE SENSOR INSTALLED AT DRAINAGE STACK .....	190
FIGURE 6-9: EPLC MEASUREMENT STATION AT 6/F LKS BUILDING, THE HK POLYU .....	191
FIGURE 6-10(A): EVOLUTION OF AIR PRESSURE AT M FLOOR, LKS BUILDING .....	194
FIGURE 6-10(B): EVOLUTION OF AIR PRESSURE AT 6TH FLOOR, LKS BUILDING .....	194
FIGURE 6-10(C): EVOLUTION OF AIR PRESSURE AT 12TH FLOOR, LKS BUILDING .....	194
FIGURE 6-11(A): PDF WITH AIR PRESSURE AT M FLOOR .....	196
FIGURE 6-11(B): PDF WITH AIR PRESSURE AT 6TH FLOOR .....	196
FIGURE 6-11(C): PDF WITH AIR PRESSURE AT 12TH FLOOR .....	197
FIGURE 6-12: STANDARD DEVIATION OF PDF & RMS OF AIR PRESSURE AT DIFFERENT FLOOR .....	199
FIGURE 6-13 CCTV AT LOWER FLOOR – SUFFERING POSITIVE PRESSURE .....	201
FIGURE 6-13: TRANSIENT TRANSMISSION, REFLECTION AND VENT/STACK RATIO CHART .....	202
FIGURE 7-1: ENHANCEMENT FOR RISK MODEL .....	211

## List of Tables

TABLE 1.1: RESEARCH METHOD OR TOOL THAT SHARED BY MORE THAN ONE	
CHAPTER .....	20
TABLE 4-1: EXPERIMENT DATA RECORD IN THE POLYU DRAINAGE RESEARCH RIG .....	89
TABLE 4-2: PARAMETERS USED IN THE NUMERICAL ANALYSIS .....	112
TABLE 5-1: 8S AIR PRESSURE RESULTS ARE FROM THE HK POLYU TEST RIG .....	156
TABLE 5-2: 18 STOREYS BUILDING INFORMATION .....	158
TABLE 5-3: 8S AIR PRESSURE RESULTS ARE FROM 18 STOREYS BUILDING .....	162
TABLE 6-1: CONDITION AND FACTORS FOR AIR PRESSURE FLUCTUATION .....	193

# **Chapter 1      Introduction**

## **1.1      SARS Outbreak: Drainage system can kill?**

In year 2003, a disease outbreak occurred in a residential estate, named Amoy Gardens, in Hong Kong. The pathogen to be responsible for the disease is a new virus, abbreviated as SARS-CoV {"SARS" stands for Severe Acute Respiratory Syndrome and "CoV" stands for coronavirus}. The transmission of this virus has induced a total of 1,755 infected cases in Hong Kong, with fatalities. In the private residential estate Amoy Gardens alone, the Department of Health in Hong Kong announced that there are 321 confirmed cases occurred with 42 fatalities reported during the epidemic period i.e. between March and April in 2003.

Environmental investigation has been conducted by the World Health Organization (WHO) in that residential estate afterwards. Their investigation report (WHO 2003) advised that one of the hypotheses to explain the Amoy Gardens outbreak was the virus transmission through a contaminated drainage stack. Besides, it was believed that the seal in water traps has dried up and thus,

lost their function to isolate the drainage pipework from the occupants' living space. As a result, design of the drainage systems has attracted attention among the public after the outbreak, when it was widely aware that a dried-up water trap can be risky and that the fatal virus may enter their flats via a dried-up trap.

Apart from the water trap, other abnormalities observed from building drainage system also caught attention among the public. In a Hong Kong Government Press Release (2004), there are complaints from public housing tenants that their flats share communal drainage pipes with adjacent units and so, they are suffered from cross-flow of sewage to (or from) the adjacent unit after toilet flushing. In response to these complaints, the Housing Authority, the governmental department responsible for the management of public housing estates, launched a "Drainage Ambassador" scheme that door-to-door inspection of the indoor drainage facilities of public housing units was conducted. During this exercise, damaged or leaking pipelines were found and repaired, together with other maintenance working such as replacing pipe brackets, and repairing or replacing water traps.



At the same time, operation and maintenance engineers, who were working in buildings with different types of use, had some other findings. The complaints they received were mainly related to drainage system performance, such as flow problems in the drainage system and components like water overshoot from water closets, cross-flow among adjacent fitments, or foul smell in rooms installed with drainage pipeline or sanitary fitments.

This research is conducted to identify an effective approach to manage risks of contamination in the drainage system to occupants in high-rise buildings due to abnormalities on sewage water flow, or improper operation and maintenance of the system.

## **1.2 Research Questions**

The overarching research question in this thesis is:

In order to enhance the performance of drainage system in high-rise building and hence to prevent recurrence of fatal incident like SARS disease outbreak, what can be done in order to rectify the current practice, if needed, for future

design; and what can be done to troubleshoot common pitfalls in existing drainage system?

To answer this overarching research question, the following lines of research questions in the subset of overarch are to be addressed:

1. Is the drainage system really responsible for the spread of virus in the SARS outbreak case? Which system component(s) appears to be more “responsible” to the viral transmission?
2. What are the possible causes or mechanisms of environmental contamination imposed from the drainage systems?
3. What are the typical abnormalities encountered during the use of high-rise drainage system, particularly in Hong Kong? How do these abnormalities come out?
4. Can any design or management solutions be provided to suit the engineering practices in Hong Kong, and to minimize the risk of environmental contamination by the building drainage system, in order to reduce the chance of abnormalities occurrence and indoor environment contamination?

### **1.3 Research Objectives**

To answer each of the research questions, it is necessary to outline the objectives to be achieved in this study:

1. To identify the critical drainage system component that is responsible for the contamination to the indoor environment.
2. To identify the causes and mechanisms of environmental contamination imposed from the drainage systems.
3. To identify typical abnormalities encountered when the drainage system is in use.
4. To propose new design and management solutions, which are applicable to Hong Kong, to reduce occurrence of abnormalities and indoor environment contamination and hence, to minimize the risk of pathogen transmission via building drainage system as well as the risk of disease outbreaks within residential buildings in future.

## **1.4 Review of Main Background Literature**

### **1.4.1 Sewage Disposal System, Public Health, and SARS Outbreak**

Sewage disposal system has played a significant role on public health (Weiss and McMichael 2004). As early as year 1850, disease outbreak via vehicle transmission was identified (Hardy 1993, Boobyer 1896, Parkes 1892). From a macroscopic perspective, there is a concern that in today's developed countries, urbanized cities can be served as a "highway" for microbial traffic (Morse 1995) which may facilitate the transmission of pathogens and increase the risk of infectious disease outbreaks (Weiss and McMichael 2004). And, Hong Kong has no exception (figure 1.1 and 1.2).



**Figure 1.1 shows a congested railway cabin where illnesses can be easily spread out via air. None of the people has prepared mask to prevent breath infection.**



**Figure 1.2 Congested buildings in Mong Kok, red circles show backlands where very short distance between buildings**

Some researchers, like Alirol et al. (2007), has proposed that urban environment could offer favourable grounds for the spread of epidemics mainly because of high population densities (Alirol et al. 2011). However, different opinions have been observed with this respect. The epidemiological analysis reported by Lau et al. (2004) on the case of SARS outbreak in Hong Kong reviewed that the available evidences did not indicate that frequent visits to crowded area lead to a higher likelihood of community-acquired infection. Their analysis also advised that even if a person lives in a residential estate with a reported SARS patient, this is not a significant factor to the spread. For the Amoy Gardens infected

cases, environmental contamination (the sewage system is, again, the suspected source) was probably attributed to the outbreaks.

The exceptional Amoy Gardens outbreak incident was mainly confined within a single building block (Block E). It implies that the existence of a route of environmental contamination within the same building have played a more significant role. A densely populated setting would probably shorten the time required for the virus to reach another person, or allows the infectious pathogens to reach a larger number of “patients” along such environmental route. Rather than solely blaming on the population density as a cause, there is research which supports that the mechanism of environmental transmission would be far more important in terms of infection control and prevention. Even though people can avoid visiting crowded area, they cannot avoid visiting toilets. Hence, there is no surprise that people have more concerns on the drainage side during the outbreak.

Due to shortage of land, there are a significant number of high-rise buildings in Hong Kong. For sewage disposal, it is a common practice to install vertical

drainage stack to collect and deliver waste water and soil from the high-rise building to the government sewer, to which the public sewer is connected with the building drainage system. Since they are interconnected, the building drainage part is considered as the “sewage system” as nominated by the epidemiological field professions.

#### 1.4.2 A closer look to the building drainage part

The prevailed hypothesis is that the aerosolized droplets, possibly contaminated with the SARS virus, were sucked from the Water Closet to the bathroom via the empty trap, and flowing back to the bathroom (Lee 2003), and Yu et al. (2003) found that such droplets were discharged to the re-entrant through the exhaust fan, and spread to the adjacent flats. In such case the virus travelled in the drainage pipework at 16/F of Amoy Garden. There is concern whether the virus travelled only at 16/F or, it also spread to the drainage pipework at other floors via the vertical stack.

Hung, Chan and Law et al. (2006) concur to the hypothesis of the vertical drainage stack transmission. Tests have been conducted, by tracer gas technique,

to prove that the airflow in the drainage stack can bring the contaminant from the 16<sup>th</sup> floor to reach to 37<sup>th</sup> floor in a similar high-rise residential building, when the water traps at both floors are emptied. Their study has assumed that the aerosolized water droplets behave like gases. Further research conducted by Lim et al. (2010) demonstrated that pathogens that can be airborne would exist in various particle forms that can float in air. Its nano-scale size allows them to move like gas molecules through the air as Brownian motion. Furthermore, in the text book “Fluid Mechanics” authored by Douglas et al. (2005), the possibility of upward air transport via drainage stack was also discussed with the supports of computer simulation results. Both the tracer gas experiment and computer simulation match the epidemiological pattern among flats 7 of the above index case.



#### 1.4.3 Plumbing Risk Management Guide from World Health Organization

After the SARS outbreak in 2003, World Health Organization (WHO) has issued a document in 2006 on the health aspects of plumbing systems and SARS outbreak in Hong Kong has been quoted as one of the reference case. The role of plumbers in risk assessment and risk management, including risk recognition, risk evaluation and analysis, risk abatement, risk acceptance and risk transfer, was discussed. The WHO risk management guidance mainly focus on the water supply side although the document covers both water supply and sanitary removal in buildings.

After reviewing the above literature, it is anticipated to focus this research on the drainage side. Risk recognition and risk abatement are applied as a basis to achieve the objective of this research which is to minimize the risk of pathogen transmission via building's drainage system as well as the risk of disease outbreaks in residential buildings in future.

## **1.5 Risk Management Model of this Research**

O'Donovan (1997) defines the term 'risk management' as: "A process where an organization adopts a proactive approach to the management of future uncertainty, allowing for identification of methods for handling risks which may endanger people, property, financial resources or credibility". On the risk management of drainage system operation, the core processes are grouped together by developing a risk management model including risk recognition, risk control and abatement, risk acceptance and monitoring. Figure 1.3 (in next page) shows the structure of the risk management model. In the next section, the items shown in the figure will be discussed separately and the methodology adopted will be explained.

## **1.6 Research Methodology**

### **1.6.1 Risk recognition**

On the risk recognition concerning drainage flow, Chan et al. (2005) reported a review on the contemporary drainage engineering practices in Hong Kong,

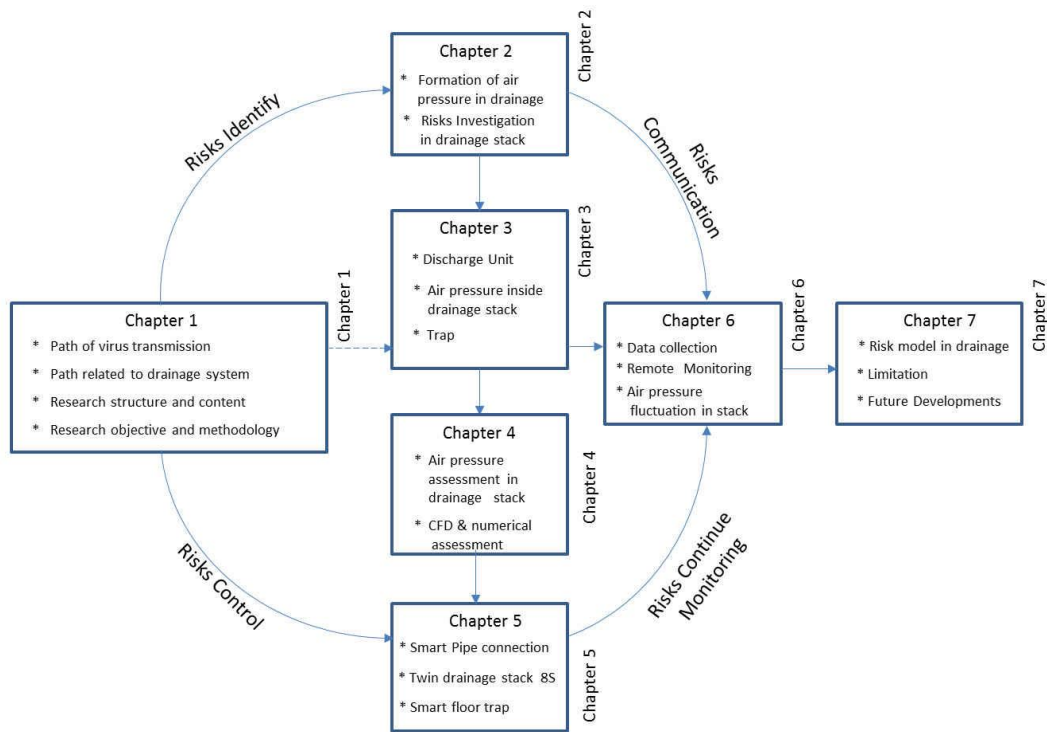


Figure 1.3 shows flowchart in Risk Management on Drainage Stack

Unnecessary bending(s) was found at the high-rise drainage stacks of some residential buildings in Hong Kong. Hydraulic jump would be created at the bending(s) of the stack toe to create positive air pressure at the stack (Wise and Swaffield 2002). This increases the risk of depletion of nearby water trap seal in floor drain traps and water closets.

This research started by an investigation on the drainage stack in Hong Kong high-rise residential building to observe how serious the positive air pressure

problem can be. To explore how a change on the ventilation pipe design can prevent positive air pressure problem, 1:1 drainage test rigs were built for field investigation. The details will be discussed in chapters 2 and 3. ‘Pearpoint’ push rod CCTV system was used to assist the visualization of flow pattern within the stack and included in chapter 3.

#### 1.6.2 Modelling the drainage system flow mechanism

Jack et al. (2005) presented a research on the investigation of the system flow mechanism by using the AIRNET model as a tool for interactive flow modeling to observe the water curtain behaviour at various air speeds, in particular the duration of “closing” of water curtain.

In this research, a different approach has been taken because the main focus is to observe how a change on ventilation pipe design would affect the stack pressure, to fulfill our objective. Computational Fluid Dynamics (CFD) simulation is found to be more useful with this respect. It can be applied to observe the outcome flow pattern at the vertical section of the stack. In Chapter 4, the flow

visualization during field investigation has been incorporated to compare the simulation outcome pattern with the real flow pattern.

### 1.6.3 Risk Abatement (I): Innovative invention on sewage stack ventilation

Cheng et al. (2008) from Taiwan introduced various design options on zoning and also various options on ventilation pipe connections. A dedicated stack was proposed for each zone. Zoning can effectively reduce the loading on the sewage stack. However, the residential buildings are tightly packed in Hong Kong. The pipework for even a single sewage stack provision is already too congested (see figure 1.4) and so, adding extra sewage stack(s) for higher zone(s) may not be feasible, especially for residential buildings with 50 storeys or more which is usually divided into 3 zones.

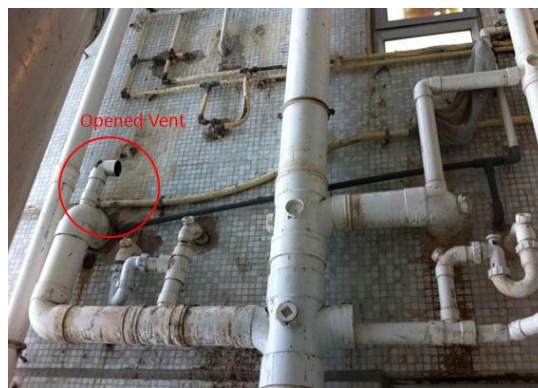


**Figure 1.4 shows a congested pipework arrangement. In addition, an opening of ventilation pipe where emits foul smell**

In addition, the facade installed with water pipework is very congested in Hong Kong. If extra sewage stack(s) is provided due to zoning division, more bending(s) may be needed to accommodate the pipework, as manifested in the case described by Chan et al. (2005), which violates their advice that bending(s) should be avoided.

In view of the above concerns, in order to cater for the congested environment in Hong Kong, an alternative design approach is needed. A patented new stack design named as “8S stack” (twin stack) is developed for this research. Chapter 4 will explain how CFD model is employed to predict the performance of 8S twin stack. Field measurement for the drainage test rigs will be introduced in Chapter 3 although the contemporary stack has been removed and replaced by the newly developed 8S twin stack. Further details will be given in chapter 5.

#### 1.6.4 Risk Abatement (II): Water trap seal retention

After the SARS outbreak, the importance on water trap seal retention attracts more attention between the engineering sector and the public. Alternative piping and floor drain trap arrangement was proposed by local researcher. It has been

proposed to connect the discharge pipe from wash basin to the floor drain's water trap (Yuen et al. 2003) such that a larger portion of water will still flow downward to the vertical stack. It is also found that a small portion of water will flow to the opposite direction to the floor drain water trap near the basin discharge pipe. The drawback of this design is that, if the floor drain is unattended, the water in the floor drain trap will be a dead-end. Water will be gathered and becomes stagnant. It is undesirable because there is no mechanism to flush away the floor drain trap water "automatically" (i.e. occupants are not required to pour water to the floor drain).

In Singapore, the governmental Sewerage Department's Code of Practice has recommended a "common trap" connection that the floor drain trap acts as a trap to the horizontal pipe. Water from wash basin and the bath will be "collected" upstream of floor drain trap. Water will then pass through the floor drain trap and, flows to the vertical stack via the horizontal pipe downstream the floor drain trap. However, there are problems with this design. The first one is flow out of the floor drain grating - water will "flood" to the floor surface near the drain grating (Yuen et al. 2003, Lee 2006). The second problem is water loss

due to evaporation still exist. In case if an occupant leaves a flat for weeks due to overseas trip, the wash basin and floor drain will be unattended and dried up and, contamination is still possible.

This research focuses on the test of evaporation loss of a trap with a typical alternative design. The trap water surface area in contact with air can be minimized by the design, as detailed in chapter 5.

#### 1.6.5 Risk Monitoring by Remote Communication System

Regarding the remote air pressure measurement of drainage system, Gormley et al. (2011) has reported a research on the use of a remote system to test whether defective water trap seal exists by inducing pressure transient. The transient reflection and the transmission of pressure waves were detected and monitored. Remote pressure transient generators, together with pressure traducers were installed to the stacks for the detection of feedback signal. According to the author team, the operation of pressure transient generation and detection system was conducted outside the building.



This sheds light on the development of a set of remote air pressure monitoring system which is installed with air pressure sensors along a stack in the selected floor levels. In addition to air pressure monitoring, this research takes one more step by conducting a probability density functions analysis to evaluate the range of air pressure that the vertical sewage stack may be encountered. The level of “risk acceptance” or the air pressure level that can be accepted becomes possible to be determined, say, by observing at which pressure level the water closets at the floors near the stack toe will or will not, have backflow or water seal overshooting problem. The remote air pressure monitoring system then serves as a tool to assist engineers to decide whether remedial measure should be implemented. Chapter 6 will present this part of the research.

Some of the research method and tools will be used in more than one section as stated in the above. Table 1 shows the chapter which a single method and tool will be demonstrated.

Table 1.1 Research method or tool that shared by more than one chapter

Item	Chapters employed the items
Drainage test rigs	Ch. 3: Primary Investigation on stack performance Ch. 4: Estimation of air pressure by CFD Ch. 5: 8S twin stack development
Flow visualization: (‘Pearpoint’ push rod CCTV system)	Ch. 3: Primary Investigation on stack performance Ch. 4: Estimation of air pressure by CFD (result comparison) Ch. 6: Remote monitoring
CFD simulation and results	Ch. 4: Estimation of air pressure by CFD Ch. 5: 8S twin stack development

## 1.7 Thesis Structure

This thesis consists of seven chapters. Chapter 1 introduces the research background which covers the main research questions and the objectives, the literature review on a wider perspective regarding sanitary drainage, its influence to public health, and also the possible transmission mechanism on the spread of virus in drainage system. A feasible methodology for the study and the thesis structure would be developed.

Chapters 2 to 6 constitute the main body of the thesis, which are focused on the investigation of the flow pattern inside drainage stack and its performance under various alternative design options. They are made by means of simulation, experimental set-up and field measurement. Detail of these methods will be discussed in the methodology section.

Chapter 2 focuses on risk recognition from the characteristics of drainage water and air flow. There is a review on the formation of hydraulic jump, problems arises from the excessive air pressure in drainage stack and the variation of air pressure during the discharge process. Malfunction of traps due to various reasons, including the influence from the air pressure fluctuation in the system, is also discussed in this chapter.

Chapter 3 covers a more detailed investigation on the flow pattern of water discharge in a drainage stack, and the performance evaluation. The drainage test rig, developed for testing the performance of stack design is also introduced in this chapter.

Chapter 4 aims to develop, by means of Computation Fluid Dynamics (CFD) simulation. It is a prediction method on air pressure inside a drainage stack ventilated under a specific design of the ventilation pipe arrangement (if vent pipe is provided). Observations on flow pattern in chapter 3 are adopted as a reference. Field measurement is conducted by the installation of stack (and ventilation) pipe with similar size and ventilation arrangement to the design that is simulated by the CFD. Comparison between simulation results and field observation is presented.

Chapter 5 introduces the development of an innovative invention for the control of air pressure inside drainage stack. The evaporation testing of a new water trap design is also presented. The new design approaches serve as risk abatement measures on indoor contamination from drainage pipe caused by flow abnormalities aroused by excessive pressure, or those by dried-up water traps.

Chapter 6 covers the risk monitoring of the determination on level of acceptance, by developing data communication and drainage stack monitoring techniques. Field application case study is also presented.

Chapter 7, the final chapter, summarizes the major research findings and draws conclusions relating to the research questions as stated in the beginning of this thesis. Based on the findings, recommendations are then made for future design revolutions and new monitoring techniques for monitoring the flow in building drainage system and water retention condition in traps.

## **Chapter 2      Risk Recognition**

### **2.1      High Discharge Loading to the Vertical Stack and its Risk**

In a high developed community and dynamic working place like Hong Kong, people spend long time in their working space due to the long working hours culture in Hong Kong. Most of the commercial buildings in Hong Kong are usually taller than 20 storeys and the maximum can reach more than a hundred storeys. Quite many of them are occupied for a long time during business days. Peak utilization depends on the usage pattern of the occupants, while usually in day time, particularly near lunch hour. For some premises such as shopping mall, night time is also the peak period. Utilization is reduced in mid-night sleeping hours. Distribution of peak time among different buildings for different purpose may vary, even if the nature of premises is similar. It is even worse when the vertical drainage stack encounters high discharge loading that the risk of internal surface scaling can be higher. It may occur earlier in high-rise buildings when compared to lower-rise premises. The stack is difficult to be accessed to conduct cleansing of the internal surface, which raise the risk of

partial blockage (cross sectional area of the stack reduced partly) or, risk of increased pressure inside to be higher.

As high-rise buildings are closely packed in Hong Kong, the discharge loading on both the under-ground and above-ground drainage system is very high.

Within a commercial complex, the usage pattern varies among different zones.

The upper tower of the complex is usually office blocks while the lower zone podium floors are mainly occupied by shops and restaurants. Discharge from office floors occurs mainly during business hours, while the discharge quantity of restaurant floors is larger during meal time, i.e. lunch and dinner hours. High usage of sanitary appliances results in a heavy waste water discharge loading to building drainage system, at a high discharge flow rate. Risk of pathogen transmission occurs in toilets is significant because of high usage of sanitary system. As a result, there is higher chance of air or water backflow from drainage pipework to the sanitary fittings inside the occupied area of toilet. It may be distributed to the air by atomization of water into aerosol mist when flushing the water closets, or by air flow via emptied floor drain traps. This kind of cross-contamination would be much more complicated to deal with, when

comparing with contact-borne transmission. Contacts on surface inside toilets, say when locking the doors of toilet compartments or, using water tap (if the switch is not the automatic sensing type), may be relatively “visible” and draw more concerns among the public. But, the risk of infection by surface contact can be reduced by cleaning the surface at risk in toilets more frequently.

The risk of cross-contamination is the lowest when the soil and sewage can be completely contained solely within the building drainage system to the government sewer without travelling to other occupied location in the building.

The common causes of failing such confinement include water backflow, blockage of pipes and ducts, and leakage or a flow of foul air from the drainage system or its vent (Wong et al. 2008a). When these scenarios occur, the risk of leakage or backflow of air or water to occupied space by airflow or atomized water mist at flushing will be higher. Foul air from drainage system can also transmit the pathogen via human bio-waste. As such, the source does not necessarily come from adjacent users but also the foul air flow or leakage from the drainage stack.



## **2.2 Risk due to failure in retaining water seal in traps**

Unstable water seals of water closet and floor traps as well as leakage of drainage pipe and sanitary appliances are common causes of failures to contain the waste and foul air within the drainage system but flows back to indoors.

Whether a water seal can function properly depends if the height of water “column” in trap is sufficient to block the smell come from drainage pipe to atmosphere. The trap fails to function if water seal is unstable. To protect the water seal at sanitary appliances, it is very important to stop smells and foul air coming from the drainage stack.

### **2.2.1 Trap seal loss due to air pressure transients at the stack nearby**

‘Positive’ & ‘Negative’ air pressure usually exist simultaneously inside the drainage stack. They affect water seal of traps in two ways. One is suction of water seal back into the drainage system due to negative air pressure. Another way is a positive air pressure built-up which pushes out the water seal from the trap. Both of them cause unstable water seals and smells will easily be emitted from drainage system to the atmosphere. Figure 2.1 shows water seal suction under negative air pressure in drainage stack. Figure 2.2 shows how positive air

pressure pushes out water seal to the atmosphere. They exist together in the drainage stack and are the main issues addressed in this research.

*Transient air flow*

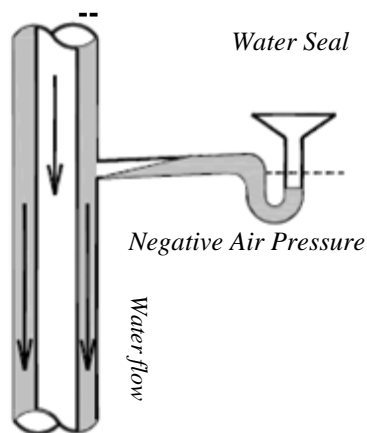


**Figure 2.1 shows negative air pressure and causes unstable water seal**

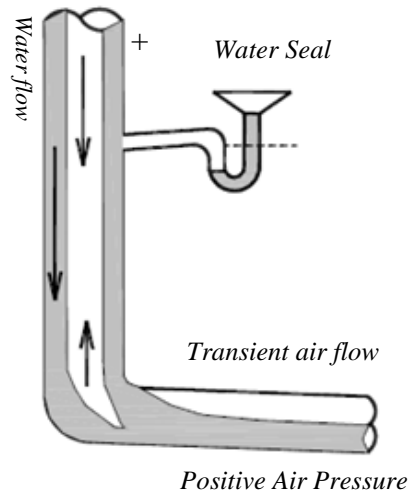


**Figure 2.2 shows positive air pressure and causes unstable water seal**

In figure 2.2, the formation of positive air pressure is always found at the toe of drainage stack. The smell flows from high air pressure to low pressure zone and goes into the atmosphere via the water closet and related sanitary equipment. If harmful virus invades our living environment say, our office, our apartment or, the related public areas, infectious diseases will be transmitted.

### 2.2.2 Causes of excessive stack air pressure near the traps

Excessive air pressure is raised due to several causes which includes blockage of drainage pipes, excessive discharge to the drainage system, and under sizing of pipes and ducts. However, they have the same outcome: water seal inside the trap becomes unstable and smell is released from sanitary appliances.

### 2.2.3 Importance of water trap seal retention

The SARS epidemic in 2003 taught us that the drainage system plays an important role for environmental public health. Empty U-traps and excess positive and negative air pressure inside drainage stacks are the main concern for risk management of building drainage systems (BDS). A healthy system requires effective design, careful installation and good maintenance to minimize these risks.

## **2.3 Risks Formation Investigation**

### **2.3.1 Formation of Hydraulic Jump and the Associated Risks**

Formation of a hydraulic jump can be explained by the conservation of energy, which includes a hydraulic equation of continuity and conservation. As shown in figure 2.3, when there is no leakage of water from the drainage system, water downfall flow rate  $Q_t$  (L/s) inside the vertical stack is the same as flow rate of horizontal pipe  $Q_h$  (L/s). This complies with the hydraulic equation of continuity.

The velocity of downfall inside the stack,  $V_t$ , is greater than the velocity of horizontal flow  $V_h$ . i.e.  $V_t > V_h$ . The residual energy is transformed from kinetic energy to potential energy. Hydraulic jump occurs at the toe of drainage stack.

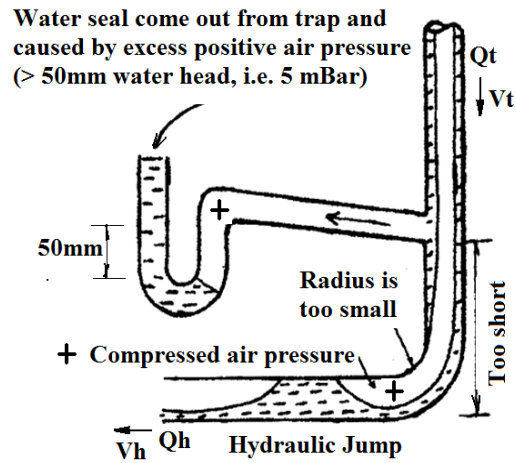


Figure 2.3 Front view shows the formation of hydraulic jump and positive air pressure at the bottom of drainage stack.

Water jump at the bottom horizontal main pipe blocks the air flow path and so, a positive compressed air pressure zone is built up at the bottom of the stack. The positive air pressure forces the water seal in the U-trap to splash back and enters the indoor environment. Hydraulic jump becomes a water curtain to stop air passing downstream, which results in the accumulation of air at the bending of the stack, to build up positive pressure.

Equations 2.1 and 2.2 below demonstrate the comparison between vertical speed and horizontal speed of discharge flow. If the vertical speed is larger than the velocity flow in an inclined discharged pipe (eq 2.3, Manning's equation),

hydraulic jump will occur. The equations\* for terminal velocity and discharge

height are shown as below (Zhu 2006, Wang and Zhang 2009):

$$V_t = 10.7 (Q_w/d)^{2/5} \quad (\text{eq 2.1})$$

$$L_t = 0.1706 V_t^2 \quad (\text{eq 2.2})$$

$$V_h = 1/n R^{2/3} S^{1/2} \quad (\text{eq 2.3})$$

$V_t$       Terminal velocity      m/s

$L_t$       Terminal Length to reach terminal velocity m

$V_h$       Manning equation

$Q_w$       Discharge flow ( $Q_t$ ,  $Q_h$ )      L/s

$d$       Diameter of stack      mm

$n$       Manning number (use 0.015)

$R$       Hydraulic Radius (assume 1/2 bore flow, use)

$S$       Gradient (use 0.01)

\*      Also reference to derivation of equations 3.5 and 3.6 in Chapter 3.

If water is discharged to a stack at which the diameter is 100mm, water falls down. After passing the bend, the water flow direction changes to the horizontal, starting from the toe of the vertical drainage stack. The declined slope of the horizontal pipe is 0.01 using 0.015 as the coefficient  $n$  for waste water, and  $R$  is hydraulic radius (0.375 by assuming half full bore). By using equations 2.1 to 2.3,  $V_t$  and  $V_h$  are estimated to be 2.4 m/s and 0.9 m/s respectively. Such a velocity difference induces hydraulic jump, accumulating positive pressure at the toe of stack.  $V_t$  is formed below  $L_t$  (1m approx.) the below discharge point.

Normally, a small variation of air pressure within Building Drainage System (BDS, less than 1 mbar, i.e. 10 mm water pressure) is normal and within expectation. However, for a BDS with high discharge loading, a higher air pressure inside the drainage stack will be induced, to break and suddenly destroy the water seal inside those traps that are located near the bottom bending end of the stack. Figure 2.4 shows water splash from a building's water closet which is a result from excess positive pressure at the stack.



**Figure 2.4 shows positive air pressure which causes water splash from a water closet – flying water drops are spreading**

Water splash is one kind of energy transfer caused by excessive positive air pressure accumulation at the toe of drainage stack. Moreover, air bubbles can last for a longer period of time in water seals when air pressure is lower. Figure 2.5 shows air bubbles coming slower from the water seal of a water closet.



**Figure 2.5 shows positive air pressure and water bubbles come from water seal of a water closet**



In Chapter 5, an innovative connection of ventilation pipe will be presented to solve the problem of excessive air pressure. Moreover, a creative invention of drainage stack is introduced. The patent invention can replace ventilation pipe and is now in application.

### 2.3.2 Malfunction of trap

A BDS review should not only consider how much air pressure will be generated by water discharge, but also to review its defense ability of the system.

Innovation of type and quality of trap are valuable for further investigation.

To assure the stability of the water seal, air balance within the drainage system is necessary. To comply with British Standard BS EN 12056 Part 2 (2000), an air ventilation pipe or device is required to protect the water seal of trap.

Malfunction of trap means that there is no negative air pressure ventilation inside the drainage stack.

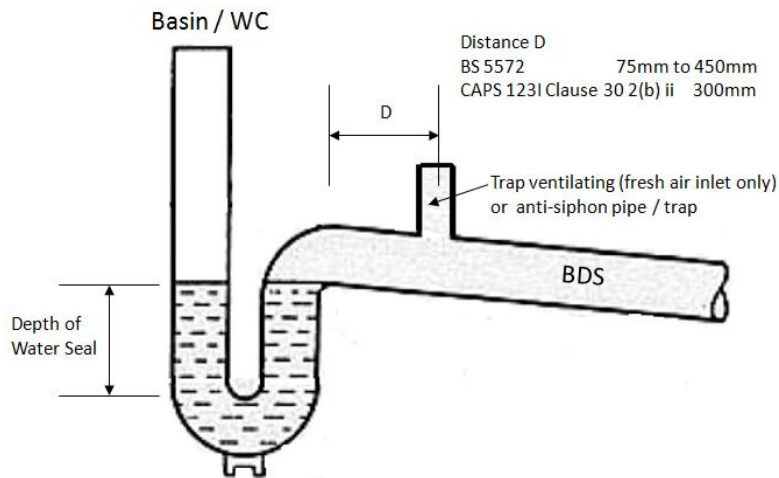


**Figure 2.6 shows standard of trap with ventilation device**

It is a usual practice to install an anti-siphon valve for a basin. The purpose of anti-siphon valve is to act as a negative pressure device. It can break the partial vacuum created that will cause emptying of the water seal in the trap. When there is a fast water flow down the main stack, suction occurs and this draws the water seal from the trap and the air from ventilation valve to balance this negative air pressure. Moreover, when the soil stack momentarily exceeds the design flushing water flow rate, the flush water mass can fill up part of the soil pipe. This mass of water compresses the air in front of it and creates a partial vacuum behind it. As a result, the pressure at the drain trap outlet always fluctuates about the vented atmospheric pressure with transient positive and transient negative fluctuation. Partial vacuum on the U-trap can draw up the

sealing water in the U-trap. The water sealing between the drain point and the main stack cannot function properly if the U-trap is dried.

Proper installation of U-traps for sealing the floor drains from the main stack is important to reduce the risk of foul air release or even the aerosolized pathogen from the bio-waste to the indoor living environment, while the air valve of anti-siphon U-trap can keep closed tightly under the testing positive pressure. Although a plastic sealing valve disc has the sealing effect (Chan et al. 2008a), the plastic sealing valve disc may deform when it is used for a period of time such that the sealing ability is reduced, leading to a malfunction at the trap. Figure 2.6 shows the weakness of a moveable non-return valve that can be damaged easily due to degradation after use, or due to an inadequate quality control during manufacturing.



**Figure 2.7 shows A gasket anti-siphon valve disc stained with rust in the U-trap**

In addition, a smart trap design will be presented to reduce the risk of trap-seal loss that the water seal can be retained for a longer period of time.

### 2.3.3 Field measurement - A case of excessive air pressure in drainage stack

The building drainage system is used for the discharge foul water and the drainage stack is a core member and collects discharge from different flats. For foul drainage, the design objectives are to limit the liquid flow and allow a greater portion of section area of the pipe for air balancing. According to common practice, only  $1/4$  to  $1/3$  of the cross sectional area of the pipe or stack is occupied by water during the discharge. The drainage stack not only discharges water but also serves as a primary ventilation pipe as well. If all the trap seals are depleted, an air path is established since the pipes and stack connect all the flats inside the building together.

To verify the possibility of airflow generation from the empty floor drain trap to the occupied space, a field investigation was performed by Hung et al. (2006) in a vacant 41-storey building. Figure 2.7 illustrates the drainage system serving the flats under investigation.

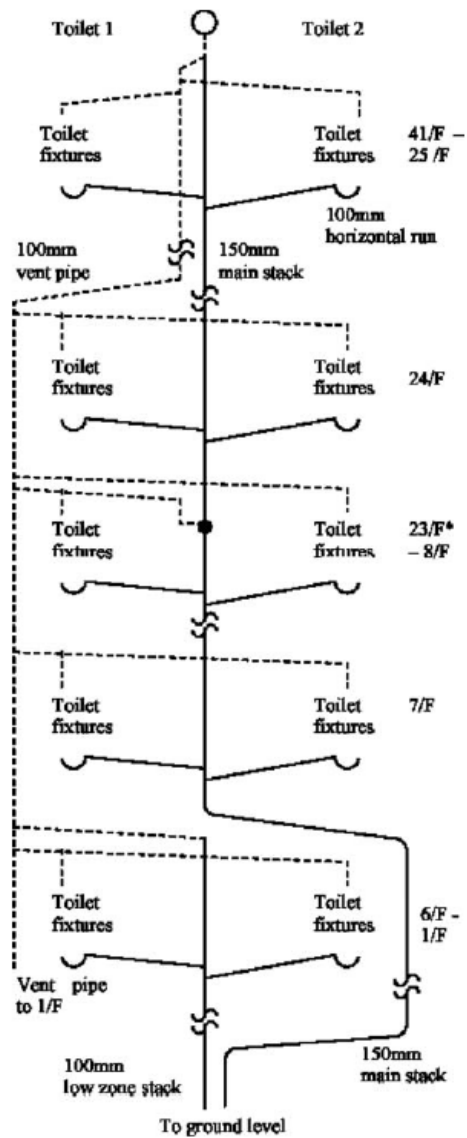


Figure 2.8 Vertical schematic of the drainage stack in the field study building.

There are two bathrooms in one flat, which are served by a single drainage stack with 150 mm in diameter. The stack is connected with a ventilation pipe of size 100 mm, installed 3 m apart from the water stack. Horizontal ventilation pipes

are connected to the sanitary appliances. Such horizontal ventilation pipes are connected to the water discharge stack, such that one horizontal ventilation pipe will be provided for every four floors.

The condition of the floor drain traps was checked by pushing a wire into the bottom of the water trap. If the trap contained any water, the wire end should emerge wet. Otherwise, if the wire end was still dry, the floor drain trap was considered to be dry. The floor drain trap at the 10th floor was found to be dry before the measurement process began. While the cause of this observation is still unknown, insufficient water-refilling to the trap during the vacant building maintenance process performed by the property management is the most likely explanation. During the investigation, a total of nine flats between floors 20 and 41 along a vertical line were selected for water discharge. Since there are two washrooms in each flat (only a single discharge stack is provided to serve both), a total of 18 washrooms were selected.

Water was discharged to the stack by turning ON both the bath tub tap and the shower head in all these washrooms. All the selected water taps were turned ON

to the maximum flow position. The discharge flow rate from each water discharge point was estimated using a flow meter cup as shown in Figure 2.9.

Total water discharge rate to the vertical drainage stack was approximately 2.3 L/s i.e. the sum of all measured water flows from discharge points, after turning ON each of the appliances and the water flow becomes steady. For all water discharge fittings, the maximum flow position was fixed during the measurement process. Near the 10th floor dry trap, a microprocessor-based anemometer was located for air velocity measurement. The instrument, Dantec 54N50 low velocity flow analyzer, measures air velocity either in centimetres per seconds or in metres per seconds.

The velocity range of the instrument is 0-100 cm/s, with a final accuracy of  $\pm 1$  cm  $\pm 5\%$  in 5- 100 cm/s, or 0- 5 m/s with a final accuracy of  $\pm 5\%$  in 0.25- 5 m/s.

The toilet door was closed and the exhaust fan was switched OFF. It was observed on the 7th to 10th floor washrooms that water was being expelled from the water closets (WCs). For this reason, the WCs were covered in order to prevent water spillage.

Under the above-mentioned conditions, the air velocity near the floor drain was measured at 3.56 m/s. A paper strip was placed near the vertical grating of the floor drain to verify the air flow direction. It was found that the air current was pushing the paper strip away from the floor drain opening (figure 2.10), which showed an airflow direction from the drainage pipe to the washroom.



**Figure 2.9 Discharge flow is measured By the cup**

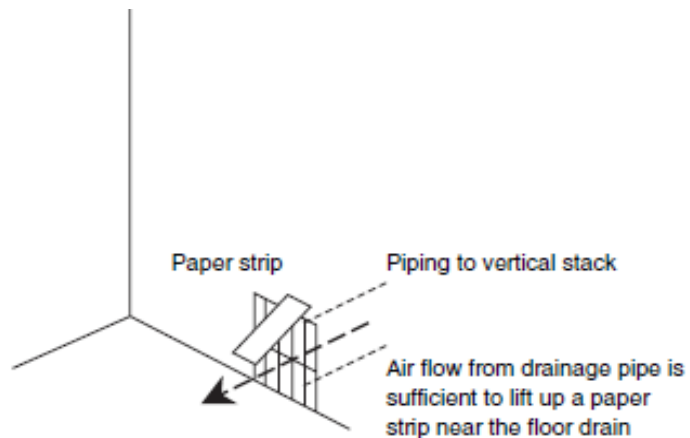
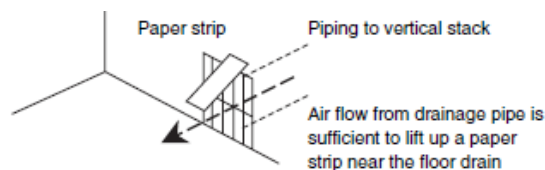


**Figure 2.10 Verification of airflow direction by placing a paper strip near the floor drain.**



by the positive air pressure created at the

1 floor. When the fluid from the upper

floors impinges upon the offset, a local surcharge condition occurs, which

propagates a positive air pressure transient, and applies positive pressure to the

water trap seal. During the case study, the floor drain trap on the 7th floor was



filled with water. Such positive pressure was high enough to force the water inside the trap to flow back to the toilet floor and lead to flooding in the bathroom. In the 10th floor dry trap case, an air flow of 3.56 m/s was measured.

The above experiment concluded that, even without air exhaust due to fan operation, the positive pressure generated in the drainage system can induce an airflow that drives contaminated air from the stack to the toilet. Instead of sizing ventilators in toilets to avoid entraining airflow from the floor drain, the investigation showed that it is far more critical to prevent excessive airflow within the high-rise drainage stack and the consequent positive pressure created at drainage stack offsets. However, the mechanical ventilation does have its main function, which is to remove odour and moisture build-up in toilets and washrooms. The mechanical ventilation system should not be undersized in order to avoid airflow created by the fan. Since airflow can actually be induced inside the drainage stack, as observed in our experiment, the best practice is to size the exhaust fan according to the toilet ventilation requirement, and adopt a self-priming design and positive pressure relieving measures to protect the water trap seal.

In Hong Kong, provision of ventilation pipework is a regulatory requirement. It is required to set up the ventilation pipe opening above the roof level of the building. However, the distance between the opening of the pipe ventilation system (e.g. at the roof) and the source of positive pressure transient (e.g. at the bottom of the stack) is usually very long, which can be more than 100 m for a typical 40-storey building. As such, it is not rare to find that the venting system in some high-rise buildings is incapable to relieve positive pressure transients, typically at the bottom end of the stack.

In occasional cases, water expulsion from WCs located on lower floors can be experienced. To cater for emergency cases, building operation and maintenance engineers should implement pressure relief measures, such as installing pressure attenuators near the drainage stack off-set location, or any critical water trap under high risk of water seal depletion. There are also rooms for improvement on the drainage system in order to reduce the risks. The measurements are not only for emergency but also for ease of management. At the design stage of a drainage system, the first step is to conduct a reasonable estimation on air pressure caused by water discharge in the system. However, it is not a common

practice in Hong Kong because the testing and commissioning approaches are usually based on past experiences only. There is no provision for testing requirements to monitor air pressure profiles even in drainage system for new buildings. The common practice among residential buildings in Hong Kong hardly monitor the air pressure inside the drainage system continuously to predict and alert the excessive air pressure inside the drainage stack during occurrence. Actual cause and the risk of foul air or foul water backflow into the flats is usually unknown among the occupants. In the coming chapters, a series of steps will be introduced on an estimation of air pressure profile in the buildings.

### 2.3.4 Hazards caused by drainage stack

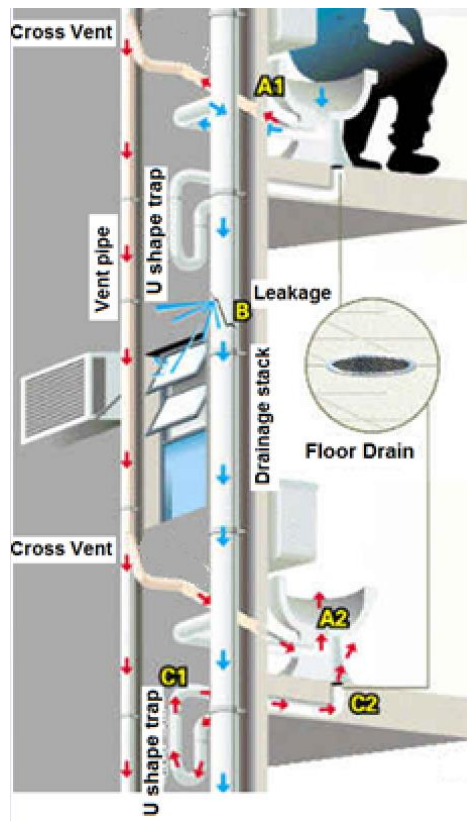


Figure 2.11 Verification of hazards are caused by drainage defects

In figure 2.11, 3 possible paths for virus transmission can be observed. Source of virus is created from water closet user (A1) of upper floor and reach lower floor water closet (A2). The second path is leakage (B) from the drainage stack which is degraded. The red path from figure 2.10 is the ventilation pipe, and the virus can reach the adjacent floor when traps C1 or/and C2 is/are emptied. All of these paths become hazards of the establishment of virus transmission path within the drainage system. While virus transmission via the drainage network attracts

more attention among the public in the 2003 SARS outbreak incident, there is risk of toxic air poisoning caused by the egress of air from drainage system. This issue has been addressed by the Council of Labor Affairs in Taiwan (2007) where incidents with death and injuries occurred at works relating to cleaning, repairing, or water proofing structures in drainage pipes due to inhalation of anaerobic air or sulphurated hydrogen gas. This also reminds building users that the risk of egressing poisonous gas from drainage system should not be ignored. The result of failure on retaining the water seal to block the foul air can be as serious as fatalities. The proposed methods to protect the water seal in traps, i.e. the defense line, are so important that the safety and health among occupants can be protected.

## **Chapter 3**

### **Primary investigation on the performance of drainage stack**

As mentioned in previous chapters, discharging water can induce a positive or negative air pressure in the drainage stack. They exist during a single discharge.

The positive and negative values fluctuate alternatively within the air pressure profile which can be obtained by theoretical prediction, or observed from field measurement.

#### **3.1 Review Assessment Methodologies for Drainage Stack**

##### **3.1.1 Discharge Units**

The total discharge flow rate from a building to the sewer depends on the usage of sanitary appliances. Every sanitary appliance has its own discharge flow rate, which can be determined by the flow volume and the time duration of the discharge of such flow volume. The structure of discharge grating is also influential. For different sanitary appliances, say basin and bath, their discharge unit is different because both their discharge pipe size, discharge volume and duration are different.

The design method published by the Institute of Plumbing (IOP, 2002) is widely adopted. It introduced a great change that unit of discharge unit is defined on discharge volume over discharge time and, the discharge flow rate of a sanitary appliance can be easily found. The discharge flow rate can be obtained from the total discharge unit directly (see equation 3.1).

$$Q = K \sqrt{\sum DU} \quad \text{Unit of } Q: \text{L/s (eq 3.1)}$$

K is a variable factor with dependence mainly on the frequency of fitment usage. This value is dimensionless and ranges from 0.5 to 2. These values are adopted from the British Standard BS EN 12056 (2000) and IOP design manual (IOP, 2002). If there are 240 water closets (WC) connected to the stack, and for each single WC the flow rate is 1.82 L/s; according to IOP design manual,  $K = 0.5$  and Q can be calculated as 10.5 L/s. While the coefficient suggested by BS EN 12056 for discharge estimation is different from the IOP manual, the results come from the above two different standards are reasonably agree with each other. Nowadays, both the IOP manual and BS EN 12056 are widely used in Hong Kong for drainage pipe design.

Estimate the discharge flow is difficult because even for the same sanitary appliance with same discharge water volume and same discharge pipe size, the grating pattern can be different. It means that the discharge duration can also be different. This also results in different discharge units. Figure 3.1 shows grating B has a higher discharge unit.

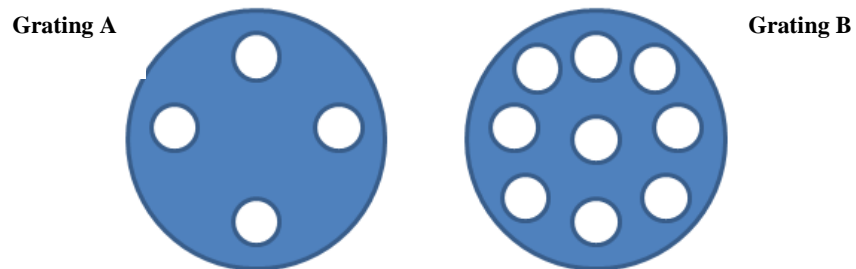


**Figure. 3. 1 Grating B has higher discharge flow rate than grating A**

The occupants' behavioural characteristic on the use of sanitary appliances can also affect the total discharge rate in the vertical stack, and this may cause flow problems due to a change in air pressure with changing discharge rate.



### 3.1.2 Formation of falling water volume

Water discharges from the branch and reaches the drainage stack with a velocity (0.5m/s is expected for 100mm branch pipe). Figures 3.2 and 3.3 show water falling from branch to a drainage stack.



**Figure 3.2** A branch jet of water striking the solid wall of a test transparent stack pipe

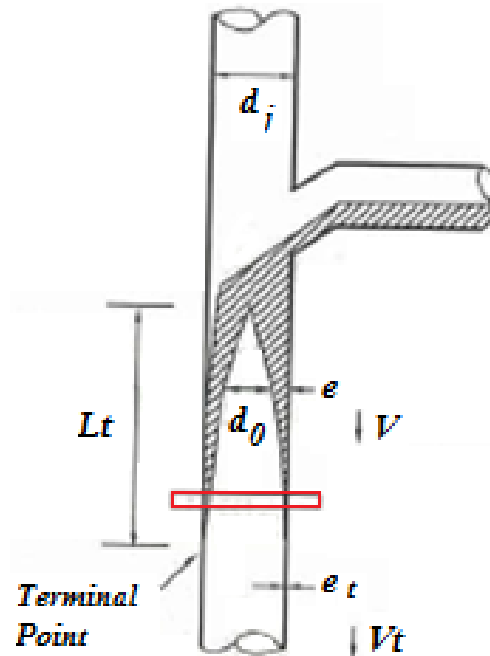


Figure 3.3 A branch jet of water flows into drainage stack and generate different velocities

From figure 3.3,

$V_t$  = Terminal velocity (m/s)

$L_t$  = Terminal Length to reach terminal velocity (m)

$d_j$  = Diameter of stack (mm)

Once the falling water volume reaches its terminal velocity and attaches to the internal wall of the drainage stack with a thickness  $e_t$ , the falling water volume looks like a uniform red ring as shown in figure 3.4:

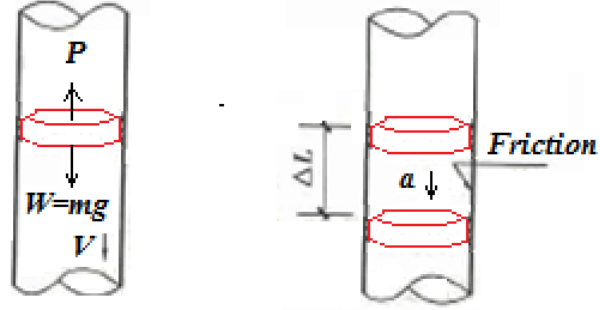


Figure 3.4 A water ring falls a depth  $\Delta L$  and reach a constant falling velocity  $L_t$

In Figure 3.4, friction  $P$  and gravity force  $W$  are reacted,

$$F = ma = W - P \quad (\text{eq3.2})$$

where  $m$  is mass of water volume passing in  $\Delta t$

$$W = mg = Q_w \rho \Delta t g \quad (\text{eq 3.3})$$

$$P = \text{friction} = \tau \pi d_j \Delta L \quad (\text{eq 3.4})$$

where  $\tau$  is friction in  $\text{N/m}^2$

For terminal velocity, velocity will be constant and acceleration  $a = 0$ , that is

$$\frac{dv}{dt} = 0$$

Substitute equations 3.2 to 3.4 into the derivative procedures adopted by

previous study (Wang and Zhang 2009) gives

$$V_t = 10.7 (Q_w/d_j)^{2/5} \quad (\text{eq 3.5})$$

$$L_t = 0.1706 V_t^2 \quad (\text{eq 3.6})$$

Equations 3.5 and 3.6 are same of equation

During a single water discharge, the water volume can have different falling velocities. The initial velocity is assumed to be zero and will increase to  $V_t$  after falling a height of  $L_t$ . In reality, the water volume is not falling along the internal wall of a drainage stack at all. Volumetric shape is also not necessary to be a red ring. The actual shape can be observed from visual inspection method as below.

### 3.1.3 Visual inspection on falling water volume

A visual inspection was conducted inside a 100mm diameter drainage stack which is installed in a domestic building. The building is 35-storey in height and the drainage stack is installed at flat 11 as shown in the layout plan (figure 3.5).

The building is a typical domestic building in Hong Kong. There are 18 flats at a single floor and can accommodate a total of almost 100 persons at a single floor.

For flat number 11 of the building, the service area is about  $30\text{m}^2$  and a 100 mm diameter drainage stack is provided for the bathroom. The stack serves along the whole vertical column of flat number 11, from the topmost 35 floors to the first floor at the bottom. The vertical height of the whole drainage stack is about 107 m. The drainage stack CCTV survey was conducted at various locations between the rooftop and G/F.



**Figure 3.5, A typical domestic building in high population density**



**Figure 3.6 A 'Pearpoint' push rod CCTV system for drainage stack investigation**

A push rod system (Pearpoint system, figure 3.6) was employed for this inspection. The push rod was attached with a camera head. The camera can be moved forward or backward (i.e. reverse direction) by pushing the rod and it can pass through the bending of the pipe.

A visual investigation had been conducted at chainage 100.9 m (near the toe of drainage stack, and chainage 0 m is the roof level). From the captured pictures (figures 3.7 to 3.9), size of water volume portion is smaller at the beginning of the discharge (front of water volume heading downward) and near the end (rear of water volume) part of the discharge. It is obvious that the largest size of water volume portion is at the middle of the whole falling water volume.

During the fall of the water volume, a thin water ring can be observed and, water falls along the surface of drainage stack. However, a large portion of water volume is shifted from the wall surface.

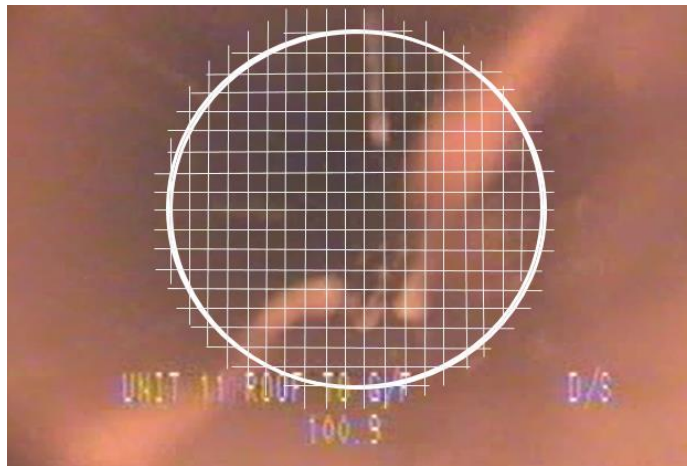


**Figure 3.7 Head of falling water volume at 100.9 m, picture shows the head of falling water which is smaller than 30% sectional area of drainage stack**

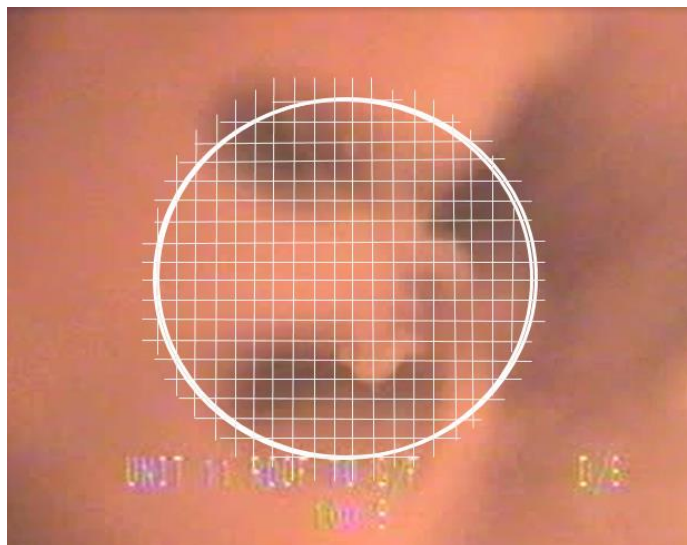


**Figure 3.8 size of falling water volume is increasing at the middle of falling water which is greater than 60% sectional area of drainage stack**

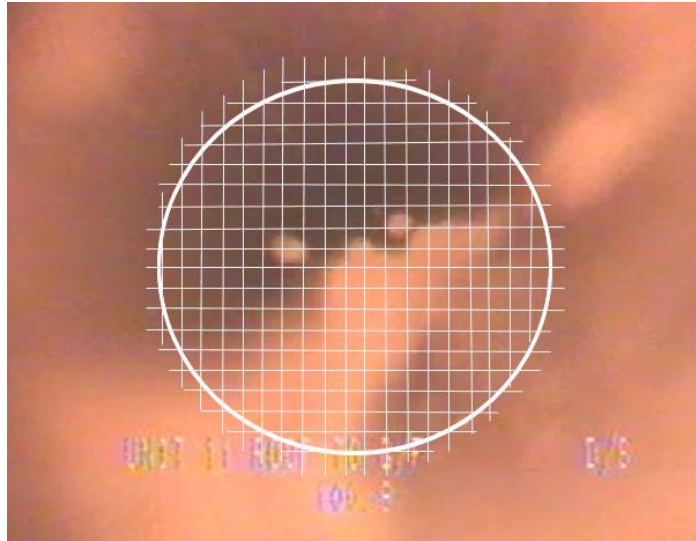


**Figure 3.9 size of falling water volume is decreasing at the end of falling water  
which is smaller than 30% sectional area of drainage stack**

As stated in section 3.1.1, the whole water volume, falling downward, is assumed to move along the internal surface of drainage stack and, the shape is assumed as a water ring with thickness  $e_t$  at terminal velocity  $V_t$ .

In the captured images above, it can be observed that the water volume is divided into two half ellipses during the fall and not in a rectangular water ring as assumed. Section of water volume can be adjusted and shown in figure 3.10:



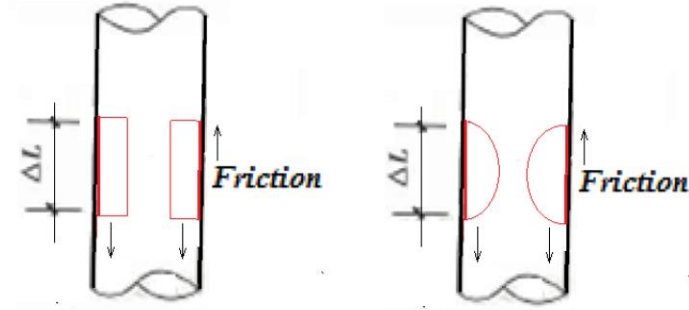


**Figure 3.10** Section of water ring can be changed from rectangle to half ellipses

From this visual inspection, the real shape of the falling water volume can be obtained. This observation, together with the information on terminal velocity and terminal distance that are available from previous mathematical derivation, provides basic concept and for further development by the CFD simulation, which will be discussed in the coming chapter.

As observed from CCTV images from figures 3.7 to 3.9, falling water volumes are divided into different parts which possess different falling velocity. The terminal velocity represents the minimum falling velocity only. In normal cases, the falling velocity in a 100 mm diameter drainage stack does not exceed 4 m/s for a water volume flow rate at 4.8 L/s (Douglas et al. 2011). Such a discharge

flow rate of 4.8 L/s is approximately equal to a simultaneous flush of 100 Water Closets (9L capacity) together at the same time.

### 3.1.4 Air Pressure inside Drainage Stack

In Chapter 2, the hydraulic jump phenomenon has been introduced. This occurs at the toe of a drainage stack (Figure 3.11). One of the risks is that it can create positive air pressure. This pressure results in drainage water and/or foul air backflow to an occupied indoor area or the atmosphere and impose a risk of contamination in indoor environment. Hence, the worst consequence can be a spread of pathogenic micro-organisms that can endanger our human health. In this chapter, the energy principles of this phenomenon are discussed and, illustrations under different velocities will be provided.

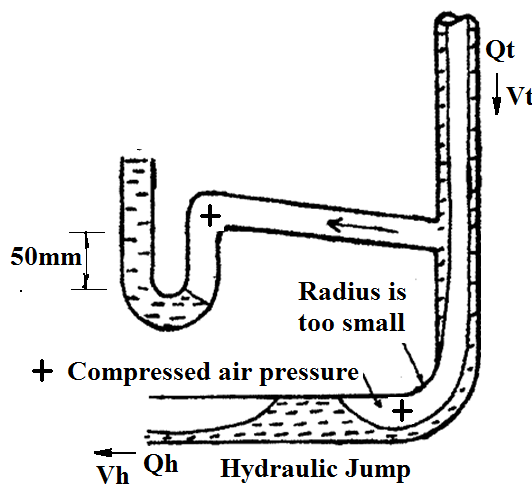


Figure 3.11 Hydraulic jump is found at the toe of drainage stack

Air pressure is the critical monitoring index to determine whether the drainage stack is under the risk of sewage water or foul air backflow towards the occupant's indoor space. The unit of pressure value can be shown as mm which is usually applied to height of water seal. 5 mbar air pressure equals to 50 mm H<sub>2</sub>O height difference when observing from the U tube. It is comparable to the height of water seal inside the trap of sanitary appliances. If air pressure inside the stack is 50mm H<sub>2</sub>O or larger, it is a significant signal that there is unstable water seal at the sanitary fitment side. The air pressure in the stack can also “press” the air to the branch and then press the water “column” inside the trap to force the trap water flow up to the floor grating for the floor drain case, or overshoot of water at the water closet. Air pressure inside the stack will not be static but fluctuating because the quantity of water discharged to the stack is changing. This can be verified by means of observation on water discharge in real system, and also by CFD simulations.

### **3.2 Drainage Research Platforms**

The development of a drainage research rig is critical for this research in order to understand the flow characteristics and to pretest a newly designed drainage system component as well as a new arrangement on piping connection. The rig also facilitates field experiments for comparison against simulation model that the embedded assumptions and operating parameters in computation model will be referred accordingly when modifying the rig setup. While one may consider conducting field measurements in a real occupied building, the flexibility is limited when comparing with test rig. The operating parameters are less controllable and it may not be permitted to retrofit the system according to the simulation inputs or piping arrangement. A drainage research test rig offers more flexibility to adjust the quantitative discharge in a more precise manner for data verification. Two such drainage research rigs have been established - one is in Hong Kong, while the other is in Japan. Their tests' data are valuable to verify the results which are generated from the coming CFD simulations.

### 3.2.1 Discharge Test in Drainage Research Rig

A 3-storey drainage test rig was built and located in the Industrial Centre of a local University in Hong Kong (Wong et al. 2008b). On the test rig, the transparent sewage pipe, ventilation pipe and cross-vent connections were demountable and the water flow could be adjustable. This test rig is a 1:1 full-scale facility for teaching and research purposes. The major topic was positive air pressure phenomenon in building drainage system. According to the experience from Hong Kong high-rise buildings, the risk of failure of the system as a result of excessive positive pressure occurred quite frequently. Calibrated data from test rig experiment could also be obtained for further investigations. The height of test rig was 7 meters (as shown in the schematic diagram figure 3.1) and equipped with a transparent drainage stack which was unique in Hong Kong. A series of access points along the stack was specified during the construction of this rig. Pressure sensors could be installed at these access points to record the air pressure profile for the whole system. Down-flow water discharge rate could be varied to observe the difference on the air pressure profile. The variation on air pressure along the transparent stack, at different water discharge flow rate, could also be obtained. The transfer tank at the

ground floor was the water source for down-flow test. The flow rate could be varied by operating the two pumps at different mode: single model or twin mode.

By pumping water to the 50 mm diameter riser, the water flow pass through a regulator which could adjust the water flow rate within the range between 150 L/min to 300 L/min. Water entered a stainless steel discharge box. The 100 mm diameter opening at the bottom of the box was connected with a 100 mm diameter transparent stack (Fig.3.2)

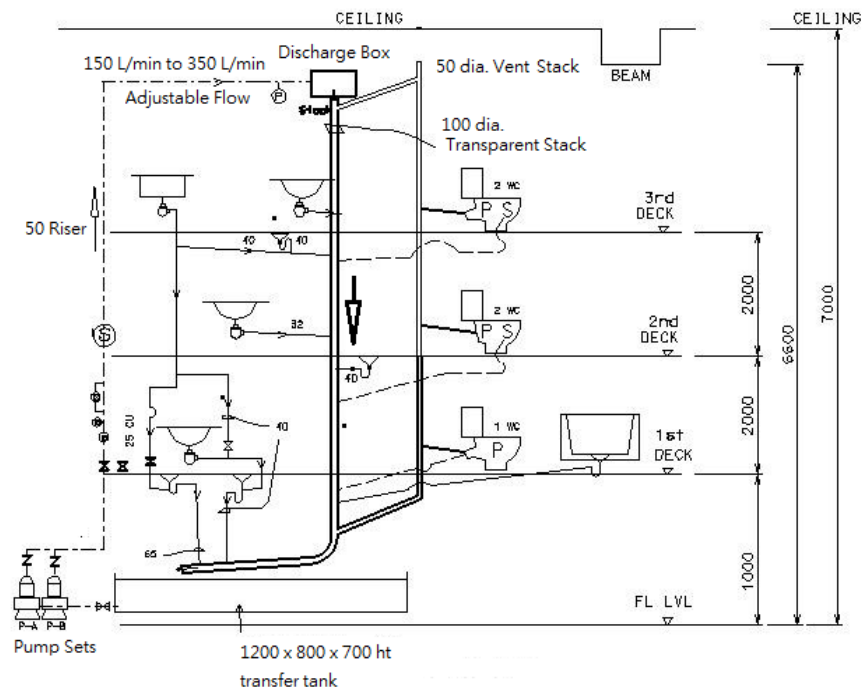


**Figure. 3.12 Schematic Drawing of Drainage Rig in the HKPolyU**

Air pressure transducers manufactured by WIKA are installed to the test rig and the accuracy is  $\pm 50\text{Pa}$ . ADAM data logger was used to receive signals from the transducers and the data was recorded.

In figure 3.5, the discharge flow was set at angular and water fall down along the transparent internal pipe wall. The centre core of the cross-section of vertical stack was air. The air could reach the top of the stack and the open atmosphere if the airflow direction was upward.

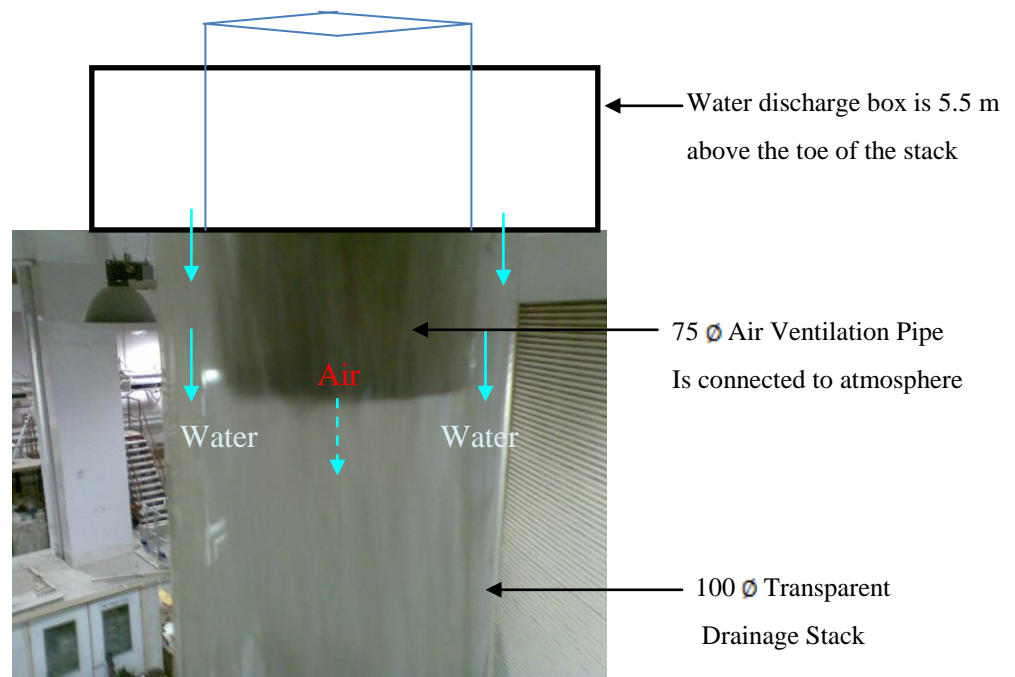


**Figure. 3.13 Water discharge from a tank installed at the ceiling**

### 3.2.2 Discharge Test in a 17-storey drainage research rig

Since the vertical drainage stack was transparent, the 3-storey rig facilitated a microscopic observation on different hydraulic discharge cases and the associated variation on stack air pressure. However, to compare the high-rise drainage system in Hong Kong, a higher test platform would be more representative.

Another drainage test rig was established by the Japan by the China National Engineering Research Centre (CNERC) in 2006 at a 17-storey building in Shiga (Zhang and Chen 2006), as shown in figure 3.14.



**Figure 3.14 17-storey Drainage Research Tower in Shiga, Japan**



This rig facilitated discharge tests according to the Japan testing standard.

Pressure sensors (Valcom – VPRN-A3), data transmitter and data loggers (OMNIACE – RT3424) with filters (9B02 - 3 Hz) were all calibrated with reference to the corresponding Japanese standard.

One set of testing data were conducted by CNERC and will be referred in this research in a later chapter. In addition, one set of air pressure profile data were collected from this research for mathematical simulation in the next chapter. The water discharge flow rate was 2.5 L/s from 17/F (as shown in figures 3.5 & 3.6).

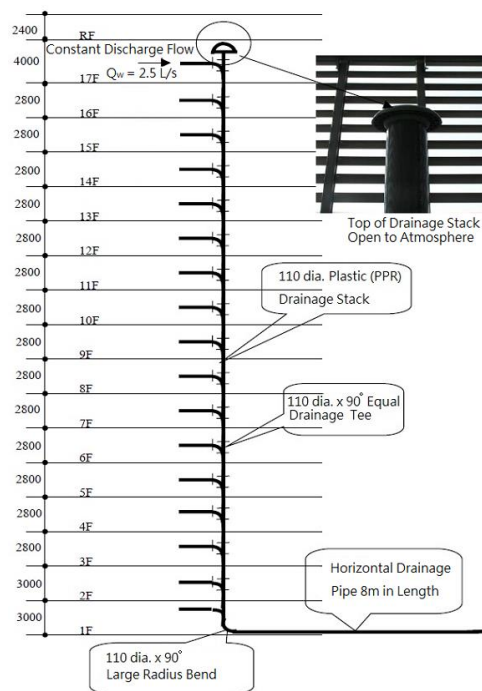


**Figure 3.15 –Configuration in research rig and a flow test discharge on the 17/F**

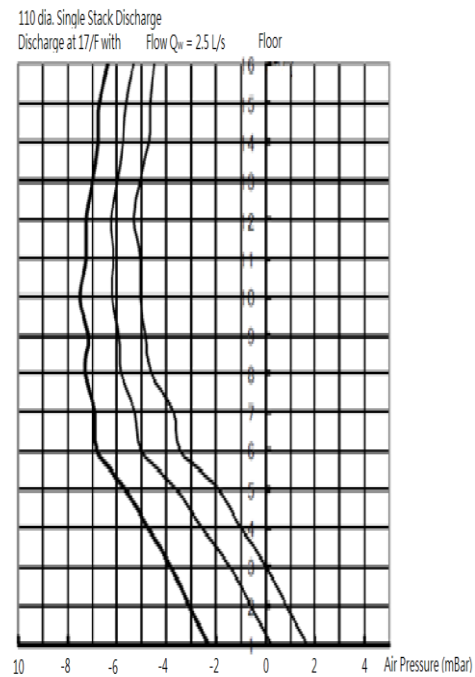


**Figure 3.16 –Air pressure profile along the 17/ F drainage stack.**

### 3.2.3 37-storey Drainage Research Tower in China

In summer 2012, a taller drainage research tower (Fig. 3.7) started to operate in China for research purpose (Zhang and Zhan 2012). The total height of the tower was 123m with 37 storeys (3m high for each storey) from the ground, with an additional storey underground (4.5m high for the underground storey). All the testing devices and accessorial devices were selected to fulfil international standards.

Advanced operating systems were incorporated to this testing tower. The PAC control system (Fig. 3.8) could realize PID adjustment of constant flow solenoid valve. A variety of switches and electric valves were also installed to control the water flow to be constant when needed. By controlling the water supply pump(s), water could be supplied to the lower and higher tanks automatically. Three meteorological stations were established to record the atmospheric wind speed, air temperature and relative humidity, together with solar radiation data via Modbus link to PAC controller on every level in the system.



**Fig.3.7** 123 m height of drainage research Tower is located at Dongguan,



**Fig. 3.8** Precise automatic valve can discharge exact water flow volume into the drainage stack and test

For constant flow experiments, the pressing sensors were set to have a measurable range between -10000Pa to +10000Pa with a resolution of 5Pa, with response cycle of 20Hz; and wave filtration of 3Hz.

Studied parameters includes the air pressure in horizontal pipes, air velocity in the vent system of the stack, surface level of water when passing through the floor drain, and the water surface level of the flow within the horizontal pipe. A pressure range of  $\pm 400$ Pa has been defined for the system as the control parameter, and the actuation control can be achieved with reference to the feedback signal from flow meter and constant flow solenoid control valve, to

deliver the desired constant flow output. Other available functions of this drainage rig include:

- ◆ Facilitates constant flow experiment
- ◆ Support ware drainage experiments
- ◆ Data acquisition
- ◆ Data analysis
- ◆ Monitoring and control

Research results from this tower are more representative to the real situation in typical high-rise buildings in Hong Kong. The tower is the only experimental institute in China that allows technical tests for high-rise and super high-rise buildings. It plays an active role for the enhancement on drainage engineering in the Chinese housing industry. In our coming research, experimental data received from the above rigs is adopted for further simulation study and data verification.

## **Chapter 4**

### **Estimation of air pressure inside drainagestack**

#### **4.1 Computer fluid dynamic (CFD) estimation**

This chapter will investigate some relevant hydraulic models and simulation methods which are suitable for this study to investigate the performance of drainage stack. Computation fluid dynamics (CFD) simulation and some numerical assessments have been executed. The results from the various approaches will be compared with the results obtained from drainage rigs experiments.

##### **4.1.1 Navier-Stokes Equations used in CFD**

Based on the Euler equations, Claude Louis Marie Henry Navier and George Gabriel Stokes modified and created the Navier-Stokes equations, or named as the N-S equations (Lappa 2009). This provides groundwork as the foundation of computational fluid dynamics (CFD) simulation which is commonly adopted in complex fluid flow modeling by breaking down the geometry into cells that to comprise a mesh. At each cell an algorithm is applied to the computation on fluid

flow within the individual cell. Depending on the nature of the flow, Navier-Stokes equations can be applicable.

According to the study by Orhan (2004), these equations arise from applying Newton's second law of fluid motion, together with an assumption that the fluid stress is the sum of a diffusing viscous term (which is proportional to the gradient of velocity) and a pressure term. Although the original Navier-Stokes equations (NS equations) only refer to the equations of motion (conservation of momentum), it is commonly accepted to include the equation of conservation of mass as well. These four equations all together fully describe the fundamental characteristics of fluid motion.

Velocity vector:  $\vec{v} = u\vec{i} + v\vec{j} + w\vec{k}$

Del operator:  $\nabla = \frac{\partial}{\partial x}\vec{i} + \frac{\partial}{\partial y}\vec{j} + \frac{\partial}{\partial z}\vec{k}$

Gradient of a scalar field, f:  $\nabla f = \frac{\partial f}{\partial x}\vec{i} + \frac{\partial f}{\partial y}\vec{j} + \frac{\partial f}{\partial z}\vec{k}$

NS equations provided motion formula as stated are:

$$\frac{\partial \rho}{\partial t} + \nabla \cdot (\rho \vec{v}) = 0 \quad \text{for continuity}$$

$$\rho \left( \frac{\partial \vec{v}}{\partial t} + \vec{v} \cdot \nabla \vec{v} \right) = \nabla \cdot \vec{\sigma} + \vec{f} \quad \text{for momentum}$$

where  $\rho$  is fluid density,  $\vec{v}$  is flow velocity vector,  $\vec{\sigma}$  is stress tensor

$\vec{f}$  is body forces and  $\nabla$  is del operator,  $\sigma$  are the normal stresses and  $\tau$  are shear stresses acting on the fluid.

Since NS equations are used as three-dimensional system, the resulting equations would be very complex and would require considerable amount of field data with spatial variants.

FLUENT is a computational fluid dynamics (CFD) software package for computer use, and employs NS equations to simulate fluid flow problems. The software employs a calculation model on water volume which is assumed to have a constant shape and not affected by air. A finite-volume method is adopted to solve the governing equations for a fluid. It provides the capability to use different physical models such as incompressible or compressible flow, inviscid or viscous flow, and also laminar or turbulent flow. In the study, air is considered as an incompressible idea gas. Geometry and grid generation is conducted by using GAMBIT, the preprocessor bundled with FLUENT.

#### 4.1.2 Air movement in drainage stack

On the simulation of air movement within drainage stack, a change of velocity is considered by Fluent, and the N-S equations employed are shown as below:

$$\frac{du}{dt} = f - \frac{1}{\rho} \nabla p - \frac{1}{\rho} \nabla \left( \frac{2}{3} \mu \nabla u \right) + \frac{1}{\rho} \nabla (2\mu \tau) \quad (\text{eq. 4.3})$$

where  $u$  is velocity,  $p$  is static pressure,  $\nabla p$  is pressure,  $\mu$  is dynamic viscosity,

$$\nabla u = \frac{\partial u_i}{\partial x_i} \quad (\text{specific volumetric dilatation})$$

$$\tau_{ij} = \frac{1}{2} \left( \frac{\partial u_i}{\partial x_j} + \frac{\partial u_j}{\partial x_i} \right) \quad (\text{shear deformation rate})$$

The following is the explanation on the equation:

$$\frac{du}{dt} \quad \text{is acceleration of air flux}$$

$f$  is body force act on unit mass of air flux

$$- \frac{1}{\rho} \nabla p \quad \text{is pressure of unit mass of air flux}$$

$$- \frac{1}{\rho} \left( \frac{2}{3} \mu \nabla u \right) \quad \text{is normal stress of unit mass of air flux}$$

$$\frac{1}{\rho} \nabla (2\mu \tau) \quad \text{is shear stress of unit mass of air flux}$$



The equation employs the standard  $k - \varepsilon$  model (turbulence kinetic energy,  $k$  and turbulent dissipation rate  $\varepsilon$ ). The simulation is applied on the two dimensional grid, which represents the air flow conditions (Steve and Chia 2013).

## **4.2 Assessment on Stack Pressure by CFD Simulation and Experiments**

### **4.2.1 Principle for the air movement inside the stack**

When water is discharged from the branch pipe and falls to the drainage stack, the water flow could be viewed as a formation from numerous small water curtains. They fall down due to gravity and are compressed downward to the air zone in the drainage stack. Since hydraulic jump obstructs the passage of air flow, compressed air will flow upward from the bottom of the stack. FLUENT is employed to simulate this phenomenon, and GAMBIT is also employed as the associated software with FLUENT. For this drainage research, 2-dimensional simulation is employed and the related grids are prepared by GAMBIT for simulation. The following represents a typical case of an installed drainage system, and to be simulated by means of CFD in this research.

The system consists of a single stack with 100 mm diameter and is 5.5 m in height. There is no ventilation pipe connection along the stack and, water falls from the top of stack.

The flow volume is approximately 2.5 L and formed by 2 half ellipse as shown in figure 4.1, with major axis of 200mm in length ( $a = 200$  mm) and the minor axis is 95 mm ( $b = 95$ mm). The water volume is assumed to fall along the wall of stack and the smallest air core is 5 mm in diameter of water volume.

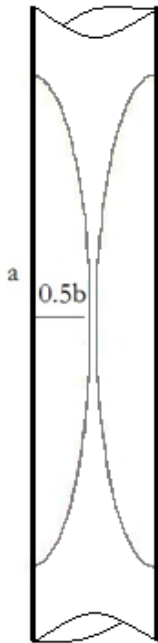


**Figure 4.1 shows water volume in drainage stack**

This is a 2-dimensional case. Assume the third dimension unit length is 1 m, water volume  $V_{\text{water}} = 1/4 \times \pi \cdot ab \times 1\text{m}$ , stack volume  $V_{\text{pipe}} = d \times 1\text{m} \times L$ ,  $L$  is length of drainage stack. Real volume of stack volume is circular shape so that real pipe volume  $V_{\text{real-pipe}} = 1/4 \times \pi d^2 \times L$

Since  $V_{\text{water}} : V_{\text{pipe}} = V_{\text{real-water}} : V_{\text{real-pipe}}$ ,

$$\begin{aligned} \text{Get } V_{\text{real-water}} &= V_{\text{water}} \times V_{\text{real-pipe}} / V_{\text{pipe}} \\ &= 1/16 \times \pi^2 \cdot ab \cdot d \end{aligned}$$

$$\text{Flow rate} = V' = V_{\text{real-water}}/0.5 = 1/8 \times \pi \cdot a^2 \cdot b \cdot d$$

$$= 1/8 \times \pi \cdot 0.2^2 \cdot 0.095 \cdot 0.1 = 0.00235 \text{ m}^3/\text{s} = 2.4 \text{ L/s}$$

$$\text{From equation 1.1 and 1.2, terminal velocity} = V_t = 10.08 \left( \frac{q_w}{d} \right)^{2/5} = 10.08$$

$$\left( \frac{0.0024}{0.1} \right)^{2/5} = 2.3 \text{ m/s and terminal drop distance for the terminal velocity } L_t =$$

$$0.1706 V_t^2 = 0.1706 (2.3)^2 = 0.9 \text{ m. For a water volume of 5 L/s, } V_t \text{ is 3 m/s and}$$

$$L_t \text{ is 1.5 m.}$$

The worst scenario is considered for this simulation, at which the terminal velocity does not exceed 4 m/s. The falling time of the water volume is also set accordingly during the simulation. Assume the initial velocity of the water volume is zero and the friction is set to be positive corresponding to the size and falling velocity of the water volume, the friction force of pipe and gravity force are balanced when the terminal velocity is set to be 4 m/s.

Assume the relationship between friction ( $F_f$ ) of internal wall of drainage stack to maximum velocity ( $V_{\max}$ ) is  $F_f = k V_{\max} = mg$ , then

$$k = \frac{mg}{V_{max}} = \frac{9.8 \text{ m}}{4}$$

$$\begin{cases} \text{When } t = 0, v = 0 \\ dv = \frac{mg - F_f}{m} \cdot dt = \left( g - \frac{kv}{m} \right) \cdot dt \end{cases}$$

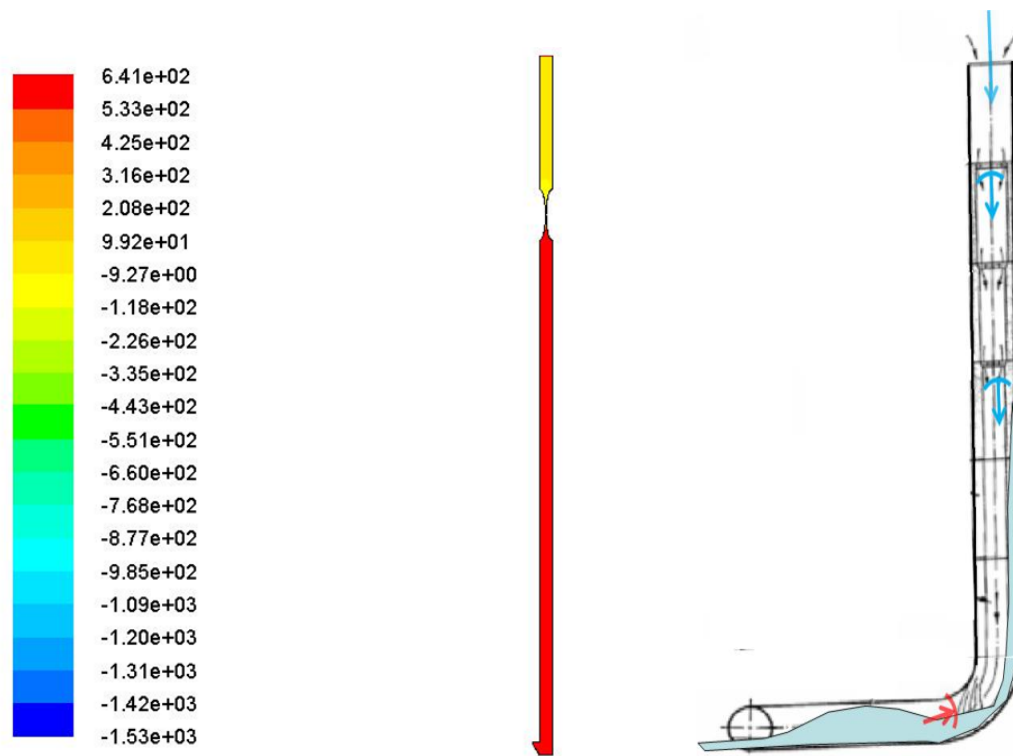
$Dv = (9.8 - 2.45 \cdot v) \cdot dt$ , by integration, a velocity equation becomes,

$$V = 4 \cdot (1 - e^{-2.45t}) \text{ m/s}$$

The velocity of the initial fall is zero and the maximum velocity is 4m/s (normally is approximately 3m/s when water flows down along the surface of drainage stack). These are applied to the computer simulation. A number of iterations have been run over. For this 5.5m height drainage stack simulation, it covers 30000 grids as prepared by GAMBIT. As the time step is very small,  $5 \times 10^{-4}$  second is used as time steps and, several iterations have been conducted.

Overall air pressure distribution could be observed from figure 4.2 and the hydraulic jump was set as shown in figure 4.3. Result shows that pressure distributions vary with time, as indicated in figure 4.4. Four peaks of negative air pressure could be observed from FLUENT simulation result. Step effect of air pressure at the centre core of water volume (figure 4.4) at time  $t = 0.5$  second

is found to be -220 Pa, the least negative value; at  $t = 1$  second, air pressure is -350 Pa; at  $t = 1.3$  seconds, air pressure is -360 Pa and at  $t = 1.5$  seconds, air pressure is -380 Pa.



Contours of Static Pressure (pascal) (Time=5.0000e-01)

Figure 4.2 shows air pressure distribution inside the drainage stack when water volume has fallen 0.5 second

Figure 4.3 shows 100 mm dia. x 5.5 m height drainage stack. Noted that hydraulic jump obstruct 80% air passage in horizontal pipe.

The result demonstrates a high air velocity in the air core of water volume. As step effect is shown to change the air pressure within discharge volume at different velocity and also different height of stack as well as time, the air pressure at different height of the stack and time should be adjusted.

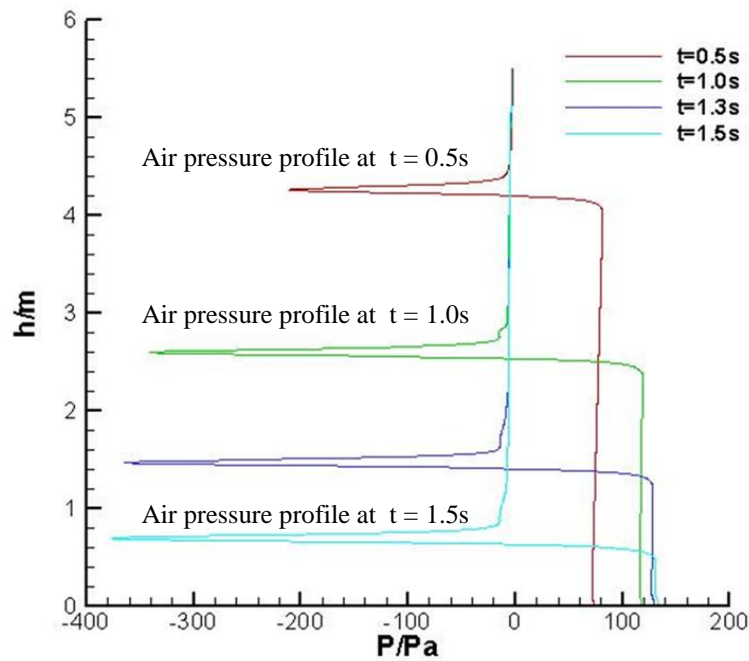
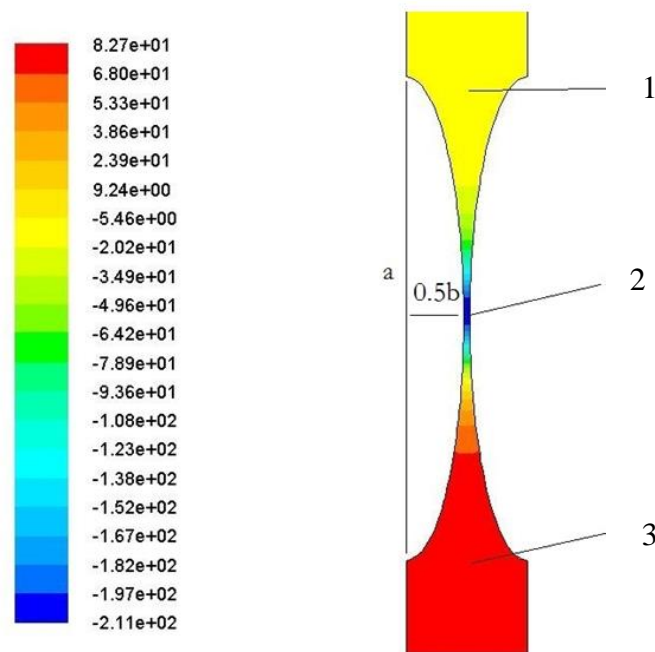


**Figure 4.4 shows different air pressure profiles at different height, different time inside water volume.**

While simulation is conducted on the water volume that falls in a single volume, the water volume could be regarded as undertaking continuous flow which results in different pressure profiles with step effects.

From figure 4.4, a continuous flow could be observed and the effect on pressure is identified from 3 water volumes at 0.5 second, 1.0 seconds and 1.5 seconds.

In actual discharge, the flow pattern should be a continuous flow and the size of volume blocks should be uneven, rather than blocks of water volume with fixed size as assumed in simulation. From figure 4.5, air pressure at zone 2 is the least because the air velocity is extremely high and this agrees with the Bernoulli's principle.



Contours of Static Pressure (pascal) (Time=5.0000e-01)  
ANSYS FLUENT 12.0

Figure 4.5 shows air pressure distribution details near water volume at  $t = 0.5$  second. There are 3 pressure zones. Zone 3 is higher air pressure and Zone 1 is lower pressure zone

Air pressure at zones 3 and 1 are higher because the flow velocity within these zones is lower. Both of the zones encounter changes on air volume in the stack and the air pressure profile for the water volume could be identified. Air pressure at zone 2 in the stack is just a step value rather than an air pressure profile. Grid size of zone 2 is 0.25mm for x direction and 5 mm for y direction, and the time unit is 0.001 second. There are over 30,000 grids in the profile and 4 hours are needed for the iteration process. Since there are 3 simulated water volumes in steps, air pressure values at the steps could be extracted from successive pressure profiles in figure 4.4.

At  $t = 0.5$  second, air pressure of water volume 1 ( $V_{0.5}$ ) at zone 1 is  $P_{1-1} = -10\text{Pa}$ , and at zone 2  $P_{1-2} = -210\text{Pa}$  at, and at zone 3  $P_{1-3} = 90\text{Pa}$ ; By the step effect, at 1 second, the air pressure of water volume 2 ( $V_{1.0}$ ) at zone 1 is  $P_{2-1} = P_{1-3} = 90\text{Pa}$ ; at zone 2  $P_{2-2} = P_{2-1} + \Delta P_{2-21} = -240\text{Pa}$ ; and at zone 3  $P_{2-3} = P_{2-1} + \Delta P_{2-31} = 220\text{Pa}$ . Similarly, at  $t = 1.5$  seconds, air pressure of water volume 3 ( $V_{1.5}$ ) at zone 1 is  $P_{3-1} = P_{2-3} = 220\text{Pa}$ ; at zone 2  $P_{3-2} = P_{3-1} + \Delta P_{3-21} = -150\text{Pa}$ ; and at zone 3  $P_{3-3} = P_{3-1} + \Delta P_{3-31} = 360\text{Pa}$ ; In air pressure profile diagram, 4 points (air



pressure Pa, height m) could be located, they are  $(-10, 4.9)$  ,  $(90, 3.5)$  ,  $(220, 1.7)$  and  $(360, 0.35)$  as plotted on figure 4.6.

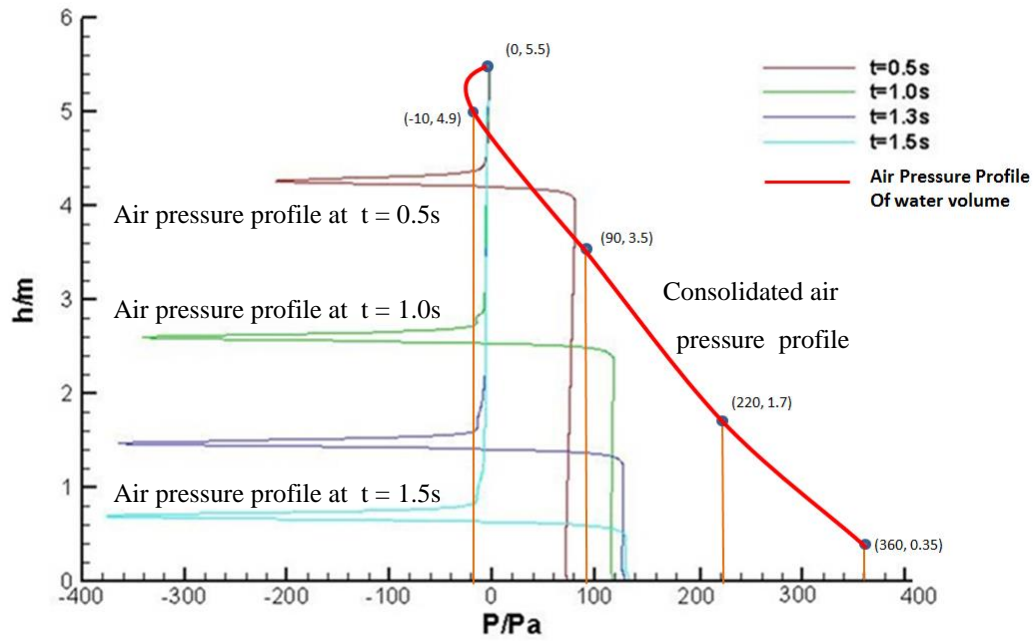


Figure 4.6 shows air pressure profile of water discharge volume

The trend equation could be identified from the regression:

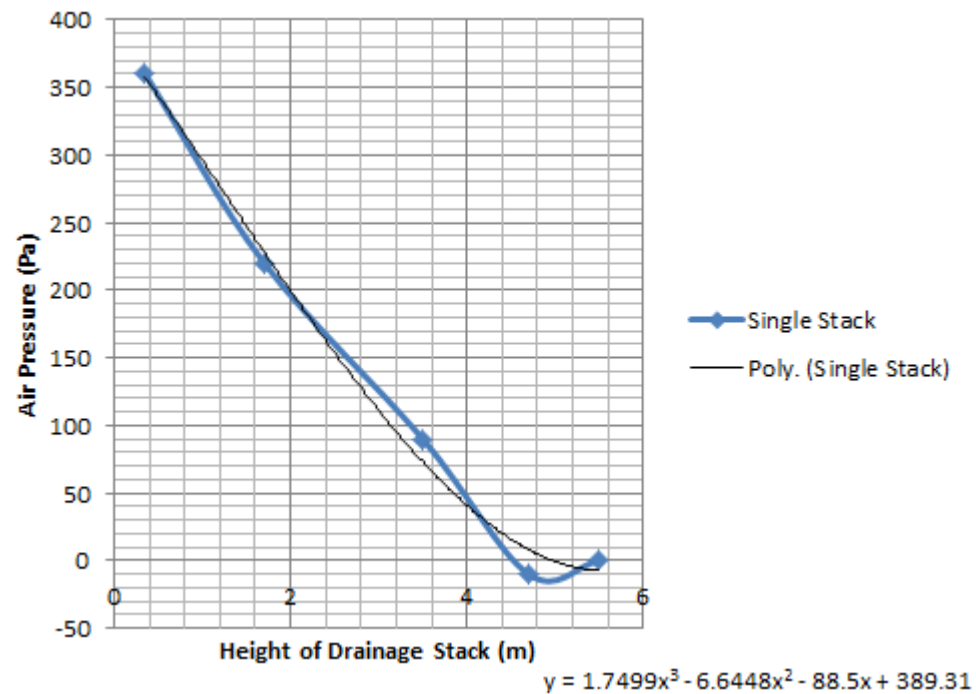


Figure 4.7 shows regression method to find a trend equation of air pressure

From the regression equation in figure 4.7, when  $x$  (height of drainage stack) = 0, air pressure is 389 Pa. Air pressure at the bottom of stack has been found. There are 5 points available to plot the completed air pressure profile. They are

$(-10, 4.9)$  ,  $(90, 3.5)$  ,  $(220, 1.7)$  ,  $(360, 0.35)$  and  $(389, 0)$

A complete air pressure profile is simulated as followed.

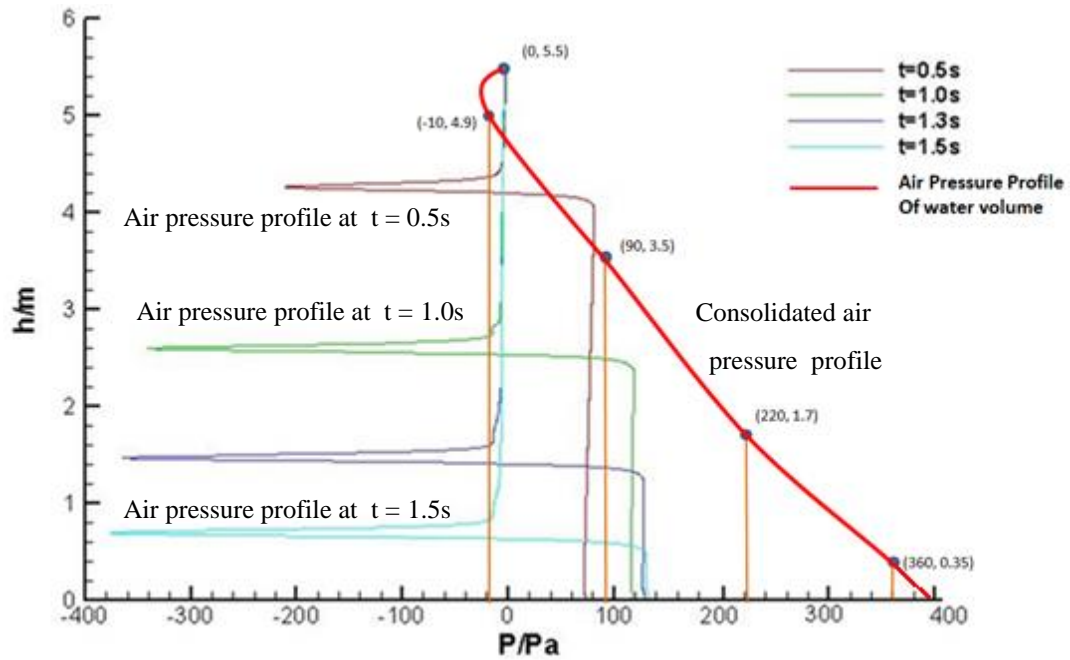


Figure 4.8 shows a simulated air pressure profile of drainage stack.

This research provides an innovative method to obtain the air pressure profile by CFD simulation using Fluent software. It is two-dimensional and also more convenient to handle while the required simulation time is more than 10 hours (when time step is set to be  $5.0e-4s$ ). 20 iterations are needed and 3000 time steps from 0s to 1.5s are simulated.

In addition to the air pressure contour, air velocity vectors could be observed from CFD simulation results as well. The information on air flow direction and the magnitude are particularly useful.

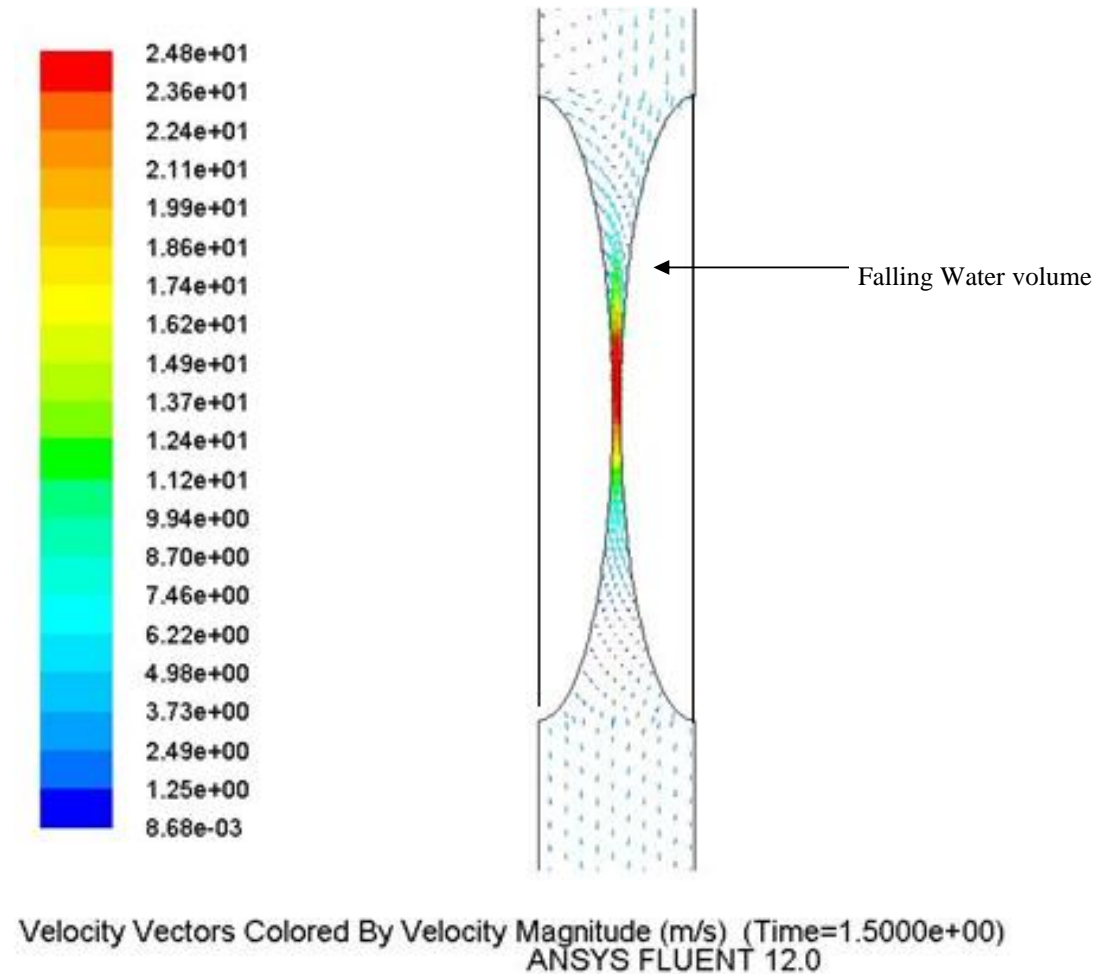
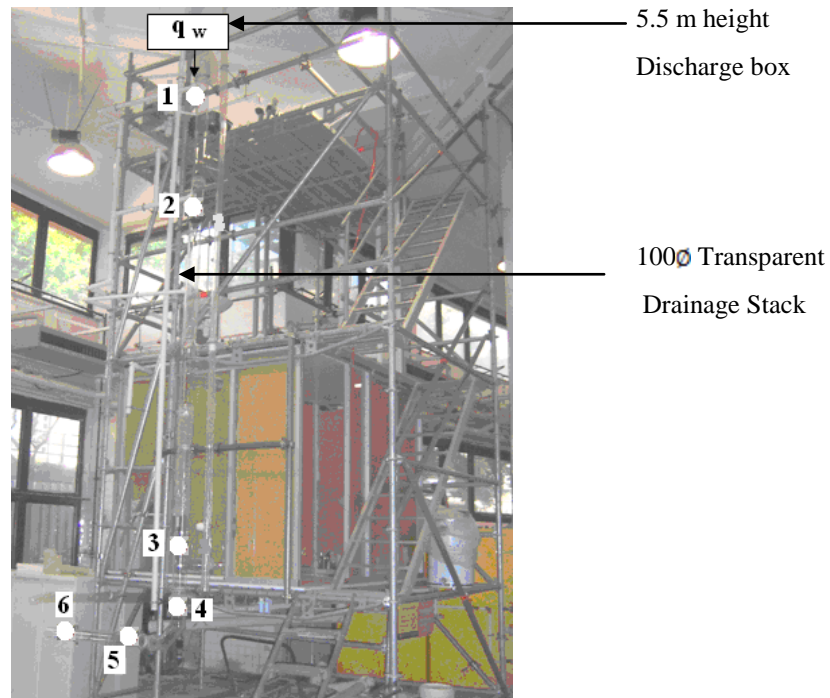


Figure 4.9 shows air vectors in the stack. Red colour arrows represent high velocity and blue colour is lower velocity.

#### 4.2.2 Data verification for CFD simulation in drainage research rig

For the field measurement conducted at the Hong Kong PolyU Drainage Research Rig (figure 4.10 in the next page), pressure sensors (WIKA) were installed at various measurement points as indicated in figure 4.11, and the data was logged by the ADAM controller connected to a computer. This experiment demonstrates an on-site testing and commissioning method to assess the air pressure profile of a drainage stack. One set of data is obtained by specifying a water discharge of 2.5 litre/s in continuous flow from the top of the stack. The water source for this demonstration is a tank located at the ceiling which is 5.5 m above the toe of the stack. Air flow was extracted from the centre of the stack.



**Figure 4.10** Air pressure measurement points 1~6 are installed along transparent 100 dia. drainage stack and horizontal pipe in HKPU drainage research rig

Between points 1 to 4, a typical pressure profile (air pressure in Pa against height m) is obtained and shown in Table 4.1, at which the air pressure is found to be negative at the discharge point and positive at the toe of the stack and, this is the location with maximum value. Point 5 locates at the crown of hydraulic jump and the air pressure is less than that of point 4. It shows that air could not pass through the hydraulic jump (point 5) via a fully opened cross-sectional area of the horizontal pipe but only via a largely reduced cross-sectional area due to the jump, while the largest positive pressure occurs at a location near point 4

(See figure 4.10). Pressure at point 6 is determined based on the air velocity of horizontal flow.

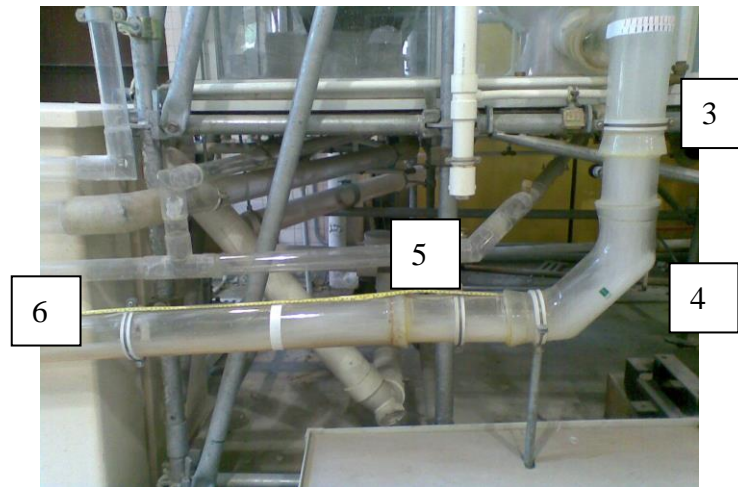


**Figure 4.11** Hydraulic jump occurs when vertical and horizontal speeds are different, trapping air at the bend

Discharge down flow  $q_w = 2.5 \text{ L/s}$

11Point	Air pressure (pa)	Height (m)
1	-50	4.7
2	50	3.6
3	200	0.9
4	390	0.3
5	80	0.05
6	140	0.04

**Table 4.1** Experiment data record in the PolyU Drainage Research Rig

The air pressure value is the mean value obtained from 3000 values (1 reading per second as set at ADAM and recorded for 5 minutes in the computer). 4 points are selected to verify simulation results and shows in Figure 4.12.

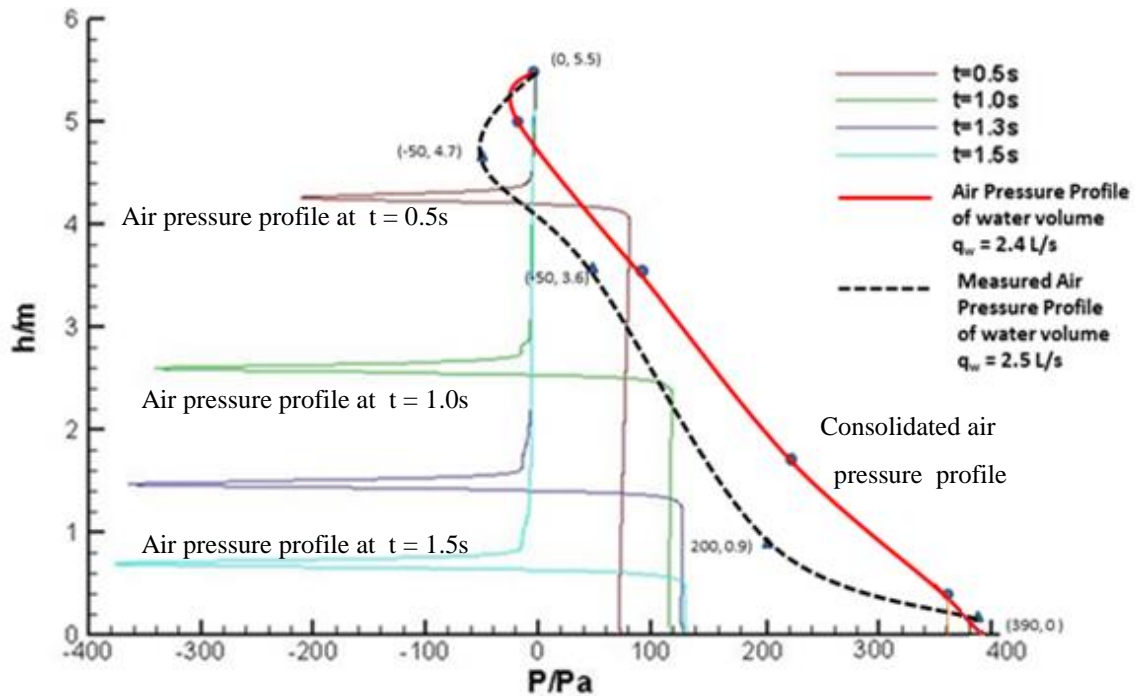


Figure 4.12 shows comparison between 2 air pressure profiles between 2 discharge flows. Red profile is estimated to 2.4 L/s flow rate and Black profile is 2.5 L/s discharges from top of stack.

Frankly speaking, using FLUENT for drainage air pressure assessment is a relatively new approach and the simulation in this research is a small scale exercise. Although more investigation is still being carried, and the method will be further developed for stacks in higher storeys to get more reference data for the real applications. Meanwhile, numerical investigation has been prepared in earlier stage. It is found that the flow in a drainage stack could be approximated as a one-dimensional process. With the assistance from drainage research



platforms, data obtained from numerical investigation evaluate the applicability and feasibility of mathematical models for drainage stack air pressure prediction.

### **4.3 Numerical Assessment - Mathematical model of Air Pressure in Drainage Stack**

Numerical assessment study is a traditional route for years and many respective researchers have developed and contributed their efforts in building service engineering problems. The Saint Venant equations, derived in the early 1870s by Barre de Saint-Venant, were possibly obtained through the application of control volume theory to investigate velocity, pressure and density of drainage air (Sleigh et al. 1998).

#### **4.3.1 St Venant Equations**

To simulate the air flows in drainage pipes or stacks, Swaffield and Jack (2004) developed a model based on St. Venant equations, which are commonly adopted to obtain numerical solutions of air flow inside the stack (Swaffield and Jack 2004). At a particular location along the stack, the air flow rate is considered as a function of time.

At first, the flow variables are considered to be function of space and time considered as a function of space and time. These variables are used in the equations of continuity and momentum which are based on below assumptions:

- ♦ The flow is one-dimensional
- ♦ Hydrostatic pressure prevails and vertical accelerations are negligible
- ♦ The resistance effects follow Manning's equation.
- ♦ The stack air flow is compressible.

As shown in Figure 4.13, using infinitesimal element analysis, we have

$$Q_2 - Q_1 = \frac{\partial}{\partial t}(\rho A \delta x)$$

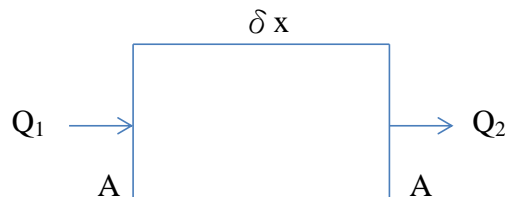


Figure 4.13 Schematic for equation of continuity

Where  $\partial Q = (\rho \partial u + u \partial \rho)$ . A, because product of  $\partial u$  and  $\partial \rho$  is neglected.

$\partial u$  and  $\partial \rho$  are the changes of velocity and density respectively in the infinitesimal element of stack length. A is the stack sectional area assumed to be a constant.

After some algebraic manipulation, the continuity equation could be written as

$$\frac{\partial \rho}{\partial t} + \rho \frac{\partial u}{\partial x} + u \frac{\partial \rho}{\partial x} = 0 \quad (\text{eq 4.1})$$

For the momentum equation, applying the 2<sup>nd</sup> law Newton to the infinitesimal length of stack pipe, we have

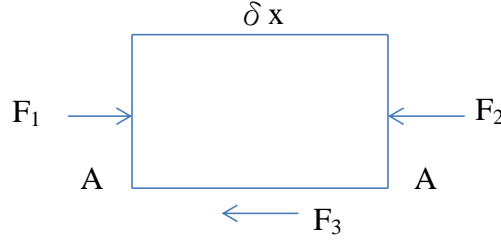


Figure 4.14 Schematic for equation of momentum

This means,  $F_1 - F_2 - F_3 = \rho A \delta x \frac{du}{dt}$

where  $F_1 = pA$  and  $F_2 = (p + \delta p)A$  where  $p$  is the pressure forces and  $F_3 (= \tau P \delta x)$  is shear force.  $P$  is wetted perimeter ( $A/P = D/4$ ),  $\tau = 1/2 f \rho u^2$ . Therefore, for the momentum equation, its partial differential form could be written as

$$\frac{\partial p}{\partial x} + \rho u \frac{\partial u}{\partial x} + \rho \frac{\partial u}{\partial t} + \frac{4 \rho f u |u|}{2D} = 0 \quad (\text{eq4.2})$$

where  $\rho$  is density of air,  $x$  is space coordinate,  $u$  is air velocity,  $D$  is the diameter of stack and  $f$  is a function of location and discharge variables. These are the equations for the prediction of drainage stack air pressure. By using a

numerical grid method, simulations with different boundaries and conditions could be carried out, as reported by Swaffield and Jack (2004).

#### 4.3.2 One-Dimensional Characteristic Lines

In a drainage stack, air pressure varies dynamically, since any small disturbance in the stack can spread at sound speed (Rotty, 1962).

The St Venant equations described in the above subsection cannot be solved explicitly except by making some simplified assumptions which are generally unrealistic for most situations. Therefore, numerical techniques have to be used. One useful and related convenient technique is one-dimensional characteristic line method, which is briefly introduced below.

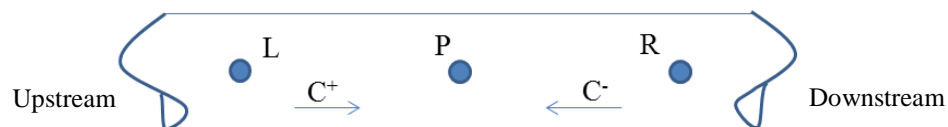


**Figure 4.15 shows movement of air caused by water discharge, 2 transients exist at same time but in opposite direction**

As illustrated in figure 4.15, there are two characteristic lines, which are denoted by  $C^+$  and  $C^-$ .  $C^+$  runs from point L to point P, and  $C^-$  runs from point L to point P. If  $x$  is space coordinate,  $t$  is the time, the two characteristic lines  $C^+$  and  $C^-$ , plotted as functions of  $x$  and  $t$ , are shown in figure 4.16

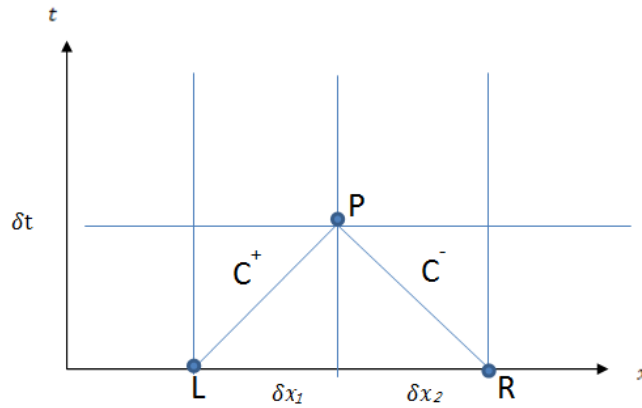


Figure 4.16  $C^+$  and  $C^-$  form 2 characteristic lines

At the time level  $t = t^n$ , at the points L and R, the velocity and pressure are known. The two characteristic lines can be simply described by  $\frac{dx}{dt} = u \pm c$ .

Hence, at the time level  $t^{n+1} = t^n + \delta t$ , the velocity and pressure at point P can be obtained by using property of characteristic line: there is an invariant along each line. Using characteristic lines and relevant initial and boundary conditions, the numerical solutions can be obtained.

.

An example, as seen in Figure 4.17, is demonstrated, the values of flow variables at the point 10 can be calculated by interpolating the characteristic lines.

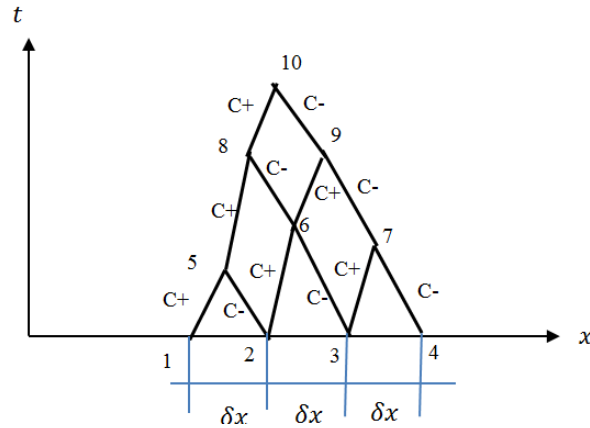


Figure 4.17 points are obtained by characteristic lines C+ and C-

In the next subsections, a new mathematical model's validation and application potential will be presented. Some related content could be found in the Ref. (Li, Wong and Zhu, 2013b).

#### 4.3.3 Mathematical Model – Characteristic Line Method (CLM)

In this subsection, a new mathematical model is presented. It is useful for predicting stack air pressure of high-rise buildings as reported elsewhere (Wong, et al., 2013a; Li et al., 2013b). This model can be treated as an appropriate extension of the St. Venant-equation model.

In the new model, step function used to describe the influence from the entrained air flow from branch pipes and an additional term are introduced to represent the gas-liquid interphase interaction of the flow. It also represents the top and base effects at the stack. Based on this model, a time-splitting based characteristic line method (TSCLM) is used to solve the governing equations. The calibration provides possible values of model parameters by using the data measured by Zhang and Chen (2006) in a real scale high-rise building test platform (HBTP) with constant water flow from branch pipes. The effects of the additional terms and the stack top and bottom conditions can be investigated numerically. The spatio-temporal evolutions of velocity and pressure are presented and discussed as follow.

The new model can predict the drainage stack base-top effects so that the stack air pressure in the HBTP can be validated and predicted.

#### 4.3.4 Governing Equations & Application on BDS

As reported in a relevant study (Wong, et al., 2013a), any small disturbance could propagate the air at sound speed. As reported by Rotty (1962), the

propagation depends on air pressure and density. Inside a building drainage system, even the small pressure disturbances induced by water discharge, the gas-liquid phase interaction at the pressure disturbances, and the base conditions of the stack could influence the propagation of air inside the stack, leading to pressure fluctuations. The water discharge draws air from branch pipes into the stack, which creates an entrained air flow. The base effect at the stack leads to a rise on mean air pressure and a reduced gas flow speed, and possibly results in a reverse gas flow at the base region. These air flow behaviours in the stack could be described by the conservations of mass and momentum.

Following the approach suggested by Swaffield and Campbell (1992a, 1992b), it is assumed that the water flow in the vertical stack is annular and so, the air flows in the stack core for convenient modeling. The friction factor describes the viscous damping mechanism of the air flow when the air flow speed is larger than the terminal speed of the discharged water. There is an accelerating effect when the air flow speed is lower than the terminal speed. The discharged water could result in an air entrainment from the branch pipe into the stack. Considering the stack air pressure to be one-dimensional and unsteady, and



assuming the pressure variation is thermodynamically isentropic, the air pressure in the stack (  $p$  ) could be represented by  $p/\rho^\gamma = \text{Const}$  , where  $\gamma = C_p / C_v = 1.4$  which is the ratio of specific heat at constant pressure to the specific heat at constant volume, and  $\rho$  is the air density. Stack range is defined as  $x \in (0, H)$  , where  $H$  is the building height. Based on the conservation of mass and momentum on the stack air flow within a building drainage system, as reported in Refs (Wong, et al., 2013a, Li et al., 2013b), the governing equations of the stack air flow should be

$$\frac{\partial \rho}{\partial t} + \frac{\partial q}{\partial x} = 0 \quad (\text{eq 4.5})$$

and

$$\frac{\partial y}{\partial x} + \frac{\partial (q^2 / \rho + p)}{\partial x} + \frac{4f}{2D} \frac{q^2}{\rho} + f_1 \rho v = 0 \quad (\text{eq 4.6})$$

while the mass flow rate is

$$q = \rho(u + v) = \rho[u + \sum_k v_k S(x - x_k)] \quad (\text{eq 4.7})$$

The water discharged from a branch pipe located at  $x_k$  results in a gaseous entrainment at a speed of  $v_k(x_k)$ . The step function  $S(x-x_k)$  has a value of zero when  $x < x_k$ , and equals to unity when  $x \geq x_k$ . It reflects the effect of discharged water, as seen in figure 4.19(a), with the total entrained air speed  $v = \sum_k v_k S(x-x_k)$ . Different from the St. Venant equations, an additional parameter  $f_1$  is introduced in equation 4.6 to take into account the complex interphase interaction and also the stack base effect. Defining the top of stack as  $x = 0$ , and the time step in simulation as  $\Delta t$ , if the stack base has relatively significant effect on the air motion when  $x > H_1$ , the  $x$ - dependent parameter  $f_1$  may be expressed by

$$f_1 = \begin{cases} -\frac{\sigma_1}{\Delta t} \cdot \frac{x}{x_N}, & \text{for } x \in [x_1; x_N]; \\ 0, & \text{for } x \in [x_1; H_1]; \\ -\frac{\sigma_0}{\Delta t} \cdot \frac{x - H_1}{H - H_1}, & \text{for } x \in [H_1; H]; \end{cases} \quad (\text{eq 4.8})$$

where  $\sigma_0$  and  $\sigma_1$  are model parameters for adjusting air flow velocity. Eq. 4.8 indicates that  $f_1$  is assumed to be linear with coordinate  $x$ . The larger the  $\sigma_0$ , the more intensive effect is found for the interphase interaction and stack base. While  $\sigma_1$  should be negative, the branch water discharge can result in the stack

top air flowing downward, causing the stack top air pressure be less than ambient air pressure. Hence, the smaller the  $\sigma_1$ , the larger effect is for the stack top.

When  $\sigma_0 = \sigma_1 = 0$ , the form of governing equations returns to the St Venant type.

The parameter  $x_N$  is used to define the stack top region, its value is assigned with respect to water discharge the high-rise building testing platform (HBTP). The value  $H_1$  is assigned according to the *convenience of numerical validation* which calibrated well with measured data from the study conducted by Zhang and Chen (2006).

The illustration of the entrained air flow speed  $v$ , as well as the terminal speed of water flow  $V_t$ , is provided in figure 4.18.

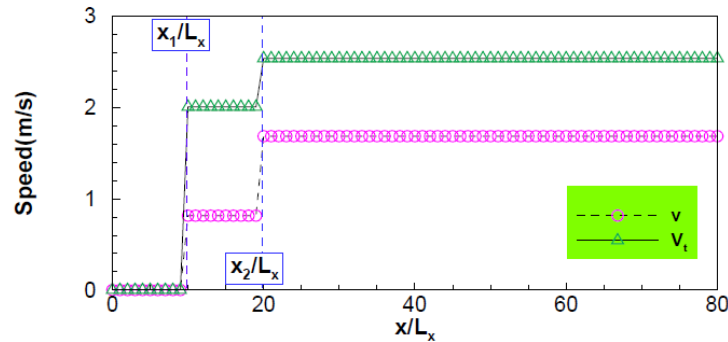


Figure 4.18: Entrained air flow speed  $v$  and terminal speed  $V_t$  for the case of  $Qw(x1) = 2.5$  and  $Qw(x2) = 21/s$ .

$$f = 0.0303(k_s/t_c)^{1/3} \quad (\text{eq 4.9})$$

where  $k_s$  is the roughness of stack wall,  $t_c(= Q_w/4DV_t)$  is the thickness of annular water flow,  $Q_w$  is the water flow rate, and  $V_t$  is the terminal speed of water flow in the stack.  $D$  represents the stack diameter;  $f$  denotes the friction factor of the air flow, which can be calculated by the following according to Jack (1998).

$$V_t = \frac{4.4034}{k_s^{0.1}}(Q_w/D)^{0.4} \quad (\text{eq 4.10})$$

Note that it has not been ascertained on how to give the air entrainment from branch pipe accurately yet, since the air entrainment is related to the gas-liquid interface, and also related to the water flow speed in the branch as well. Therefore, for a convenient numerical verification, a simple approximation is adopted.

The branch water flow is considered to fill the pipe partially, and the cross sectional area of the region filled with water can be expressed as

$$A_b = \frac{D_b^2}{8} (\theta - \sin \theta) \quad (\text{eq 4.11})$$

As shown schematically in figure 4.19, the discharged water carries air from the branch pipe into the main stack, leading to a pressure drop on air at the corresponding locations connected to the branch pipe.

$$A'_b = \frac{D_b^2}{8} (2\pi - \theta + \sin \theta) \quad (\text{eq 4.12})$$

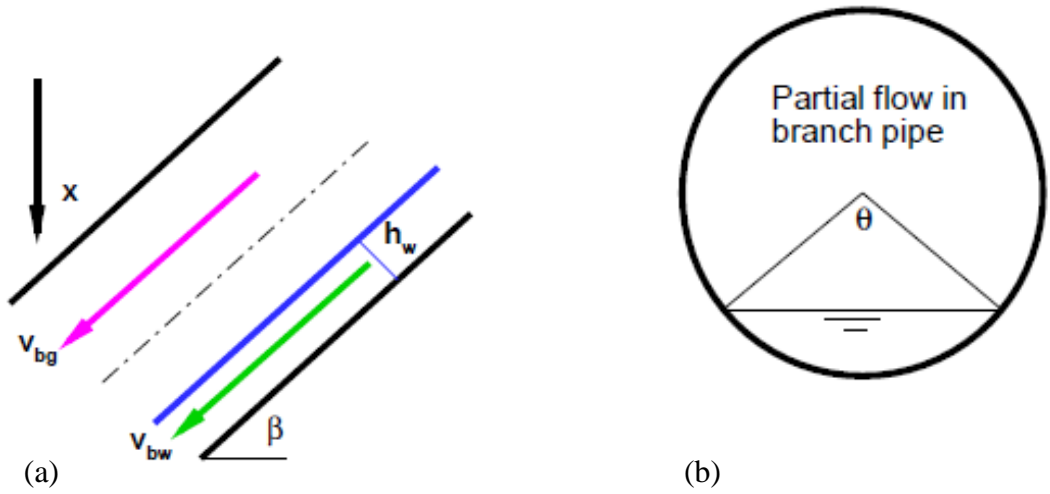


**Figure 4.19: (a) Schematic of the branch discharging, and (b) schematic of partial water flow in a branch pipe. Note that the branch water flow leads to the entrained air in the branch pipe flows into the stack.**

The cross sectional area for the air flow region in the branch pipe is expressed as,

speed  $v_{bw}$  [ Figure 4.19(a)], the velocity  $v_k$  can be approximated as

$$v_k = 4 \left( \frac{A'_b}{A_b} \right) Q_w(x_k) \sin(\beta) / (\pi D^2) \quad (\text{eq 4.13})$$

The inclined angle  $\beta$  is used together with angle  $\theta$  to determine the entrained air flow rate. The initial air speed  $u$  and relative air pressure in the stack are both assumed to be zero.

The intermediate height  $H_1$  indicates a partition which divides the stack into the upper part and the lower base part. The base part of the stack is stagnant for the air flow, leading to an increase on mean air pressure in the lower base part. Since the top and the base parts are respectively associated with the model parameter  $\sigma_1$  and  $\sigma_0$ , a time splitting based characteristic line method (TSCLM) can be utilized for air pressure prediction, which will be described in details in the following sections.

#### 4.3.5 Numerical Method

The air pressure inside a building stack is usually calculated by seeking the solutions of the St Venant equations by characteristic line method. The previous studies have implicitly considered the effect of air entrainment by imposing proper boundary conditions. However, the present governing equations (eqs 4.5 - 4.6) have explicitly reflected the effects on the stack air pressure  $p$  due to the water discharge process, as well as the interface interaction and the stack base condition. The mass balance of gaseous flow in the stack is described in a conservative form.

To predict the air pressure inside the drainage stack by using time splitting algorithm suggested by Abarbnel and Gottlieb (1981), which also suggested by Karniadakis (1991), the governing equations (4.5-4.6) can also be written in the form of Euler equations:

$$\frac{\partial \mathbf{u}}{\partial t} + \frac{\partial \mathbf{F}}{\partial x} = 0 \quad (\text{eq 4.14})$$

at which

$$\mathbf{u} = [u_1, u_2]^T = [\rho, q]^T, \quad \mathbf{F} = [q, q^2/\rho + p]^T \quad (\text{eq 4.15})$$

Together with the additional equations

$$\frac{\partial \mathbf{u}}{\partial t} + \mathbf{S} = 0 \quad (\text{eq 4.16})$$

In which

$$\mathbf{S} = [S_1, S_2]^T = \left[ 0, \frac{4f}{2D} \frac{q^2}{\rho} + f_1 \rho v \right]^T \quad (\text{eq 4.17})$$

The superscript T denotes the matrix transposition. The corresponding Jacobian matrix is as follow, which has two eigenvalues.

$$\mathbf{A} = \begin{bmatrix} a_{11} & a_{12} \\ a_{21} & a_{22} \end{bmatrix} = \begin{bmatrix} \frac{\partial F_1}{\partial u_1} & \frac{\partial F_1}{\partial u_2} \\ \frac{\partial F_2}{\partial u_1} & \frac{\partial F_2}{\partial u_2} \end{bmatrix} \quad (\text{eq 4.18})$$

$$\begin{aligned} a_1 &= \frac{1}{2} \left[ a_{11} + a_{22} - \sqrt{(a_{11} - a_{22})^2 + 4a_{12}a_{21}} \right] = \frac{q}{\rho} - c \\ a_2 &= \frac{1}{2} \left[ a_{11} + a_{22} + \sqrt{(a_{11} - a_{22})^2 + 4a_{12}a_{21}} \right] = \frac{q}{\rho} + c \end{aligned} \quad (\text{eq 4.19})$$

where  $c = \sqrt{\partial p / \partial \rho}$  which is a speed of sound,

According to the previous work by Swaffield et al. (2004), the friction factor  $f$  in the source term (S) has to be negative, if the air flow speed ( $q/\rho$ ) is less than the terminal speed ( $V_t$ ), and the term S has to be positive when  $q/\rho$  is larger than  $V_t$ . The time-splitting based characteristic line method (TSCLM) is detailed and used to solve the Euler-type equations (3.25), and the characteristic line method (CLM) can be used together with the above. Hence, the solutions can be sought as follows:

$$\begin{cases} \left( \frac{q}{\rho} \right)_j = (\zeta_1 - \zeta_2)_j / 2 \\ (c)_j = (\zeta_1 - \zeta_2)_j (\gamma - 1) / 4 \end{cases} \quad (\text{eq 4.20})$$

where  $c$  is the sound speed, and  $\zeta_1$  and  $\zeta_2$  are defined by

$$\zeta_1 = \frac{q}{\rho} + \frac{2c}{\gamma - 1}, \quad \zeta_2 = \frac{q}{\rho} - \frac{2c}{\gamma - 1} \quad (\text{eq 4.21})$$



which are respectively the first and second invariance along the characteristic lines:

$$\frac{dx}{dt} = \frac{q}{\rho} + c, \quad \frac{dx}{dt} = \frac{q}{\rho} - c \quad (\text{eq 4.22})$$

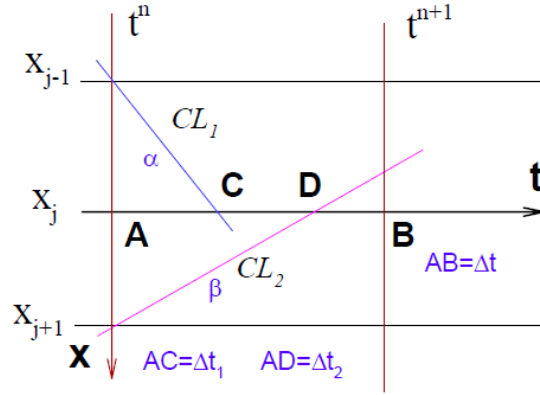


Figure 4.20: Schematic of CLM, Point B is solved by characteristic line CL<sub>1</sub> and CL<sub>2</sub>

Let  $\zeta_1 = \alpha, \zeta_2 = \beta$ , In fact, we see that along the characteristic line CL<sub>1</sub>:  $\alpha = \text{Const}$ , while for characteristic line CL<sub>2</sub>:  $\beta = \text{Const}$ . As shown schematically in Fig.4.20, we have

$$\alpha_B = \alpha_A + \Delta t / \Delta t_1 (\alpha_{j-1} - \alpha_A)$$

$$\beta_B = \beta_A + \Delta t / \Delta t_2 (\beta_{j+1} - \beta_A), \text{ where}$$

$$\Delta t = 0.988 \Delta x / M_1,$$

$$\text{Where } M_1 = \max_{\text{for all } j+1/2} (a_1 + a_2)$$

and

$$\Delta t_1 = \Delta x / (u_{j-1} - c_{j-1}),$$

and

$$\Delta t_2 = \Delta x / (u_{j+1} - c_{j+1}),$$

Noted that  $a_1$  and  $a_2$  are two eigenvalues of Jacobian matrix  $A$  given by equations 4.18 and 4.19. Therefore, equation of 4.20 can be arrived.

Based on equation (4.16), the time splitting algorithm indicates that the following equations can be applied to further improve the accuracy of the solution.

$$\begin{cases} \frac{\partial p}{\partial t} = 0 \\ \frac{\partial q}{\partial t} = -\frac{4f}{2D} \frac{q^2}{\rho} - f_1 \rho v \end{cases} \quad (\text{eq 4.23})$$

Assume the ambient pressure and density are respectively  $p_0$  and  $\rho_0$ , let

$$A = \sqrt{\gamma p_0 / \rho_0}, \quad A_1 = 1 + \Delta t \cdot \frac{4f}{2D} \left( \frac{q}{\rho} \right)_j, \quad \text{it is seen that}$$

$$\begin{cases} \rho_j^{n+1} = \left[ \frac{(c)_j}{A} \right]^{2/(\gamma-1)} \\ q_j^{n+1} = \frac{1}{A_1} \left[ \rho_j^{n+1} \left( \frac{q}{\rho} \right)_j - \Delta t (f_1 v)_j \frac{\rho_j^n + \rho_j^{n+1}}{2} \right] \end{cases} \quad (\text{eq. 4.24})$$

where  $(c)_j$  and  $\left( \frac{q}{\rho} \right)_j$  are the CLM-based solutions of Euler-type equations as given by Eq. (4.20).

The boundary conditions are stated as the following. At  $x = 0$ , we assume

$$\rho(0) = \rho_0, \quad q(0) = 0 \quad (\text{eq. 4.25})$$

At  $x = H + L_x$ , the relative pressure and mass flow rate can be expressed by

$$\begin{cases} P(H + L_x, t) = (p - p_0)/10 \\ \quad \quad \quad = b_0 + b_1 \cos[2\pi c_0 t / (H - H_1) + \phi] \\ q(H + L_x, t) = q(H, t) \end{cases} \quad (\text{eq. 4.26})$$

where  $b_0$  is the time-averaged bottom pressure, and  $b_1$  is the magnitude of bottom pressure fluctuation.  $\phi$  is the phase angle, and  $c_0 (= \sqrt{\gamma p_0 / \rho_0})$  is the speed of sound under ambient condition. The CLM method can be used afterwards, to predict the values of  $\rho$  and  $q$  at  $x = H$  can be predicted.

The time-splitting based characteristic line (TSCLM) method described in the foregoing section is used to predict the gaseous pressure in a drainage stack installed at a high-rise building testing platform with 17 floors, and the flow rates of water discharged from the branch pipes are set to be constant. As shown in figure 4.21, the measured stack air pressure and its peak values (suggested by Zhang and Chen 2006) are referred to calibrate the model parameters such as  $\sigma_0$ ,  $\sigma_1, \beta, b_0$ , and  $b_1$

For the experiment conducted at the high-rise building test platform encompassed by Zhang and Chen (2006) in Shiga of Japan, the experimental data was recorded in 2006; and the relevant calibration on the apparatus was conducted with reference to the Japanese standard given by the Engineering Societies there. The air pressure was measured by pressure sensors VPRN-A3 of VELCOM. Using the digital signal transmitter 9B02 of COLIN with a filter of 3 Hz, the collected pressure signals were recorded by the data logger OMNIACE-RT3424 of COLIN. The calibrated parameter values are given in Table 4.2, where  $\theta_k$  are the discharging angles at  $x_k (k = 1, 2)$ , and the values

of other parameters such as the stack roughness and diameters are also given.

observed that the use of parameter  $\sigma_1$  during computation can definitely make of average pressure curve (and also the pressure peak curves) closer to the measured data at the top region of the stack. The peak pressure values are expected to be  $P_{av} \pm \sqrt{2}\sigma_p$  where  $P_{av}$  and  $\sigma_p$ , are respectively the time-average pressure and its root-mean square value, because the approach of peak value prediction is absolutely correct if the stack air pressure oscillates in a harmonic mode.

$P_0 = 1.0 \times 10^5 \text{ Pa}$	$\rho_0 = 1.25 \text{ kg/m}^3$
$\gamma = 1.4$	$k_s = 1 \text{ mm}$
$L_x = 0.56 \text{ m}$	$D = D_b = 100 \text{ mm}$
$x_1/L_x = 10$	$x_2/L_x = 20$
$Q_w(x_1) = 2.5 \text{ l/s}$	$Q_w(x_2) = 2 \text{ l/s}$
$\theta_1/\pi = 0.55$	$\theta_2/\pi = 0.5$
$b_0 = 10 \text{ mmH}_2\text{O}$	$b_1 = 45 \text{ mmH}_2\text{O}$
$\beta/\pi = 1/9$	$\emptyset = 0$
$\sigma_0/\Delta t = 0.01$	$\sigma_1/\Delta t = -0.05$
$H_1/L_x = 60$	$x_N = x_2$

**Table 4.2: Parameters used in the numerical analysis.**

Figure 4.21 shows the comparison of pressures with experimental data. The differences in between are mainly due to the stack air pressure due to the top and base effects, and also the gas-liquid interphase interaction. The St Venant equations can just be taken as a simplified model in predicting the air pressure inside building drainage stack system.

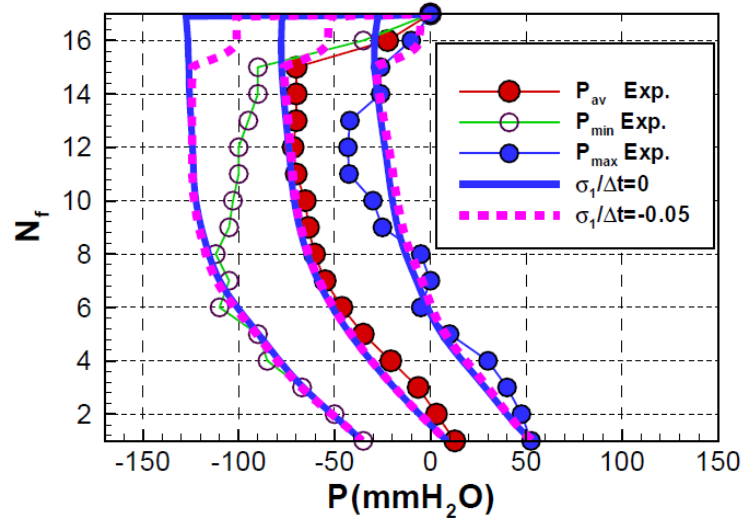


Figure 4.21: Comparison of air pressures with experimental data. The peak pressures ( $P_{min}$ ,  $P_{max}$ ) are calculated by  $P_{av} \pm \sqrt{2} \sigma_p$ , where  $\sigma_p$  denotes the root mean square value of the pressure fluctuation. The number of floor is calculated by  $N_f = (H - x) / (10Lx) + 1$ , where  $H$  denotes the building height,  $Lx = 0.28\text{m}$  represents the length scale used in the simulation. Air pressure unit is  $\text{mmH}_2\text{O}$  is same as 10 mBar

The potential of the present model can be further recognized by observing the parameters' sensitivity in the proposed mathematical model, and the spatial and temporal evolutions of air pressure and velocity in the stack, which will be discussed in details in the subsections below.

#### 4.3.6 Sensitivity Factors to $\sigma_0$ and $\beta$

As discussed in previous sections, the sensitivity of numerical solutions to the two parameters  $\sigma_0$  and  $\beta$  can be explored by comparing the distribution of time-averaged relative pressure and the pressure peaks plotted as functions of the number of floors  $N_f = 1 + (H - x)/(10L_x)$ . The effect of the velocity-adjusting parameter ( $\sigma_0$ ) on the distribution of peak pressures can be observed in figure 4.22, while the values of other parameters are listed in Table 4.2. As observed from figure 4.22,  $\sigma_0$  is the dominant parameter for the time-averaged pressure distribution in the stack. The larger the value of  $\sigma_0$ , the smaller the pressure peak values, and this indicates that  $\sigma_0$  can be used as a key parameter during the calibration of stack air pressure.

The distribution of peak pressure can also be influenced by branch entrainment, which depends on angle  $\beta$  when angle  $\theta_k$  takes the values as given in Table 4.2. Figure 4.23 shows that angle  $\beta$  has a significant impact certainly, when accounting the stack air pressure and its peak.



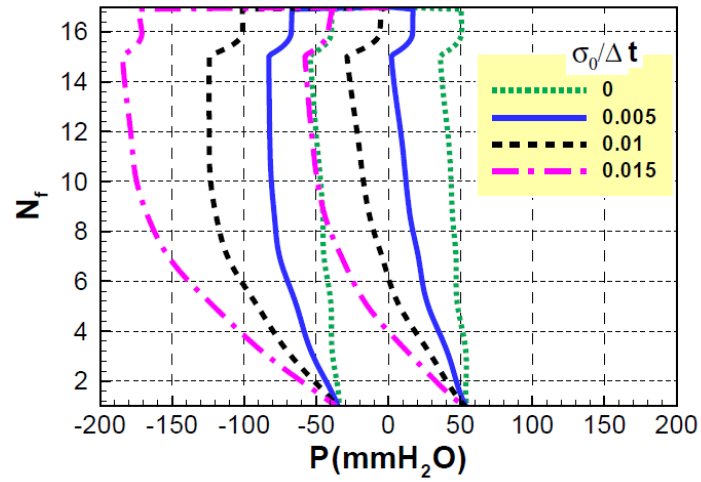


**Figure 4.22: Parameter  $\sigma$  effect on predicted peak pressures in the stack**

The suction pressure increases with the increment of  $\beta$ , which indicates that the stack pressure is sensitive to the air entrainment from branch pipes.

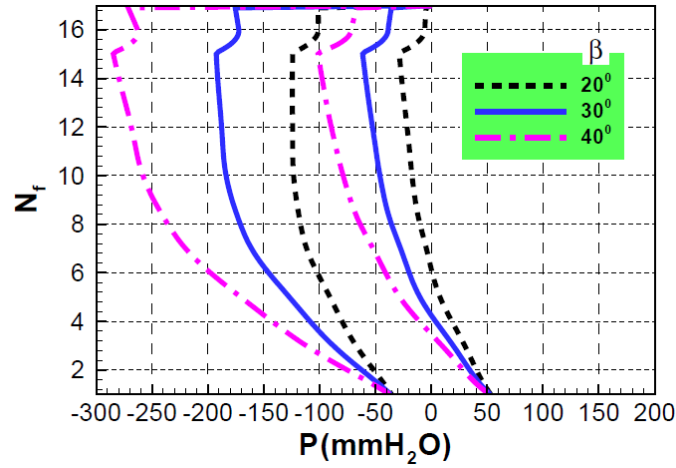


Figure 4.23: Parameter  $\beta$  effect on predicted peak pressures in the

#### 4.3.7. Evolutions of velocity and pressure

The distributions of time-averaged peak pressures in the stack are closely related to the velocity and pressure evolutions in the stack, as shown in figures 4.22 and 4.23. Using the parameters listed in Table 4.2, the simulation can incorporate a temporal evolution of pressures at two locations within the stack, as illustrated in figure 4.24(a). For  $t > 1$ , the time-dependent pressure fluctuates approximately in harmonic and quasi-periodic waves, while the time-average value and the oscillation amplitude are evidently depend on the stack location  $x/L_x$ . The time period of pressure fluctuation is approximately  $H/c_0$ . Since the pressure oscillation is quasi-periodic, as shown in figure 4.21, the peak pressures can be

approximated by multiplying the root mean square of pressure fluctuation

$\sigma_p$  with a factor of  $\sqrt{2}$  because it is clear that  $\frac{1}{2\pi} \int_0^{2\pi} (\sin \gamma)^2 d\gamma = \frac{1}{2}$ .

Corresponding to the pressure fluctuation given in 4.24(a), the velocity fluctuation history in the time range of  $t \in (1, 5)$  is shown in figure. 4.24 (b).

According to entrained speed  $v$  given in figure 4.18 with respect to the blue-curve, the total velocity  $q/p$  at the bottom of the stack would have a positive peak velocity of about 2.0 m/s. With respect to the dashed-black curve, at the location of  $x = H_1$ , the minimum value of  $q/p$  velocity is closed to - 1.0m/s.

Approximately the harmonic and quasi-periodic fluctuating behaviour can also be found in the speed  $u$ -evolutions. Figure 24 also reveals that the pressure peak corresponds to  $u$ -velocity valley at a given location, and vice-versa.

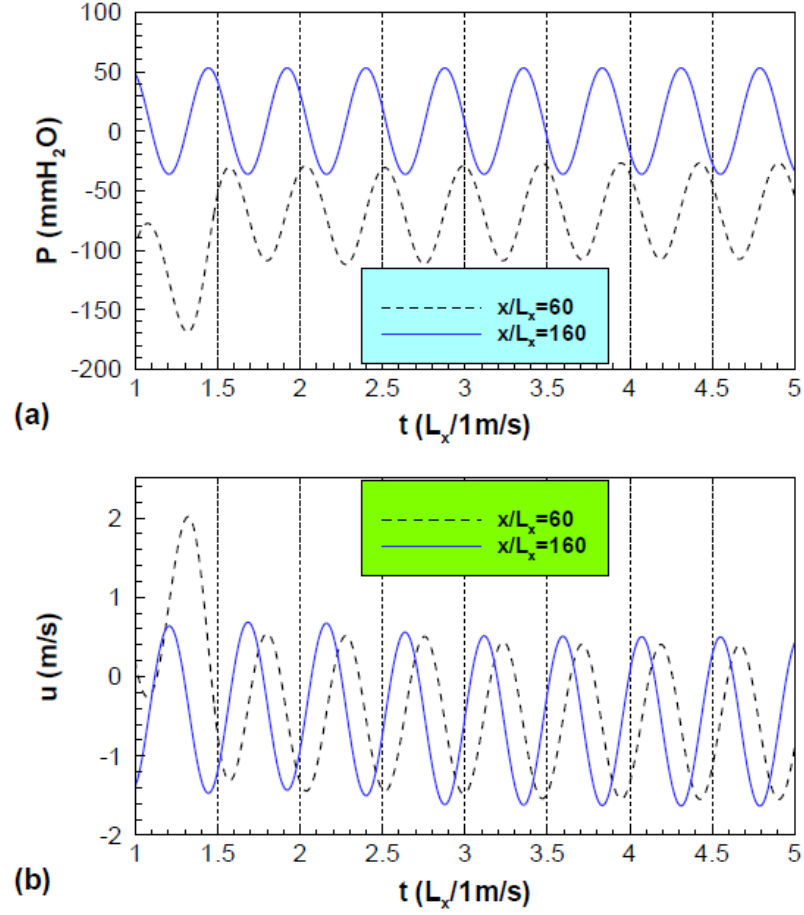


Figure 4.24: Evolutions of pressure  $P$  (a) and velocity  $u$  (b) at different locations in the building stack.

The spatiotemporal evolutions of pressure and velocity are shown in figures 4.25-4.26. Both figures are shown in a *flood* mode. Using the calibrated parameter  $\sigma_v/\Delta t = 0.01$ , the air entrainment leads to a decrease of stack air pressure  $P(x, t)$ , as shown in figure 4.25.

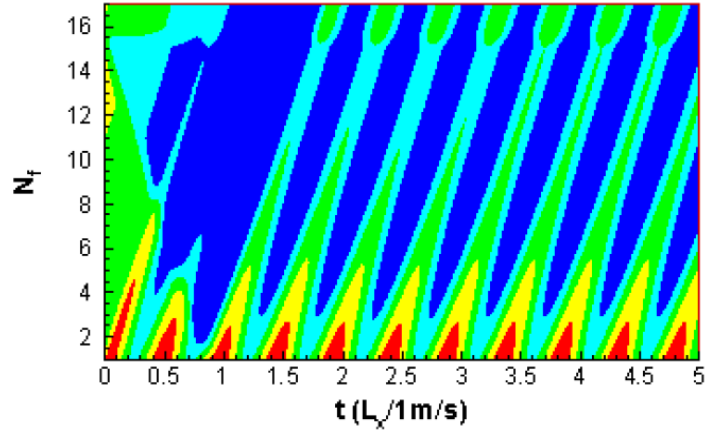


Figure 4.25 Spatiotemporal evolution of pressure in the time range of  $t \in (0, 5)$ . Note that the pressure contours are labeled by -60, -30, 0, and 30mmH<sub>2</sub>O. For the blue color zone,  $P < -60\text{mmH}_2\text{O}$ ; For the cyan color zone,  $P \in [-60, -30)\text{mmH}_2\text{O}$ ; for the green color zone,  $P \in [-30, 0)\text{mmH}_2\text{O}$ ; for the yellow color zone,  $P \in [0, 30)\text{mmH}_2\text{O}$ ; and for the red color zone,  $P \geq 30\text{mmH}_2\text{O}$ .

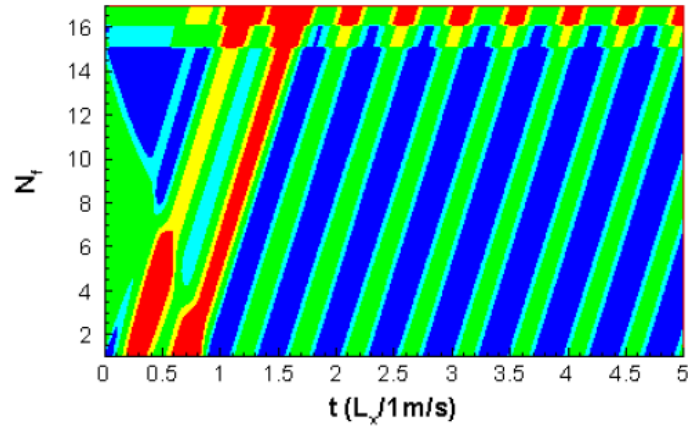


FIGURE 4.26: Spatiotemporal evolution of  $u(x, t)$  in the time range of  $t \in (0, 5)$ . The  $u$  contours are labeled by -0.5, 0, 1, and 1.5m/s.

The pressure is calculated by  $(p - p_0)/10$ , and the unit is mmH<sub>2</sub>O (1 mmH<sub>2</sub>O equals to 10Pa). The absolute pressure  $p$  is calculated by assuming the gaseous

flow to be isentropic, i.e.  $p/\rho^\gamma \equiv \text{Constant}$ . The  $P$  – contours are labeled by -60, -30, 0, and 30, indicating that when  $t > 1$ , the stack air pressure  $P$  varies with the time in a quasi-periodic mode due to the boundary conditions adopted in the calculation. Stack air pressure  $P$  also varies with time in a quasi-periodic mode as a result of the boundary conditions adopted in the calculation. This spatial-temporal  $P$  – evolution indicates the gas flow in the building stack is oscillating under the influences of the branch discharging, gas-liquid interphase interaction, and stack top and base.

Figure 4.26 illustrates the evolution of  $u(x, t)$  ( $= q/\rho - v$ ). The speed  $u$ -contours show that the velocity is generally positive on the floors when  $N_f \leq 15$ , and  $t > 1$ , it is oscillating around zero (m/s), and its value slightly depends on the stack location.

In summary, from the present mathematical and numerical work, it is found that the traditional St Venant equations model can be extended appropriately, so that the stack air pressure can be predicted favorably.

#### **4.4. Comparison between CFD and Mathematical Model**

CFD simulation by FLUENT employs two-dimensional analysis to deal with real discharge scenario in drainage stack, which produces air pressure distribution diagram, air velocity diagram and velocity vector diagram at different time steps. In this research, the air pressure of water volume at  $t = 0$  second, 0.5 second, 1.3 second and 1.5 second are considered and the corresponding air pressure values are obtained. At each time step, there are three water volumes. As the water volume is falling in the stack, the highest air pressure is found at the head of water volume and the lowest is at the rear portion. All of them can be graphically presented. Maximum air velocity can be found in the centre of water volume.

Data measured from the 3-storey drainage research rig generally agrees with the results from simulation. However, the simulation requires a very long duration on calculation not only because of the iteration process, but also the adjustment required to refine the whole simulation model. A typical case is that air pressure can be induced due to the fall of water volume. In the simulation model, falling water volume is separated into different volumes with same size at different

locations inside the drainage stack at different time with different velocity. Air pressure, between the water volumes, is connected to form a pressure profile. In addition, preparation works are required to create the geometry (by using GAMBIT to form grids and to define related simulation boundaries) and the calculation time is extremely long that 20 iterations are needed for each case, and total iteration time requires is longer than 10 hours.

As introduced, N-S equation is adopted in this CFD simulation, thus the flow should match with the assumptions governing the N-S equations. Advanced mathematical theories are applied to develop mathematical model to support the research. CLM method is one dimensional and considers only the movement of air transient. These can speed up the analytical and calculation process. The accuracy can be further improved by considering more details regarding the flow, in particular for the details that are not addressed by the simulation tool adopted in this research.



FORTRAN is a traditional program language which is widely applied in engineering simulation. Users can define the equations and settings according to their own need. The result has to be obtained in different files by this approach, which requires more time to prepare the outcome presentation.

Drainage stack simulation is used to predict air pressure profile for a high rise building. This simulation integrates computation programming and field measurement data on air pressure obtained from real site, to enhance the accuracy of simulation. More flexibility can be gained from the mathematical model. The number of branches in drainage system which undergoes multi-discharge can also be edited to make the simulation agrees more closely to the real situation. The limitation for this research is that more field measurement data from other high-rise drainage rigs is needed to refine the simulation. In our case, the highest research rig in China can provide more testing data for the simulation. In fact, the drainage system installed in most of the real buildings can be served as test rigs to build up more valuable data to form a database. Super-high-rise buildings are easily found in Hong Kong and the drainage

system inside is the best test rig for the simulation research for those super high buildings.

One may ask the reason of carrying out both the CFD simulation and the numerical studies in this research. CFD is relatively easier to be handled by more people for drainage research and therefore, benefits more people. In the coming chapter, the research will focus on the risk abatement by relieving the excess air pressure inside vertical drainage stack by adopting new design, including smart trap connection to prevent dry by evaporation, smart connection of stacks, and also 8S design that is patented and owned by the Hong Kong Polytechnic University. For existing buildings, the model developed in this chapter can be employed to understand the problem of excess air pressure when it occurs. The case in a 18-storey core building of the Hong Kong Polytechnic University, named Li Ka Shing Building, will be presented in chapter 6 to demonstrate how the model can be used for the aid of risk assessment in drainage stack problem. By integrating all of these, the risk management model can be implemented to address drainage failure in buildings.

## **Chapter 5**

### **Control of Air Pressure inside Drainage Stack**

The case investigation in section 2.3.3 of Chapter 2 shows how the drainage system fails to drain away the sewage safely and results in sewerage and foul air backflow to other flats when there is excess air pressure in the stack. The simulation study in chapter 4 offers a tool to predict the air pressure in a stack and hence allows a qualitative anticipation on the risk of failing to drain away the sewerage safely without cross-contamination to other flats. Proper prediction on stack air pressure can also assist the anticipation on the stability of water seals in a trap. As the height of the water seal is typically 50 mm, this also means the air pressure to be exerted onto the water seal in traps should not exceed 5 mBar. Otherwise, foul air or even infectious virus (if any) will travel from the trap to the indoor air.

From the risk management point of view, prevention by enhanced design and problem remedial are both important and should not be neglected. In this chapter,

prevention by enhanced design will be addressed, including the use of a Smart Connection and Smart pipe.

## **5.1 Smart Pipe Connection**

There is no doubt that water discharge will induce air flow inside the drainage stack. Air flows from higher air pressure zone to lower air pressure zone. As water discharge goes downward and its boundary attracts the air from atmosphere to enter the stack via the topmost opening.

### **5.1.1 Usage of ventilation pipe**

A ventilation pipe is critical to drainage discharge system. In the Hong Kong Legislation CAPS 123I, regulation 30 requests every trap should be connected to a ventilation device. The ventilation device should be installed within 300 mm from the trap's outlet to protect stability of water seal. In normal case, water seal is 50mm in height, which can resist an air pressure of 500 Pa. Ventilation pipe is a major device to balance the excess air pressure inside drainage stack. From experience in Hong Kong, a 50 mm diameter ventilation pipe always meet the minimum requirement and is generally regarded as acceptable; while in this

scenario, air pressure can easily exceeds 500 Pa in the drainage stack. In this case, foul air may come out from the stack and contaminate the living space. As a general practice, cross-ventilation pipe should always be provided for every 5 storeys to meet the design requirement. However, such a common practice may not be adequate, especially for the lower floors.

#### 5.1.2 Principle of smart cross ventilation pipe connection

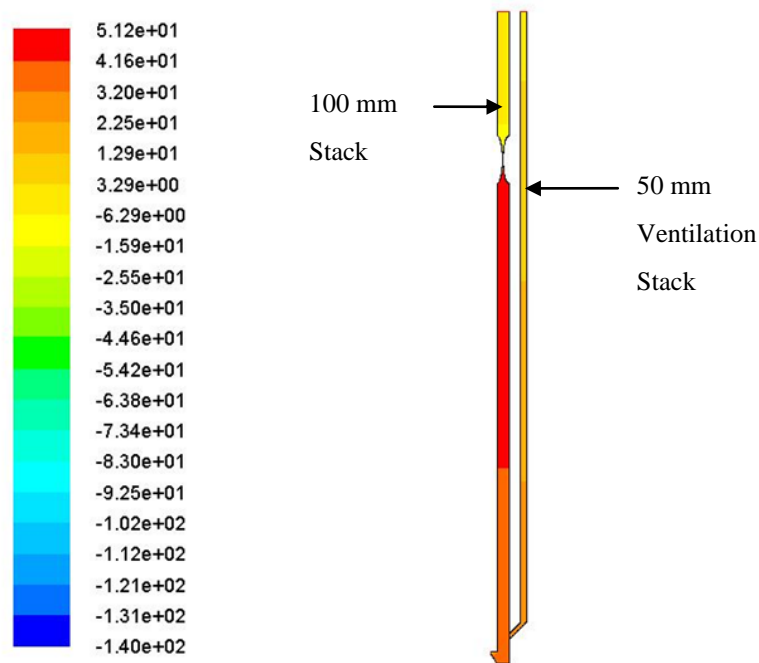
The principle of smart connection is simple with the installation of an additional cross ventilation pipe at an appropriate location of BDS. A demonstration of the effect of a cross ventilation pipe on stack air pressure is performed by FLUENT.

As the number of cross ventilation pipes has increased, loop length of ventilation pipe is shorter which increase air pressure balance inside BDS. Air pressure inside BDS will be decreased.

Using the case in chapter 4 (figure 4.3), the system is single stack system. Water discharge flow rate is 2.4 L/s and the maximum positive air pressure at toe of stack (0.3 m height) is about 400 Pa. FLUENT will be used to prepare different cases for drainage rig of HKPolyU: Case 1 is to install ventilation pipe only, case 2 is to add a cross ventilation pipe near the top of stack and the last case to

install one more cross ventilation at the middle of stack. Different pressure profiles are listed to compare their capacity of air pressure balancing. Obviously, air pressure balance capacity is increasing due to additional provision on cross ventilation to the system. All of them can release air pressure by means of 20 mm passage (suppose hydraulic jump which blocks 80% of 100 drainage pipe).

#### 5.1.2.1 Case 1 –Install ventilation pipe only (time = 0.5 second)



Contours of Static Pressure (pascal) (Time=5.0000e-01)

**Figure 5.1 FLUENT simulates a 50 mm ventilation pipe which installed at the toe of drainage stack to form a one pipe system. Pressure diagram shows air pressure can be released by ventilation pipe.**

Similar to the methodology adopted in Chapter 4, air pressure profile is prepared from four points.

They are points of (-7, 4.9), (52, 3.5), (99, 1.7), (151, 0.35) and (158, 0)

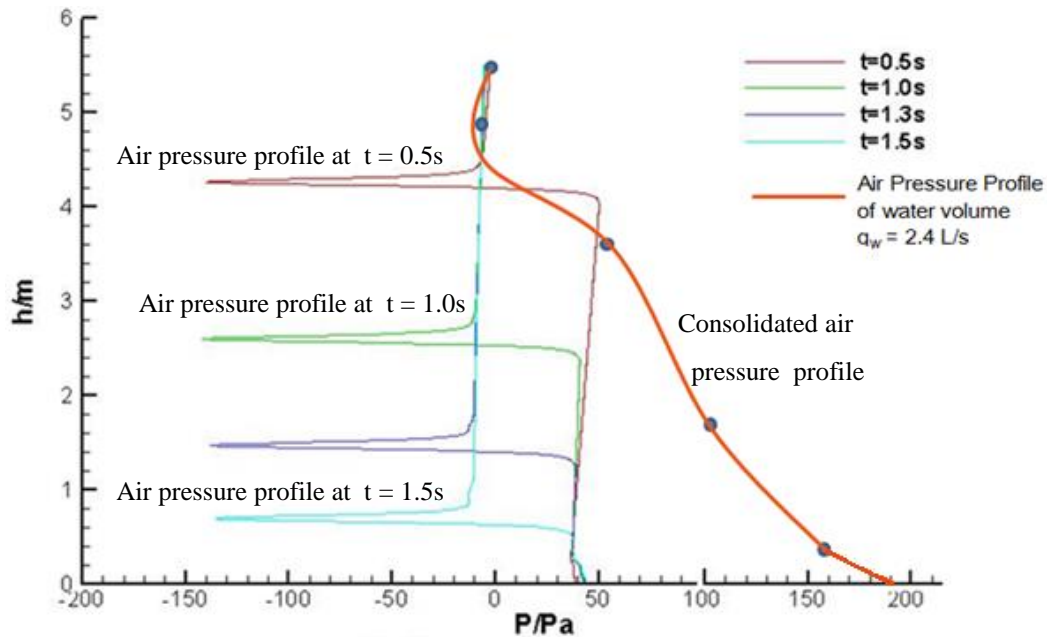


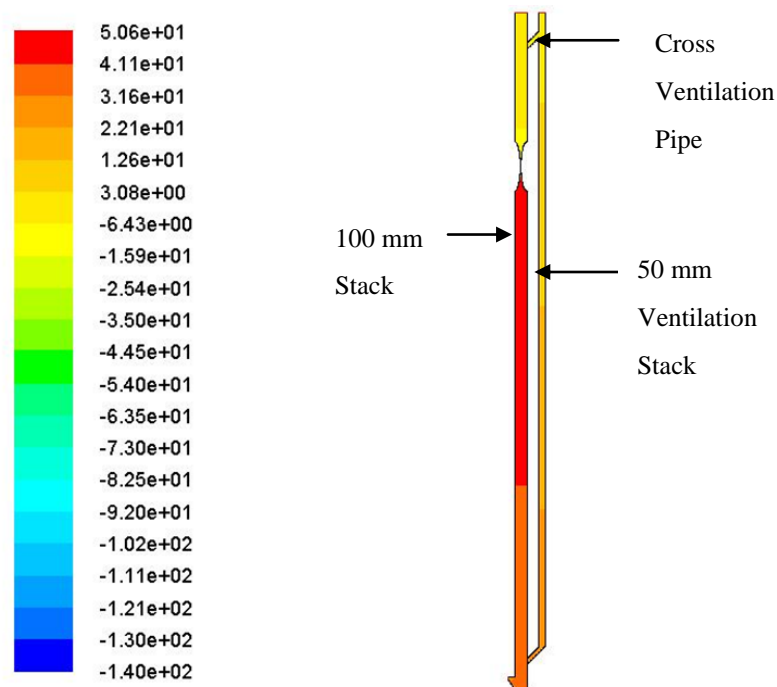
**Figure. 5.2** shows air pressure profile of one pipe system (case 1). It is a large reduction of positive air pressure which is compared with single stack system (figure 4.7)

Simulation will be conducted and more cross ventilation pipe(s) would be provided for an enhancement on design between drainage stack and vertical ventilation stack (similar to the modified one pipe system). Normally, one drainage cross-ventilation pipe will be installed at every 5 storeys and the vertical distance between two cross ventilation pipes is approximately 15 m. For

a better performance on relieving air pressure, the vertical distance will be decreased to 5 m for case 2 and 2.5 m for case 3 as described below.

#### 5.1.2.2 Case 2 – Install cross ventilation pipe to one pipe system (t = 0.5 s)

Case 2 is one pipe system with one cross ventilation pipe, drainage stack is ventilated and form a ventilation pipe circuit.



Contours of Static Pressure (pascal) (Time=5.0000e-01)

**Figure 5.3 shows the one pipe system which is installed a cross ventilation pipe near top of drainage stack**



Similar to the methodology in Chapter 4, air pressure profile for case 2 (figure 5.4) is plotted at four points. They are points (-5, 4.9), (45, 3.5), (93, 1.7), (141, 0.35) and (148, 0).

These points provides a plot on air pressure profile as case 1 and the vertical distance between cross ventilation and toe of ventilation connection is 5 m.

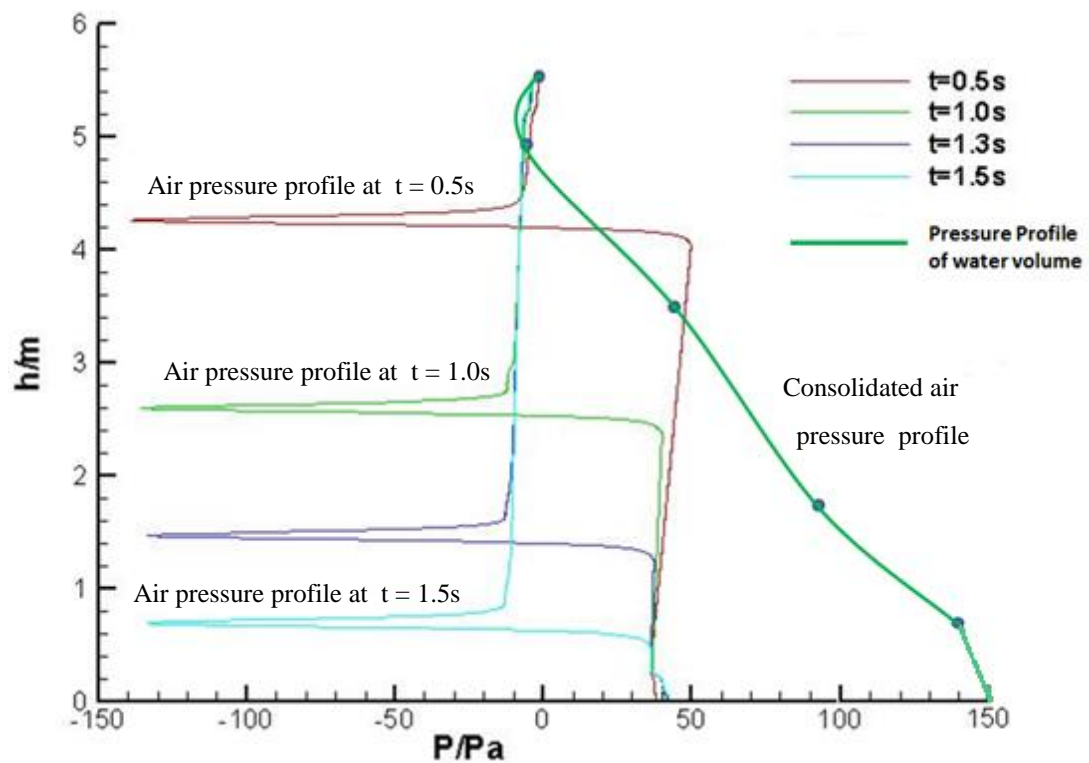
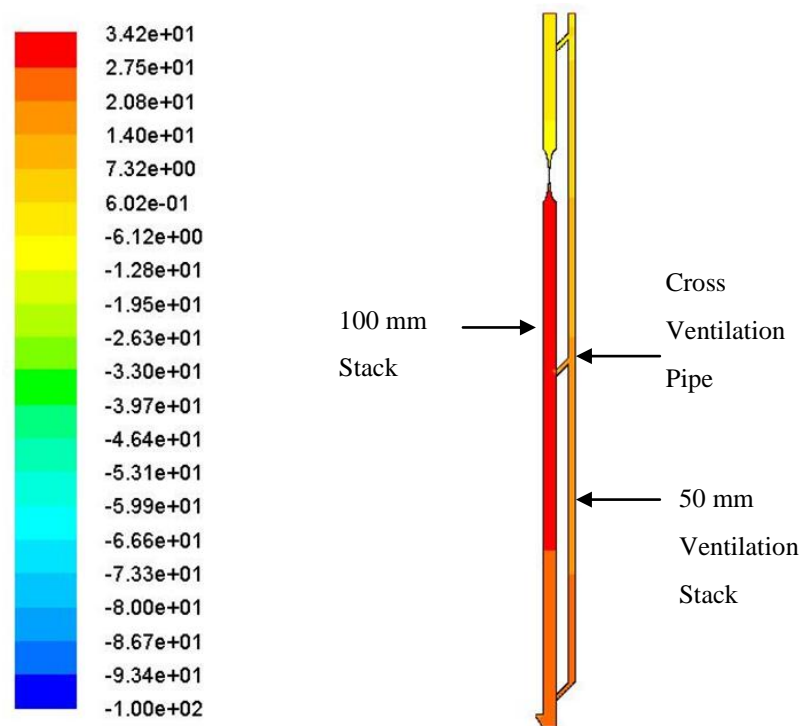


Figure 5.4, air pressure profile of case 2 – one pipe system with one cross ventilation pipe

From the air pressure profile for case 2, air pressure inside the drainage stack decreases slightly when compared with case 1. In case 3, one more cross ventilation pipe is to be added at 2.5 m height level of drainage stack.

#### 5.1.2.3 Case 3 –Install ventilation pipe and 2 cross ventilation pipes (t=0.5s)

for one pipe system



Contours of Static Pressure (pascal) (Time=5.0000e-01)

**Figure 5.5 shows the one pipe system which is installed two cross ventilation pipes near top and middle height of drainage stack (case 3).**

Similar to the methodology in Chapter 4, air pressure profile is plotted from four points. They are points of (-5, 4.9), (30, 3.5), (87, 1.7), (133, 0.35) and (140, 0)

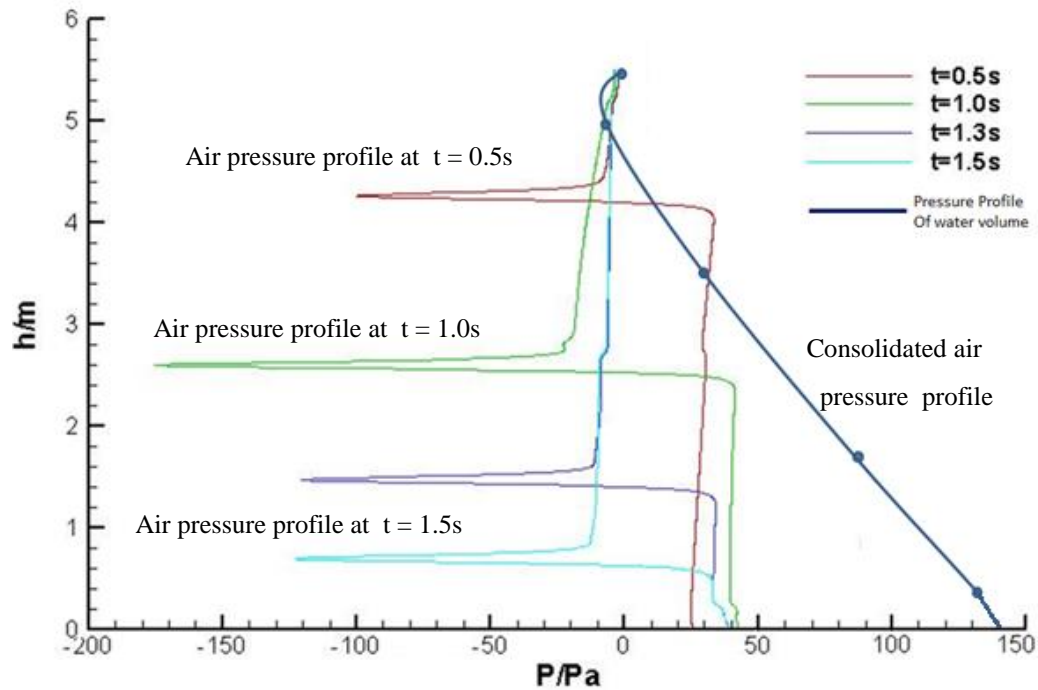
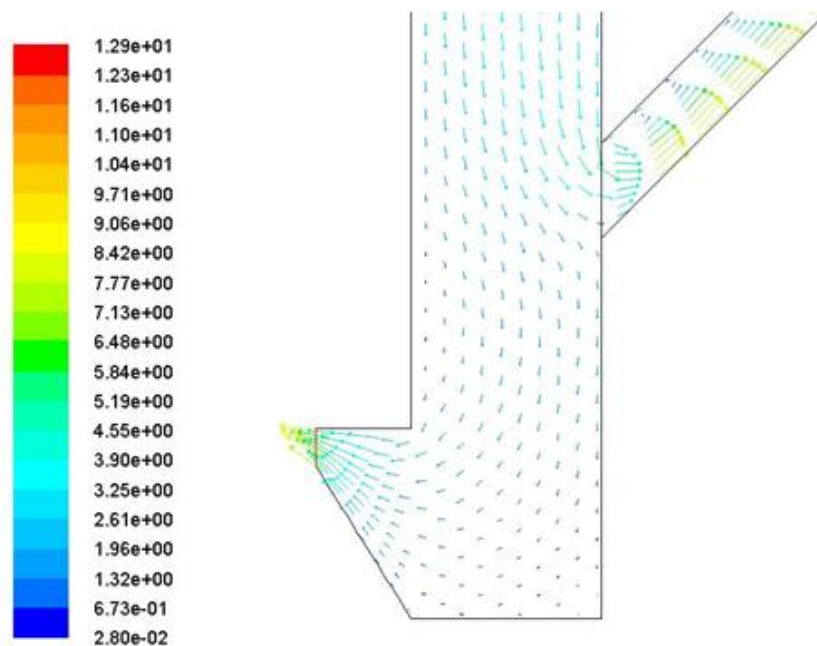


**Figure 5.6, air pressure profile of case 3 – one pipe system with two cross ventilation pipes**

From the air pressure profile of case 3, slight improvement on decreasing air pressure inside the drainage stack is observed, when comparing with case 2.

Based on FLUENT simulation from previous cases, air pressure deduction can be achieved by means of adding ventilation devices.

Once the single drainage stack (without ventilation pipe) becomes one pipe system (ventilation pipe installed), there is a significant decrease for the air pressure inside the drainage pipe. Figure 5.7 shows air velocity vector diagram at toe of the stack and at the horizontal branch pipe.



Velocity Vectors Colored By Velocity Magnitude (m/s) (Time=1.5000e+00)

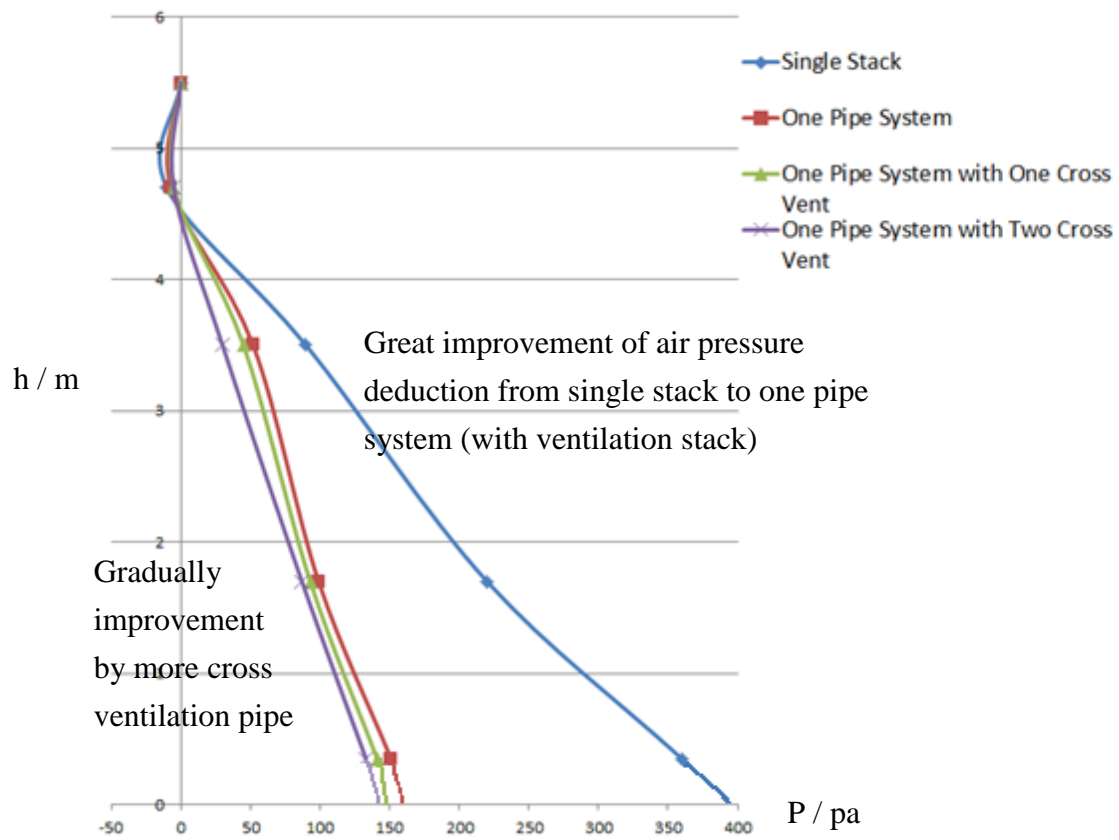
**Figure 5.7 shows the air velocity vector at toe of 100 drainage stack and connect a ventilation pipe**

Figure 5.7 shows that a water volume at 1.5 seconds can release the air pressure at toe of stack by ventilation pipe. This case assumes a 20 mm gap can functions to release air at 100 mm diameter horizontal pipe. For case 2 and 3, cross

ventilation pipes are installed at drainage stack, it shows gradual improvement on decreasing the air pressure of the main stack.

#### 5.1.2 Data verification

Verification of air pressure reduction can be conducted by adding related air pressures into a chart. Smart connection of cross ventilation pipes is applied at suitable position of drainage stack. It solves the problem of excess air pressure effectively.



**Figure 5.8, air pressure profile of different systems are shown, they include single stack, one pipe system, one pipe system with one cross ventilation and one pipe system with two ventilation pipes**

Different ventilation drainage systems are plotted in figure 5.8. A single stack system is the minimal provision for ventilation and drainage stack serves as both a ventilation stack and a water discharge stack. For a one-pipe system, there are two vertical stacks, one is the drainage stack; and another is the air stack which is connected to the toe of drainage stack. A one-pipe system with a cross ventilation pipe provision is a modified one-pipe system. The number of cross

ventilation pipe can be defined as the Density of Cross Ventilation Pipe (DCVP)

as an index at a typical floor. For a single stack system, DCVP is 0.

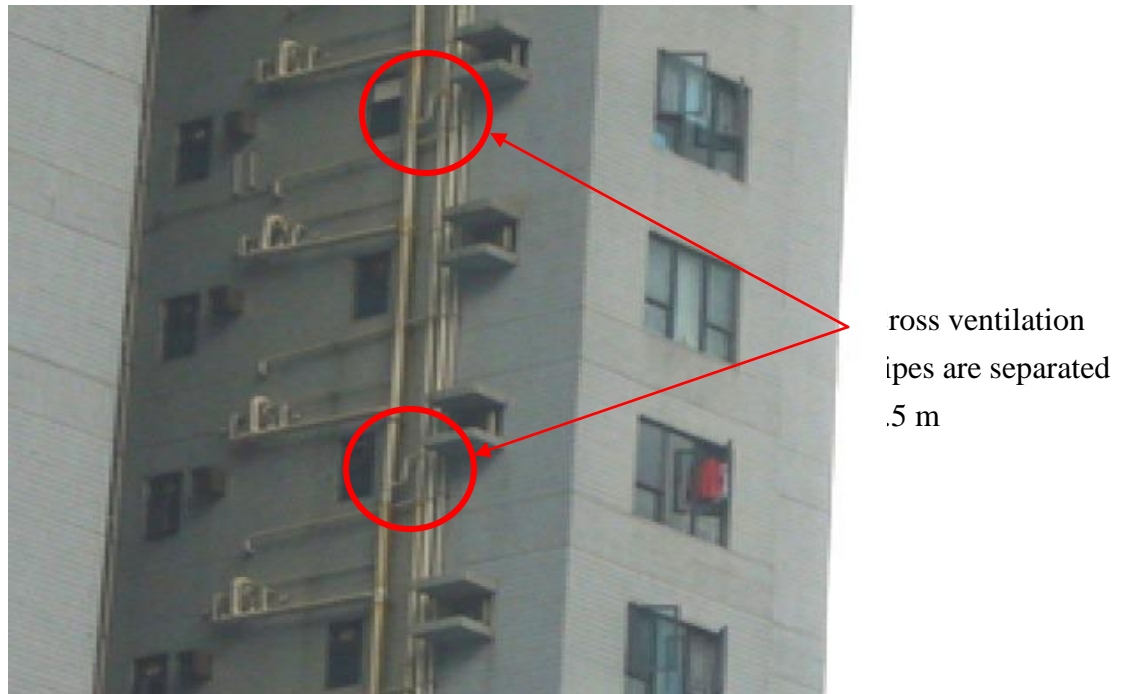


**Figure 5.9, shows a real case that cross ventilation pipes have vertical spacing 5.5 m**

For the installation as shown in figure 5.9, the vertical distance between the cross ventilation pipes is 5.5 m (3 floors), and hence  $DCVP = 1/3$ . From previous simulations, it is no doubt that by increasing DCVP the air pressure problem of BDS can be solved more effectively. Figure 5.10 shows a typical case to reduce the positive air pressure excessively. DCVP is 1 (1 cross ventilation pipe per floor).

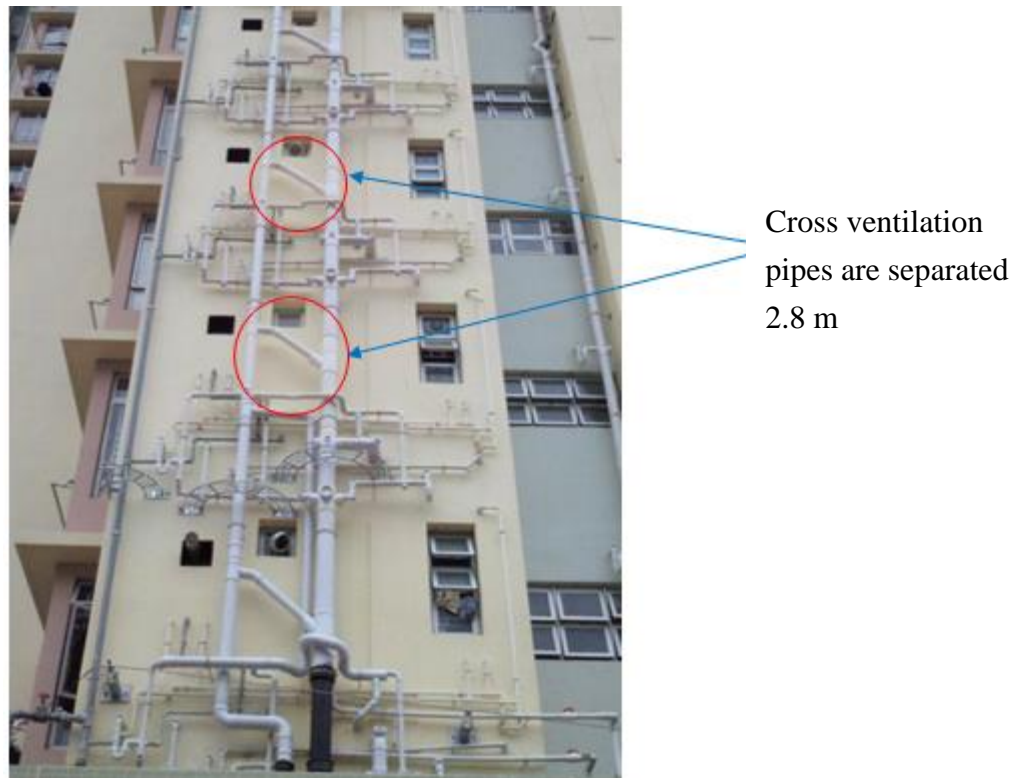


**Figure 5.10, shows a real case that cross ventilation pipes have vertical spacing 2.8 m**

The connection is functional balanced air pressure. However, it is not a popular design today. Although it can improve the performance of air ventilation aid, more pipe works are required. Even though the aged drainage stack is scaled and its internal diameter is reduced, problem of excessive air pressure can still occur. Increase DCVP seems to be a solution to solve air pressure problem but this will occupy more space.



For a special case, if a water closet is found to have a water seal suffering vibration and depletion. A smart connection is suggested to increase its DCVP to 2 (2 cross ventilation pipes per floor). Excessive air pressure accumulation at the water closet can be solved if the discharge point at drainage stack is within the 2 cross ventilation pipe.

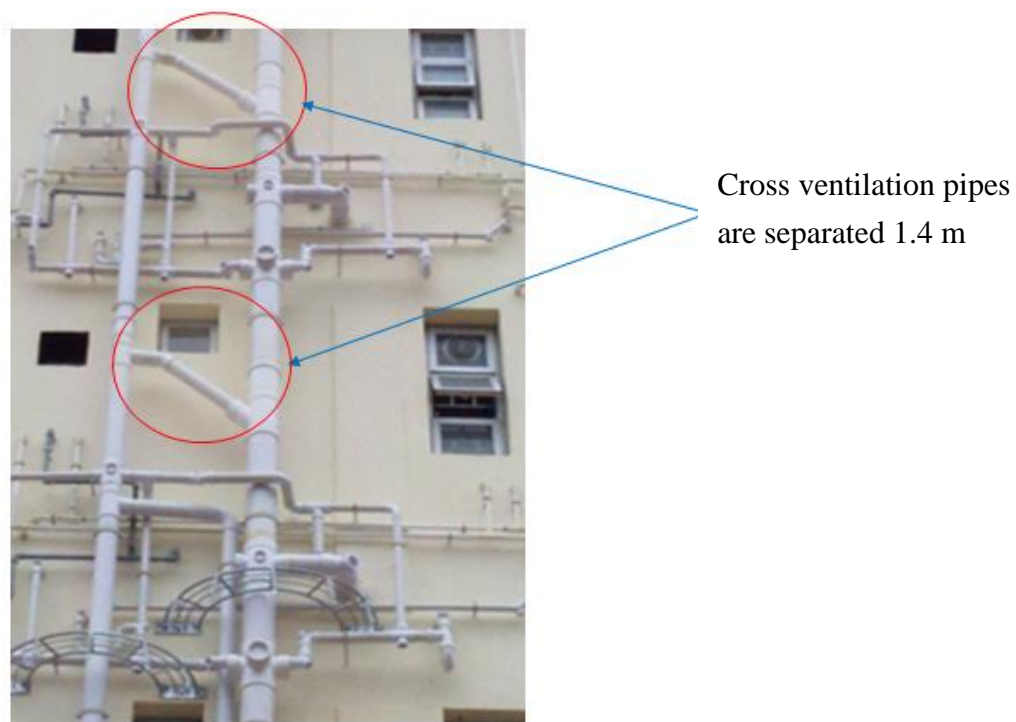


**Figure 5.11, shows a simulated case that cross ventilation pipes have vertical spacing 1.4 m**

However, if  $DCVP = 2$ , it may not be acceptable from the architect's point of view because there are too many pipes connected. As such, too much space is occupied by the pipes, which may result in a negative appearance of building.

Figure 5.11 shows a simulated case for  $DCVP = 2$ .

## **5.2 Innovation of a Twin Drainage Stack System (8S)**

This section describes an innovative drainage stack named “8S”. “8” presents twin pipe and “S” stands for stack (drainage stack). Comparing with BDS with ventilation pipe provision, 8S can thoroughly solve the problem of excessive air pressure in drainage stack and also reduce the space occupied by pipe. It is because 8S has its own ventilation pipe and the DCVP of this stack design exceeds 100.

### **5.2.1 Idea of 8S twin stack**

8S is run in a self-balance of air pressure. Theoretically, when water volume falls down, it generates higher air pressure and lower air pressure (Chapter 4, figure 4.6 zone 3 and zone 1 respectively). Air pressures can self-compensate and do not affect water seal of sanitary appliances.

8S is a drainage stack and its shape looks like the shape ‘8’ from plan view. Actually, 8S is formed by a twin drainage stacks connected with central-ventilating channel (CVC), as shown in figure 5.12.

Once discharge occurs in high-rise building drainage system (HBDS), the twin stack performs its dual functions at each side - one is drainage stack and the other is ventilation pipe at the same time.

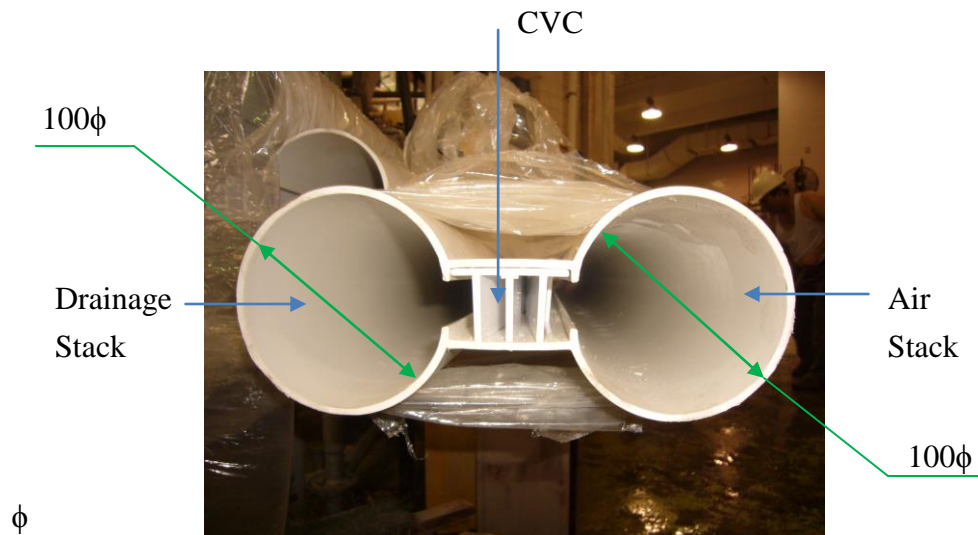


**Figure 5.12, shows plan view of 8S**

The CVC is actually same as a Cross Ventilation Pipe (CVP) but DCVP is over 100.

Air balancing depends on its two arms to maintain equilibrium. In 8S, CVC is the arm to balance the air pressure with higher efficiency. Figure 5.12 shows top views of 8S - LHS is for drainage discharge, RHS is for air stack and CVC is the balancing device for air pressure.

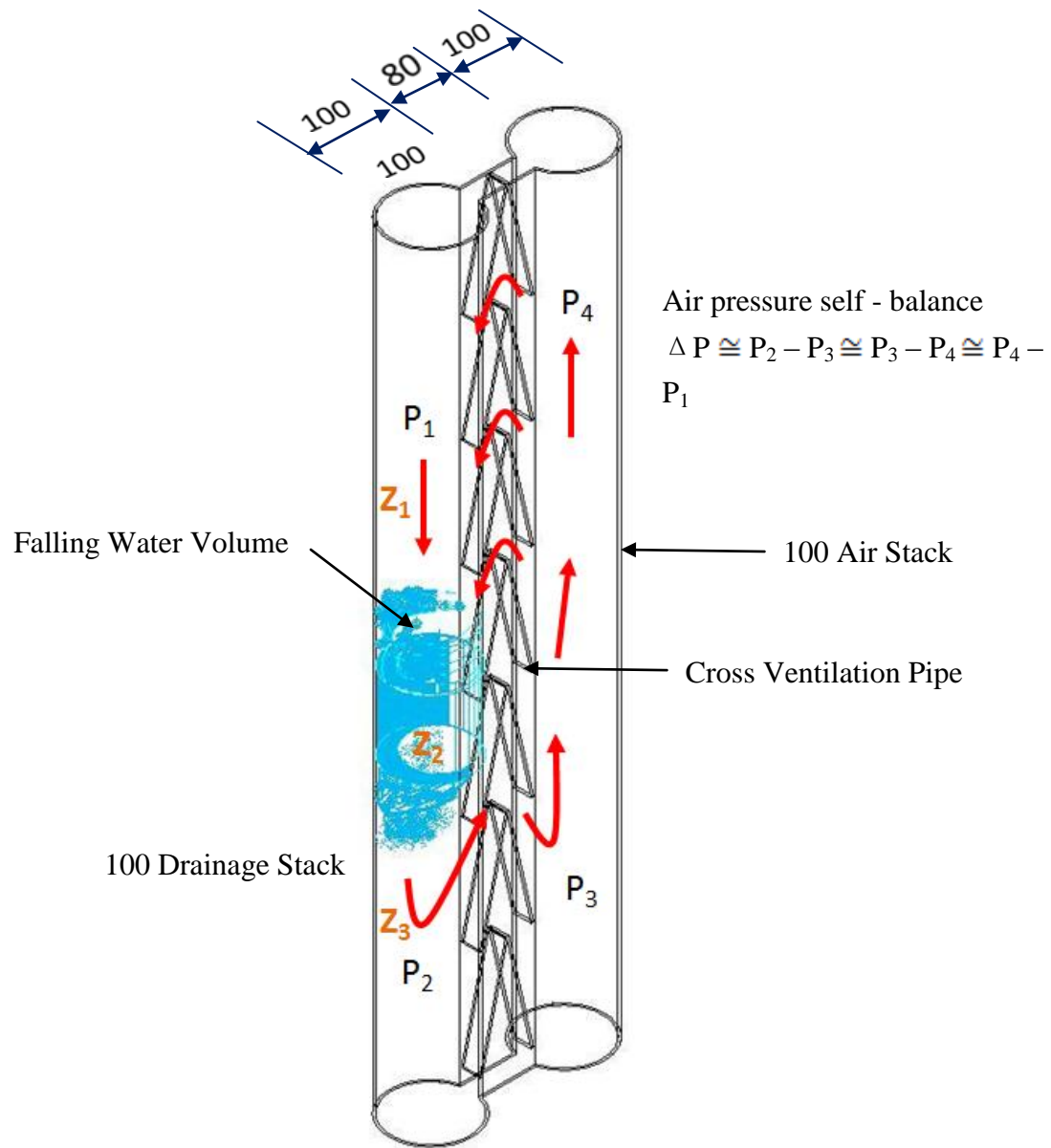
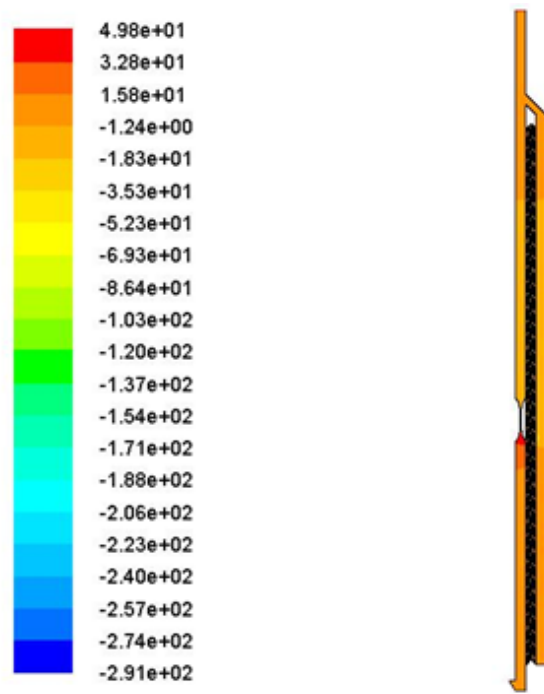


**Figure 5.13, shows structure of 8S which drainage stack and ventilation stack are connected by CVP**

As air flows from higher pressure zone to lower pressure zone, an ideal scenario is that the air will follow the route  $P_2 \rightarrow P_3 \rightarrow P_4 \rightarrow P_1$ . Air pressure at various positions is induced when the water volume falls downward, the pressure at various positions trends to “cancel out” within them.


### 5.2.2 CFD simulation for 8S

Similar to previous chapters' simulation, FLUENT is used to simulate whether the twin drainage stacks can perform the expected function when there is a water fall from the horizontal branch to the vertical stack. Three types of systems are under investigation: single stack, one pipe system and, modified one pipe system. The third type has two different arrangements on the cross ventilation pipe: with 1 cross ventilation pipe and 2 cross ventilation pipes. Height of the water flush is 5.5 m height and for all types of drainage system arrangements, the discharge quantity is set to be the same (2.4 L/s). Finally, the 8S twin stack system should also undergoes the same simulation process as well, for comparison with traditional design options..



Contours of Static Pressure (pascal) (Time=1.0000e+00)

**Figure 5.14, shows structure of 8S which drainage stack and ventilation stack are connected by CVP**

The simulation was conducted in the similar manner as Chapter 5. Water volume falls from the height level of 5.5 metres at the drainage stack, but the difference is that ventilation stack is connected to the top region of drainage stack. The summit of drainage stack is 6 m in height. This set up is similar to the traditional one pipe system but it equips with a large number of  shapes cross ventilation channels (CVC).

From figure 5.14, it can be observed that positive air pressure is induced at the head of falling water volume at  $t = 1$  second after falling. Air pressure can be well digested by all ventilation devices within the 8S twin stack, including the ventilation stack and CVC.

Figure 5.15, shows the zoom-in diagram for the water volume. Air pressure values at various locations (i.e.  $P_1$  to  $P_4$ ) are listed as below:

$$P_1 = -4 \text{ Pa},$$

$$P_2 = 5 \text{ Pa},$$

$$P_3 = 3 \text{ Pa}, \text{ and}$$

$$P_4 = -1.8 \text{ Pa}$$

The results follow exactly the desired pattern  $P_2 > P_3 > P_4 > P_1$ .

From the result of simulation, CVCs would encounter an extremely low pressure. Those CVCs contact the head of water volume and induce a local negative pressure. The air pressure is very small but agrees with the assumption. 8S twin stack performs very well to release the air pressure within the drainage stack.

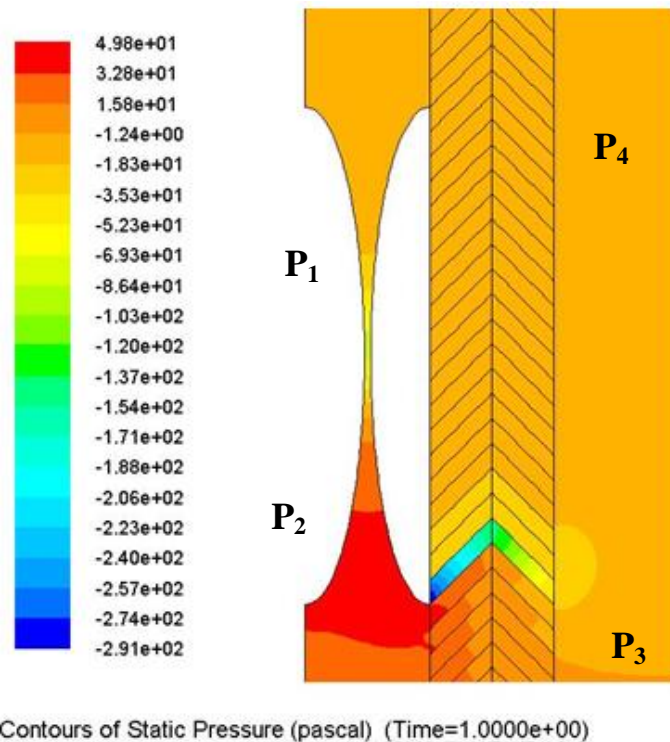


**Figure 5.15, shows air pressure contour near falling water volume at falling time  $t = 1$  second**

From figure 5.16, air is well ventilated via the CVCs at the head of falling water volume at falling time  $t = 1$  second. Positive air pressure at the water volume can be released along the fall and no positive air pressure would be “accumulated” at the lower drainage stack. A large portion of air flow vectors are ventilated via



the ventilation stack, while the CVCs are observed to allow a small portion of the air flow vectors to flow across. In order to show that 8S twin stack possess allows a larger degree of air ventilation.

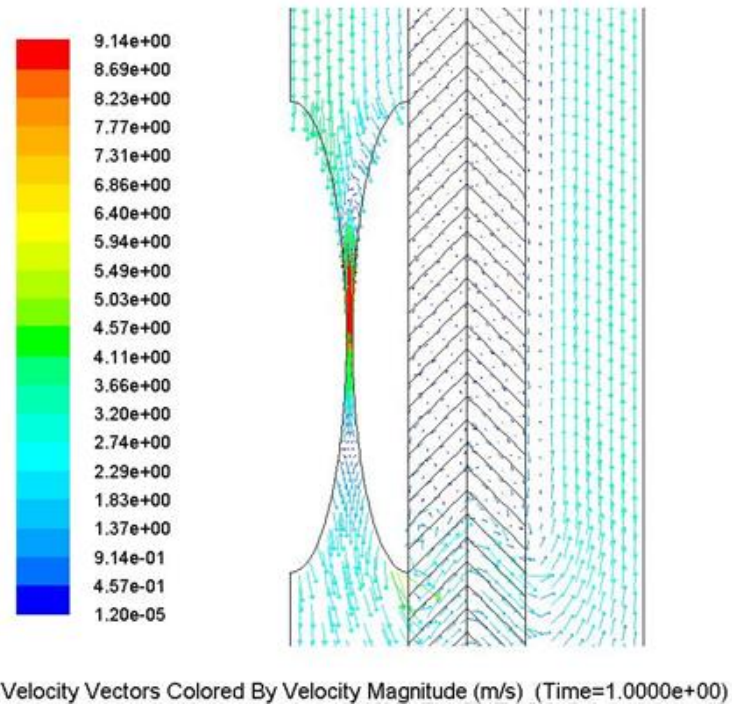
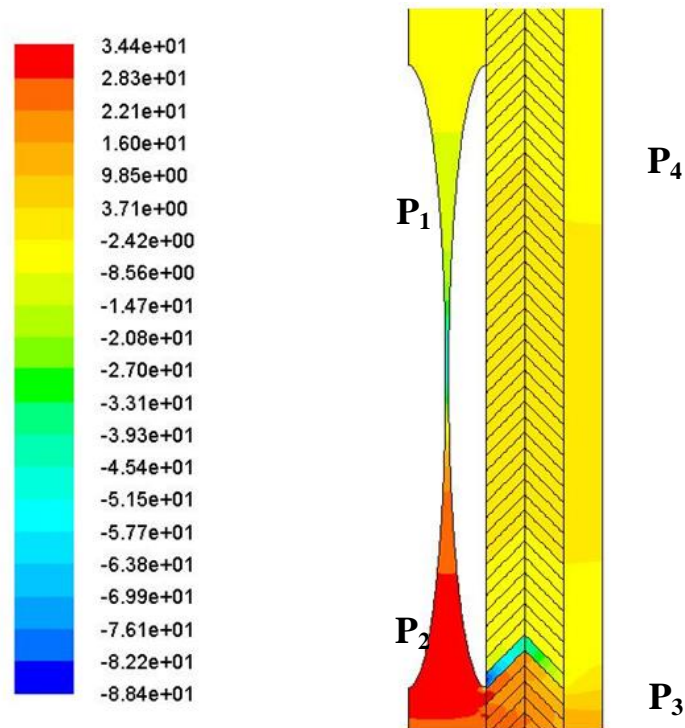


**Figure 5.16 shows air velocity vector diagram which is near falling water volume at falling time  $t = 1$  second**

In figure 5.17, another simulation is conducted with a larger discharge volume of the water fall. The water discharge flow rate is 5 L/s during this part of simulation. It doubles the quantity of previous discharge trials (2.4 L/s), and moreover, the diameter of ventilation stack decreases to 50 mm. When time  $t =$

0.5 seconds after the falling of water volume, air pressure self-balancing can be achieved obviously in figure 5.17



Contours of Static Pressure (pascal) (Time=5.0000e-01)

**Figure 5.17, shows air pressure self-balance effect when ventilation stack = 50mm, water volume = 5L per second and falling time  $t = 0.5$  second**

$P_1 = -14 \text{ Pa}$ ,

$P_2 = 34 \text{ Pa}$ ,

$P_3 = 9 \text{ Pa}$ , and

$P_4 = -8 \text{ Pa}$

This also follows the expected pattern  $P_2 > P_3 > P_4 > P_1$

From the above results, 8s twin stack has been proved to possess self-air balance capacity again, which is also large enough to self-balance an unexpected air transient induced inside the drainage stack.

According to typical local basic design thinking, the quantity of water discharge flow of 2.4 L/s & 5 L/s can be perceived in the following discussion. From the design manual of the Institute of Plumbing (2002), the quantity of discharge flow can be expressed as

$$Q = K\sqrt{\sum du}$$

Where Q is the discharge flow and K is the frequency constant.

Suppose in a commercial building complex,  $K = 0.7$  according to IOP design manual (Tildsley et al. 2002), if the discharge appliance is a water closet and the highest water consumption is assumed to be a 9L cistern, the discharge unit (D.U.) approach can be adopted.

Since the discharge unit is 2 L/s for commercial building, 2.4 L/s and 5 L/s water discharge flows equal to respectively 6 and 26 water closets flushing simultaneously inside a real building. In reality the case of 5 L/s occurs rarely but the probability of occurrence is definitely not zero.

For a twin stack consist of a pair of 100 mm drainage and ventilation stacks together, the test of the 5 L/s simulation and its set-up is the same as 2.4 L/s discharge test. Although their discharge quantity is doubled, test results indicate that the air pressure contour (figure 5.18 and figure 5.19) for 5 L/s water discharge is almost the same as 2.4 L/s discharge simulation. This shows that the 8S twin stacks perform its function even whe the water discharge flow rate is abnormally high.

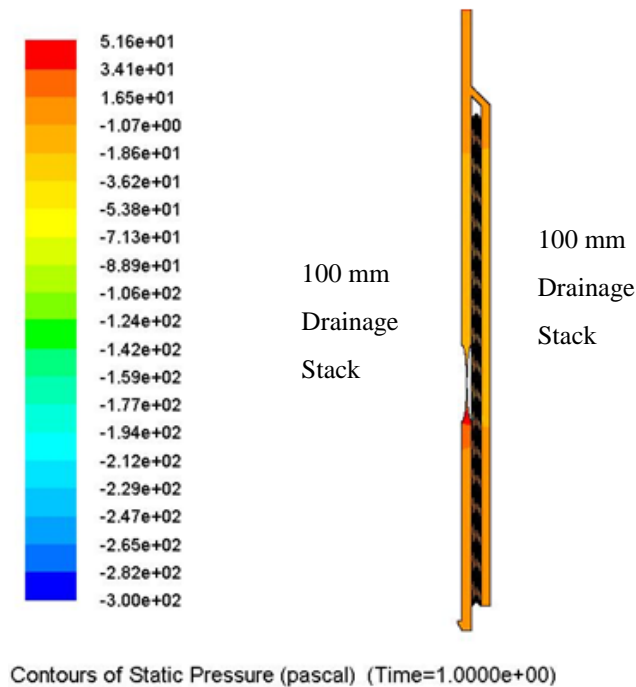
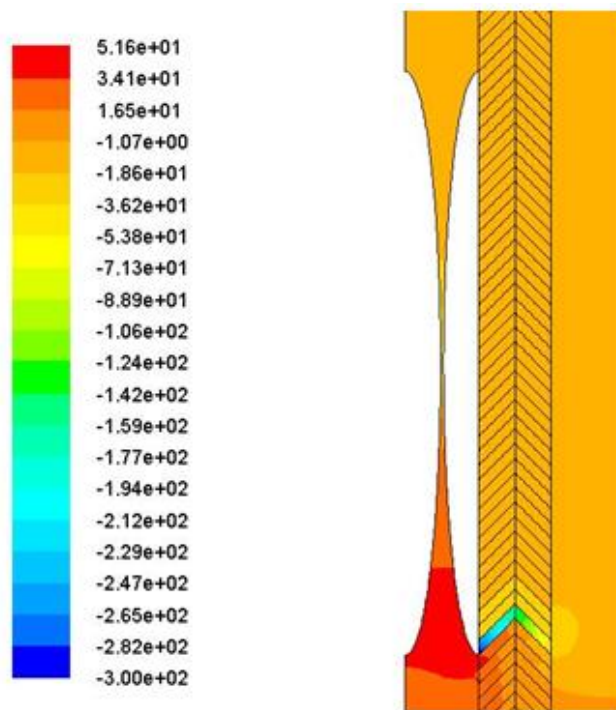


**Figure 5.18, shows air pressure contour of drainage stack at falling time  $t = 1$  second and discharge**



Contours of Static Pressure (pascal) (Time=1.0000e+00)

Figure 5.19, shows air pressure contour diagram which is near falling water volume at falling time  $t = 1$  second and discharge volume = 5 L/s

### 5.2.3 Comparison between 8S and other connection CFD simulation.

The air pressure result of water volume (2.4 L/s) is shown in figure 5.20

Air pressure profile at  $t = 0.5s$

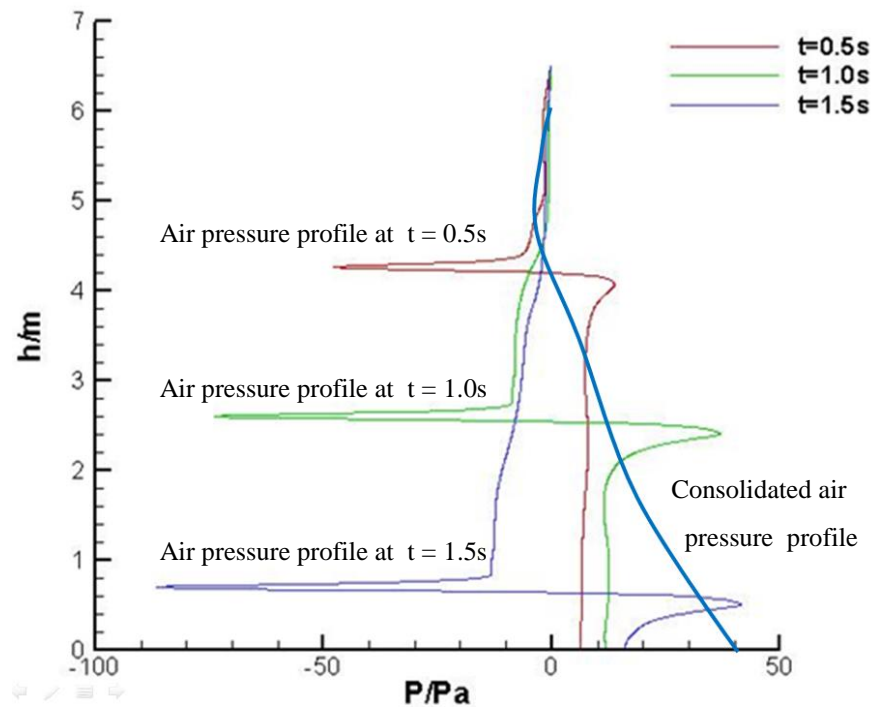


Figure 5.20, shows air pressure diagram in the 8S drainage

In the pressure diagram (figure 5.20), when water volume falls at time  $t = 1$  second, the air pressure at (35, 2.4) decreased suddenly from 35 Pa to 10 Pa.

CVC is anticipated to play a role on releasing the air pressure. 35 Pa is discarded and the latter value of 10 Pa is considered regarding the pressure profile data.

The air pressure profile for the 8S twin stack can be plotted from the following related points (0, 6), (-1, 5.5), (-1, 4.7), (7, 3.5), (20, 1.7), (37, 0.35) and (41, 0).

As the discharge volume and height are 2.4 L/s and 5.5 m respectively, which are the same settings of other connections; the plot of air pressure profiles diagram is similar to figure 5.8.

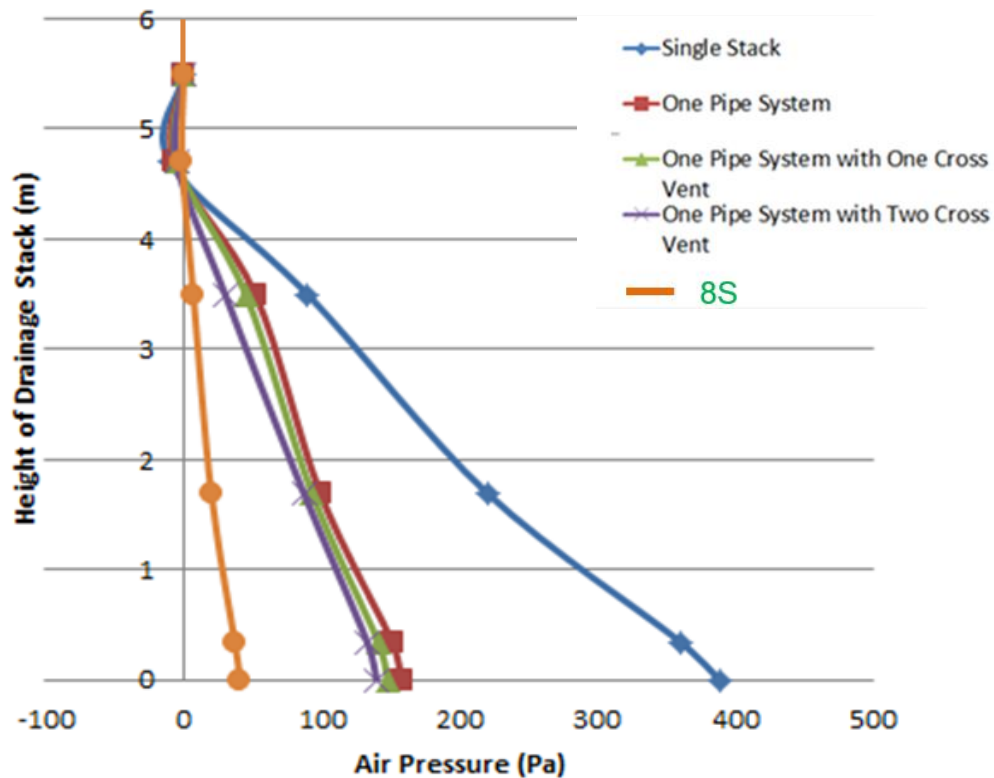


Figure 5.21, shows air pressure profile of 2.4 L/s discharge in 8S drainage stack

Figure 5.21 shows the air pressure profile diagram which compare different drainage connections options. In the 1<sup>st</sup> case, positive air pressure occurs at the toe of drainage stack, and for this single stack system its greatest value is 390 Pa.

Once the drainage stack is equipped with ventilation stack, the system becomes a one pipe system. This is the 2<sup>nd</sup> case that positive air pressure at toe of stack decreases to 158 Pa. For 3<sup>rd</sup> and 4<sup>th</sup> cases which is installed with cross ventilation pipe between the drainage and ventilation stacks. Here, the air pressures further reduce to 148 Pa and 140 Pa respectively. It shows the importance of ventilation provision to the main drainage discharge stack, which dominates a large part air pressure reduction (232 Pa). Cross ventilation pipe is effective to balance air pressure but its capacity is not enough and just to decrease 10~20 Pa. The ventilation ability also depends on their distance of separations between the cross pipes, 5 m separation between cross ventilation pipes can decrease 10 Pa and 2.5 m separation reduces 20 Pa.

The 8S twin stack has CVC (about 250 ventilation channels) which is provided along the drainage stack and ventilation stack. From the results, air pressure at the toe is 41 Pa. It shows that 8S twin stack achieve an outstanding efficiency to release positive air pressure and, a sharp deduction is observed when comparing to one pipe system (the positive air pressure is reduced by more than 120 Pa).



The simulation results of 8S twin stack show its merit while it is far more important to conduct field verification by a real water discharge process at a real installation. The tests are not only conducted at the 5.5m drainage research rig but also conducted at a 18-storey real building.

#### 5.2.4 Validation in Drainage Research Rig and real building

A series of tests have been conducted to verify the performance of 8S stack.

##### 5.2.4.1 Comparison with Drainage Research Rig of the Hong Kong PolyU

A series of hydraulic tests have been held in the Drainage Research Rig in the Hong Kong Polytechnic University.

Height of water discharge is 5.5 m and the water volume would be slightly greater than the simulation value (2.4 L/s).



**Figure 5.22, shows the setting up of 8S in Drainage Research Rig of HK PolyU**



**Figure 5.23, shows small air pressures which are observed at the toe of stack**

Flow (L/s)	Point 1 (pa)	Point 2 (pa)
3.3	50	20
4.2	80	50

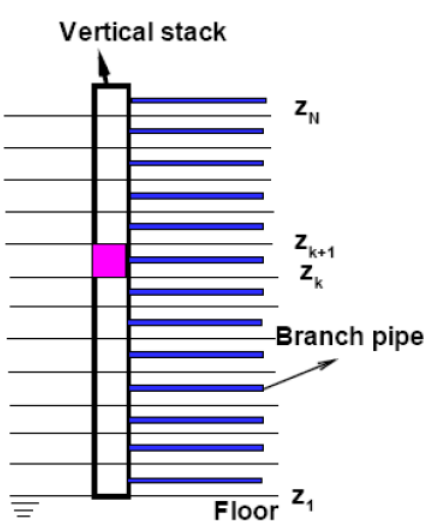
**Table 5.1, shows low air pressures which are found at the toe of the stack**

The air pressure transducers are located at the toe of 8S. The configuration of the test is the same as the previous test mentioned in section 4.2.2. Observed from the simulation result, the positive air pressure at the toe is 41 Pa for a 2.4 L/s water discharge flow rate, which agrees generally with the measurement result at the toe of 8S twin stack (positive air pressure of 50 Pa for a 3.3 L/s water discharge). Moreover, figure 5.23 shows that no hydraulic jump can be observed during the whole discharge process. There is no doubt that 41 Pa is very small and it equals to 4 mm water pressure head which can be considered as zero or negligible air pressure.

8S twin stack can effectively solve the problem of excess positive pressure, and additional tests will be conducted in a real building.

5.2.4.2 Comparison with a real building

The building has 18 storeys which is a typical residential building in Southern China. The test configurations are listed as below: material of 8S twin stack is uPVC with a wall thickness of 3 mm. Internal diameter of the whole twin stack is 2 x 100 mm which are connected together by a 100 mm width CVC.



Stations	Heights (m)
Toe of Stack	0
1/F	1.5
5/F	13.8
11/F	28.6

Table 5.2, shows station points of pressure transducers

Figure 5.24, shows station points of pressure transducers



**Figure 5.25, shows 8S setting-up for a domestic building in Dongguan, China**

There are 3 pressure transducers installed at the drainage stack. The specification of these transducers is WIKA  $\pm 50$  pa, IP65 (figure 5.26). The logger ADAM 6017 (figure 5.27) is used.



**Figure 5.26, shows a WIKA air pressure transducer installed at 8S**



**Figure 5.27, shows a ADAM logger and computer for data collection**

As shown in figure 5.25, there is one water closet per floor and the closets from all floors (within a zone) are connected to the 8S twin stack. Every water closet discharges water at a flow rate of 1.5/s. The water discharge rate is controlled by the electrical box as shown in figure 5.28. All water closets can be operated to flush at same time and for a definite input time period.

In order to deliver a maximum discharge to the drainage system, all water closets are set to discharge with a controlled time delay for successive floors. Water volumes from each floor combine in the stack to form a single larger water volume.



**Figure 5.28, shows control box for flushing of water closets**

Several tests are conducted and table 5.3 shows part of the data obtained from the flushing tests. Two set of data were obtained, one set from the 100mm diameter drainage pipe test, and the other from the 100 diameter 8S twin stack. Water discharge flow rate is between from 4.5 L/s to 25.5L/s, which varies according to the number of flushing water closet in the trial.

	Discharge (L/s)	Discharge Floors	1/F (mBar)	5/F (mBar)	10/F (mBar)
8 S	4.5	15~13	-1.31	-2.14	2.63
	9.0	12~7	0.23	-1.29	1.56
	25.5	18~2	0.20	-0.18	2.30
100 Stack	4.5	15~13	2.02	-1.53	-0.9
	9.0	12~7	5.96	-4.31	-0.89
	25.5	18~2	38.46	-11.41	-10.97

**Table 5.3, shows air pressure reading at different station points for different discharge flow**

Observed from Table 5.3, it is clear that 8S twin stack installation can effectively reduce the large positive air pressure at the lower storeys. It is supported by a reduction of more than 10 mbar negative pressure at 5/F and, a reduction of 36 mbar positive pressure at 1/F, compared with the tradition 100 mm stack. While at 10/F the negative pressure at the traditional stack would change to a slightly possible pressure for the 8S twin stack case, the magnitude of air pressure at 10/F is still decreased by some 8 mbar.

The 8S twin stack is expected to solve air pressure problem typically in high rise buildings. Simulation and field verification show that the 8S twin stack is able to perform its expected function. By reducing the magnitude of air pressure within the drainage system, risk of failure including foul water back flow and escaped



air flow from drainage system to the indoor environment can be minimized to offer a safe and health indoor environment.

### **5.3 Smart Floor Trap**

SARS outbreak in 2003 shows the threat on a communicable infection that human body has little or no immunity to the new pathogen. Intensive research is conducted on the transmission mechanisms of pathogens inside a building. According to the report released to the public from the delegate investigation team from World Health Organization (2003) suggested the plague occurred in Amoy Garden could be a result of SARS virus transmission via the re-entrants and the drainage stacks of the residential buildings. The awareness on the importance of water seal inside the trap in drainage systems was raised. The Hong Kong government has advised the public frequently that the traps should be filled up by water all the time.

Floor drain traps in the bathrooms and kitchens were often neglected by building occupants who fail to keep the traps filled up with water. One reason is that Hong Kong people tend to mop the floor during cleaning while wet cleaning is relatively seldom. If the air pressure within the drainage system cannot be properly relieved,

the water seal could deplete to allow the smelly foul air flows from drainage system to the living environment.

### 5.3.1 Smart water seal refilled floor trap

A smart pipe connection as shown in figure 5.29 can solve this problem. The floor traps will be refilled by a smart tee which delivers waste water to floor trap.

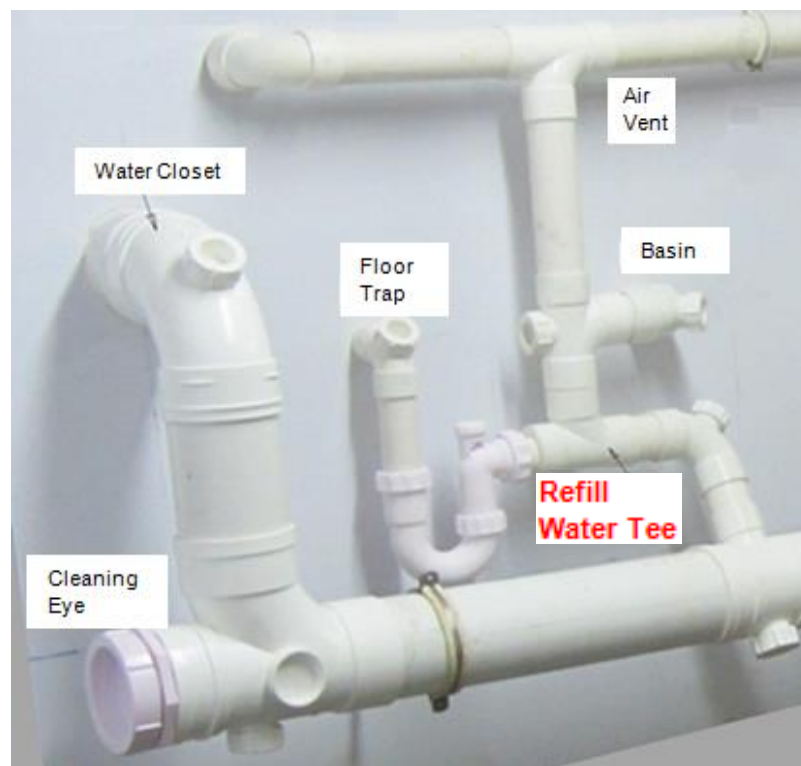


**Figure 5.29, shows a smart pipe connection to refill water to floor trap**

In figure 5.29, a floor trap becomes “smartly connected” that water seal can be refilled to ensure that the water seal inside will not lose nor becomes empty. This

reduces the risk of contaminated air flow from drainage stacks into indoor spaces if the floor drains can retain the water longer against drying and evaporation, without changing the currently adopted design and sizing practice of drainage system. The coming research describes a new design of floor traps which reduce the rate of evaporation of the water seal. This chapter also describes the method to evaluate the performance of smart trap at a test rig.

#### 5.3.2 Smart floor trap

Smart trap is a bell type floor trap. The most significant difference compared with traditional floor drain trap is that a large buffer space is provided to recover the trap depletion (water seal) by evaporation (Chan et al. 2008b). Smart trap emphasizes a new principle: Safety of floor trap is not only depends on the height of the water seal, but the contact surface of water to atmosphere is equally important to resist water loss. An innovative design of minor consumed trap is illustrated. The appearance of floor traps in figure 5.30 and figure 5.31 are the same, but they vary in the ability of water retention.

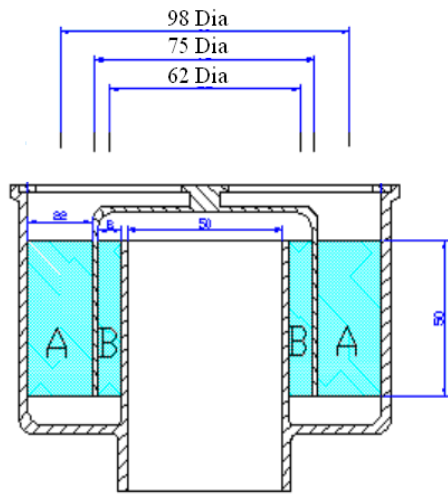


**Figure 5.30 Bell type floor trap**

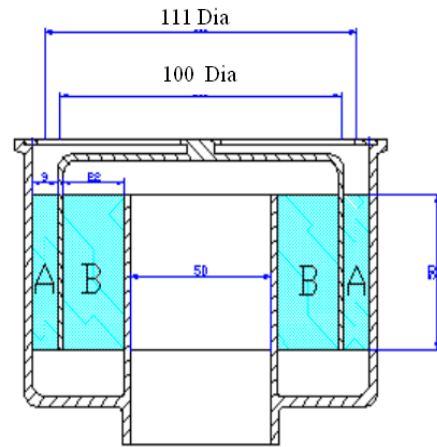


**Figure 5.31 Bell type smart floor trap**

The operating principle of the smart bell is not complicated. There are two tiers of water seals, tier A and tier B in the floor trap. The tier contacts with the atmosphere suffer evaporation under an outside air velocity. More important is that the evaporation is caused by temperature difference between the inside and outside of the trap as well. Of course outside air velocity is also a factor for evaporation. From figure 5.31, the estimated contact area of water seal in tier A and tier B in normal bell floor trap is expressed below:

Area of water seal  $F_A = 22 \times 98 \times 3.14 = 6769.84 \text{ mm}^2$

$$F_B = 8 \times 62 \times 3.14 = 1557.44 \text{ mm}^2$$

Total area of water seal  $F_T = 6769.84 + 1557.44 = 8327 \text{ mm}^2$

Total consumption of water seal  $\omega_T = F_T \times 50 = 416364 \text{ mm}^3$

Total suction of water seal  $\omega_S = F_A \times 50 = 338492 \text{ mm}^3$

Daily evaporation of water seal  $\omega_E = F_A \times 2 = 13539.7 \text{ mm}^3$

Residue of water seal after suction  $\omega_R = \omega_T - \omega_S = 77872 \text{ mm}^3$

Safety period of water seal (no. of day)  $= \omega_R / \omega_E = 77872 / 13539.7 = 5.8$

From the result, the trap is easy to empty and smell will be easy come from the drainage system and may cause health problem.

From figure 5.32, Smart trap has a smaller contact area of water seal in tier A, it minimize the water loss from the seal. The trap owns a large tier B for refilling water seal that is reduced in tier A. Estimation is made for the retention period of the water seal which is much longer than the traditional traps as shown in figure 5.31.

The calculation is shown as below:

$$\text{Area of water seal} \quad F_A = 8 \times 111 \times 3.14 = 2788.3 \text{ mm}^2$$

$$\text{Total area of water seal} \quad F_T = 6769.84 + 1557.44 = 8327 \text{ mm}^2$$

$$\text{Total consumption of water seal} \quad \omega_T = F_T \times 50 = 416364 \text{ mm}^3$$

$$\text{Total suction of water seal} \quad \omega_S = F_A \times 50 = 139415 \text{ mm}^3$$

$$\text{Daily evaporation of water seal} \quad \omega_E = F_A \times 2 = 5576.64 \text{ mm}^3$$

$$\text{Residue of water seal after suction} \quad \omega_R = \omega_T - \omega_S = 276949 \text{ mm}^3$$

$$\text{Safety period of seal (no. of days)} = \omega_R / \omega_E = 276949 / 5576.64 = 49.7$$

The water seal loss in smart bell trap would be larger if tier A is too large.

Efficiency of water recovery is also too low in this case.

### 5.3.3 Verification on the evaporation rate of smart trap

An experiment has been conducted to verify the evaporation rate of smart trap to compare its performance with a traditional P trap. An air chamber is constructed for these purposes.

#### 5.3.3.1 Evaporation Model

"Aerodynamic Method" is a widely applied to calculate evaporation (Jensen 2010). This method is an approximation and adopted in this investigation. This method is documented and requires measurement on temperature and vapor pressure at two heights above the surface are required, together with the speed of air outside the trap.

The equations for evaporation estimation is:

$$E = -\rho * L * k * u_{star} * (q_2 - q_1) / \ln(z_2/z_1)$$

where E is evaporation,  $\rho$  is air density, L is the latent heat of vaporization, k is von Karman's constant,  $u_{star}$  is the friction velocity,  $(q_2 - q_1)$  is the specific humidity difference between the air and the "air film" near the water surface,  $\ln$  is natural log,  $z_2$  is the height of the dew point temperature measurement location, and  $z_1$  is a height near the water surface.

$\rho$  can be approximated as 0.0012 g/cm<sup>3</sup>, where <sup>3</sup> means exponent to the 3rd power.

L is approximated by 598 cal/g.

k is 0.38

wind speed is in cm/s.

ustar is assumed to be one tenth of the wind speed.

air pressure is in mBar.

height of temperature measurement point is in cm;  $z_2$ .  $z_1$  is also in cm.

To be determined are: the vapor pressure in mBar ( $e_2$ ) for the air dew point temperature (at  $z_2$ ); and the vapor pressure in mBar ( $e_1$ ) for the water temperature at  $z_1$  (which will be close to the dew point near the water surface because the air there is almost saturated) by using the following equation:

$$e = C0 + C1*T + C2*T*T + C3*T*T*T + C4*T*T*T*T + C5*T*T*T*T*T + C6*T*T*T*T*T*T$$

where

$$C0 = 6.11$$

$$C1 = 0.4437$$

$$C2 = 0.014289$$

$$C3 = 0.000265065$$

$$C4 = 0.00000303124$$

$$C5 = 0.000000020340809$$

$$C6 = 0.00000000006136821$$



where the temperature  $T$  is in degrees C; it is noted that each coefficient is multiplied by as many  $T$ s as the number in the coefficient.

The specific humidity (dimensionless),  $q_2$  (at  $z_2$ ) and  $q_1$  (at  $z_1$ ) can be estimated by the following equation:

$$q = (0.622 * e) / (P - 0.378e)$$

Using the above information, evaporation can be estimated.

#### 5.3.3.2 Test in an Air Chamber - Evaporation Test

The inner size of air chamber is 600mm (Length) x 500mm (Width) x 500 mm (Height). It possesses a steel case for insulation. The temperature and air flow inside the test chamber can be controlled by a heater and an exhaust fan. All floor traps are installed below and outside the chamber and accessible such that the water seal height inside the trap can be measured.



**Figure 5.32 Trap Test Rig**

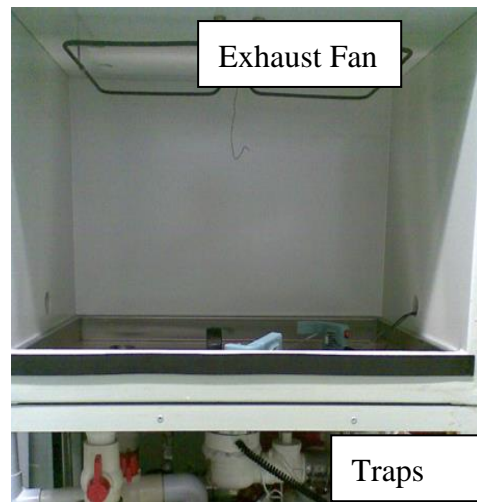


**Figure 5.33 An air chamber is for**

Figures 5.32 and 5.33, shows the test rig the testing. Evaporation occurs due to different temperatures which are measured inside and outside of the traps. A heater is installed below the steel case to adjust the temperature of air surrounding the traps.

Measurement result is listed below:

$$Z2 = 38.1 \text{ cm}$$

$$Z1 = 21.1 \text{ cm (near water surface)}$$

$$T2 = 28 \text{ }^{\circ}\text{C}$$

$$T1 = 30.7 \text{ }^{\circ}\text{C}$$

$$V_{\text{Wind}} = 100 \text{ cm/s}$$

Evaporation is calculated by model

$$E_{\text{P Trap}} = 0.01886 \text{ cal/cm}^2/\text{s}$$

$$= 789.27 \text{ W/m}^2$$



**Figure 5.34 P-trap at floor drain**

Measured data:

$$Z2 = 19.7 \text{ cm}$$

$$Z1 = 1.9 \text{ cm (near water surface)}$$

$$T2 = 28 \text{ }^{\circ}\text{C}$$

$$T1 = 31.9 \text{ }^{\circ}\text{C}$$

$$V_{\text{Wind}} = 100 \text{ cm/s}$$



**Figure 5.35 Smart Bell floor drain trap**

Evaporation Rate is calculated by,

$$E_{\text{Smart Trap}} = 0.00711 \text{ cal/cm}^2/\text{s}$$

$$= 297.4 \text{ W/m}^2$$

### 5.3.3 Finding in the test

The evaporation rates of P trap and Smart trap are compared as follow:

$$= \frac{E_{P \text{ Trap}}}{E_{\text{Smart Trap}}} = \frac{789.27}{297.4} = 2.6$$

From the figure 5.34 (P trap), and figure 5.35 (smart bell type floor trap), although the size of Smart trap is larger, its evaporation is 2.6 times less than the 50 mm diameter P-trap.

The special feature of smart trap, which reduce the contact area of trap seal water exposed to the air, is successful to reduce the evaporation and hence, reduce the risk of water seal depletion inside the traps at the sanitary fixture. Smart trap improves the reliability of drainage system in high-rise building because:

- The loss of water seal of trap can be minimized.
- No potential hazard of water loss due to the siphonage effect in the system.
- Two tier of water seals are provided to ensure fast recovery of water.
- Unlike the outdoor water floor trap, the smart bell trap will be installed in indoor area. Only discharge pipe is to make connection between the trap to main horizontal discharge pipe. It means that no floor trap is placed outdoor. It not only avoids depleted water seal but also improves the appearance of external pipe connections. The only adverse effect of internal floor trap is that it has to be placed in separated floors. So, it is more difficult to carry maintenance if the floors are belonged to different owners.

#### **5.4 Some suggestions on future work: identifying emptied traps along a stack**

Regarding the emptied trap, it is recommended that for future research, the feasibility of automatic detection on depleted water seal in traps can be investigated. Actually, some preliminary research has been started already.



**Figure 5.36 : schematic diagram for the data transmission system testing**

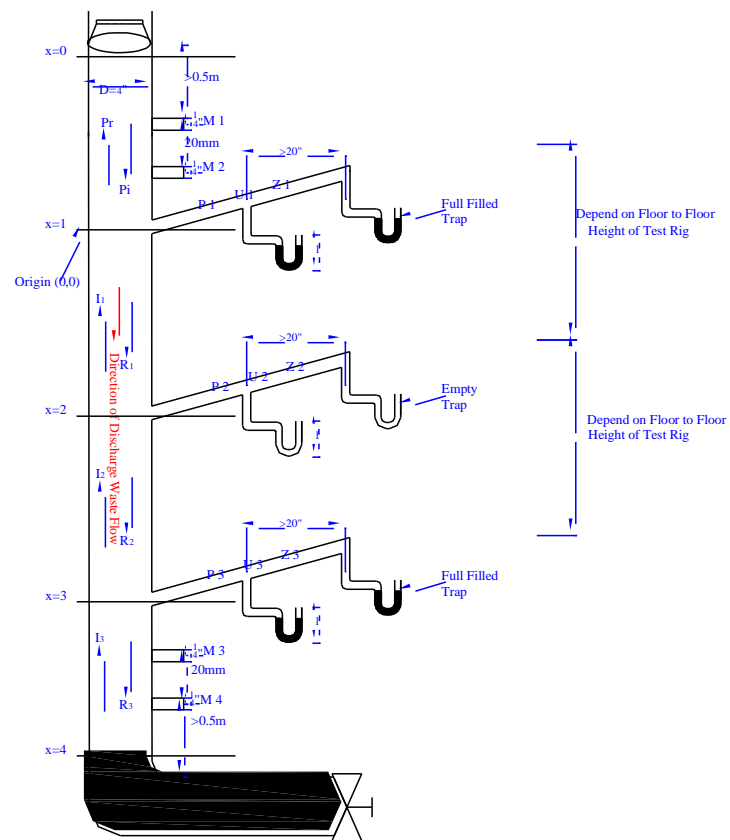


**Figure 5.38: The schematic diagram of test rig for empty trap detection**

In figure 5.36, the test rig for sound transmission inside drainage rig is established in drainage research rig of the Hong Kong PolyU. In figure 5.37, this schematic drawing shows the set-up that the convenience of regular and routine checking of all system traps has been enhanced to prevent any unidentified dry or semi-depleted traps before the experiment. The acoustic impedance technique with an indication of depleted traps in the pipe system would ensure that the system is complied with performance standards. This research objective is to perform the simulation (at which the ability can be confirmed) using sound impedance and sound transmission loss properties within building drainage and vent systems, which may be used to identify those defective trap seals.

More research is needed to investigate the sound transmission characteristics of the drainage system for various combinations of empty and sealed traps. Finite element methods can be employed to solve the unknown parameters by using computer software such as MATLAB. The frequency concerned is at the first eigenfrequency of the pipe, such that plane wave propagation inside stack and

pipes should be sufficiently separated apart from the branches. Although this limits the feasibility of the research at present, it is expected that such a research is useful to manage the drainage system, once the separation requirement between stack and pipes can be reduced in future research.



## **Chapter 6**

### **Drainage Monitoring and Communication Systems**

The effective monitoring on the drainage system at real building requires data acquisition of the operating parameters within the system. This chapter describes a unique data logging at the drainage stack. It can record air pressure data in the stack continuously within the defined logging period. In addition, this chapter also introduces an advanced analysis technique on the air pressure data from drainage stack.

#### **6.1 Data Collection of Air Pressure inside the Stack**

In Hong Kong, many high-rise buildings suffer problems in drainage system. Examples include aged pipes and stacks with scaling, as well as blockage inside the pipework. This may result in an increase on the air and water pressure within the system. Risk of leakage may also become higher if the discharge rate increase. At the same time, the internal diameter of pipework gets smaller due to scaling and, the pressure inside the scaled pipe will further increase. Different from other building services systems such as air-conditioning or electrical

system provided with a number of options available in terms of monitoring devices and computerized control algorithm, there is a lack of detection devices and protocol available for the performance monitoring on drainage system.

#### 6.1.1 Data Collection in a Real Building – Li Ka Shing Building

The Li Ka Shing building (LKS) is the tallest building in The Hong Kong Polytechnic University and is located at the centre of the campus. There is a restaurant at 14<sup>th</sup> floor, a student computer centre at 3<sup>rd</sup> floor to 4<sup>th</sup> floor, and all other floors are offices. Utilization of the sanitary appliances at the 3<sup>rd</sup> and 14<sup>th</sup> floors is relatively higher throughout the whole day when compared with the other floors. An investigation was made in April 2008 whereby 3 air pressure survey points were installed on the main foul-water stack (150mm diameter) of the building, on the mezzanine (M) floor, the 6<sup>th</sup> floor and the 12<sup>th</sup> floor respectively. The objective of the research is to determine the air pressure distribution of the main stack and how it varied. This building is used as a measurement platform and real pressure values are online logging.

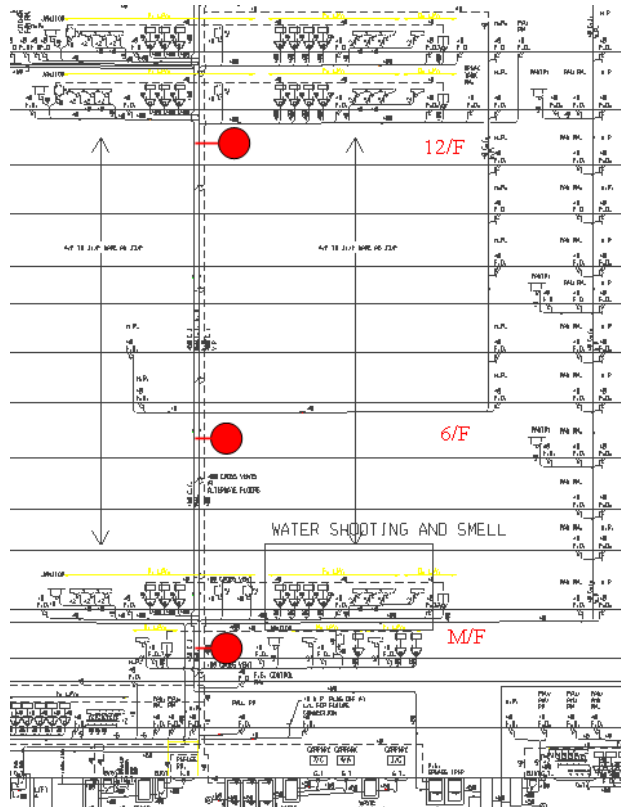


Figure 6.1 – Schematic drainage diagram for 150 dia. Main stack and air pressure survey points



Figure 6.2 – WIKA air pressure transducer is installed at 6/F 150 drainage stack



Figure 6.3 – WIKA air pressure transducer is installed at M/F 150 drainage stack

### 6.1.2 Air fluctuation behaviour in a drainage system in LKS

The purpose of data analysis not only limit to defining the alarm level from the collected data, but also lead to a better understanding on the air pressure characteristic of the main drainage stack.

#### 6.1.2.1 Data collection at M/F of LKS

As observed from figure 6.4, the average air pressure inside the stack was 1.18 mbar (with a maximum at 5.57 mbar and a minimum of -0.59 mbar). The peak period of utilization was between 11:45 a.m. to 2:15 p.m., i.e. during the lunch period.

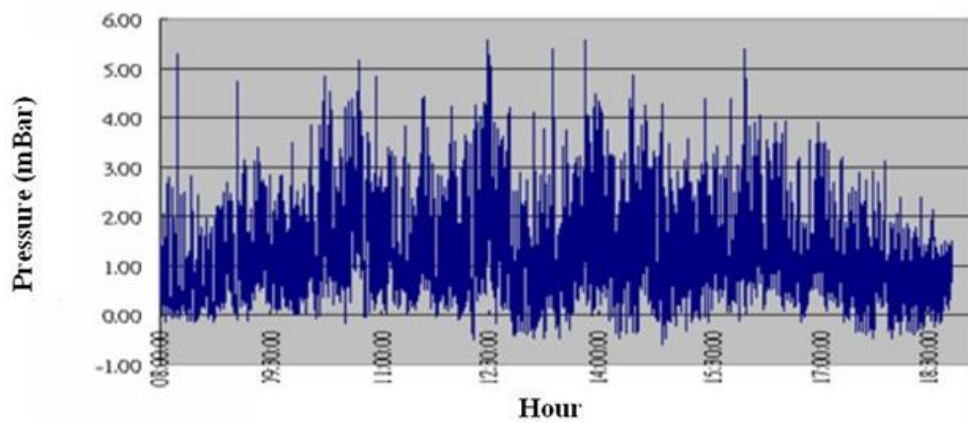


Figure 6.4 – Air pressure inside 150 stack at M/F, Li Ka Shing Building

#### 6.1.2.2 Data collection at 6/F of LKS

Observed from figure 6.5, the average air pressure is -2.28 mbar (with a maximum at 2.38 mbar and minimum of -7.32 mbar). There is no significant variation or maxima at a particular time. Air pressures in the stack at 6/F appears to be more stable than that at the M/F.

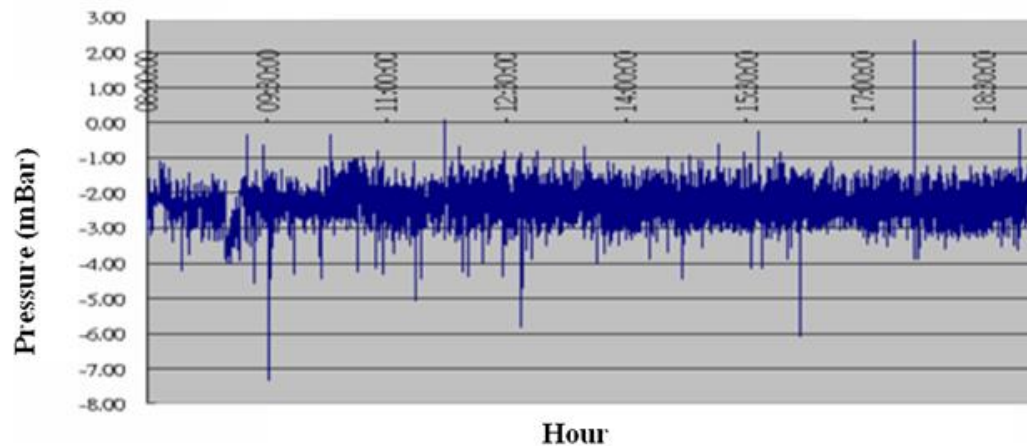
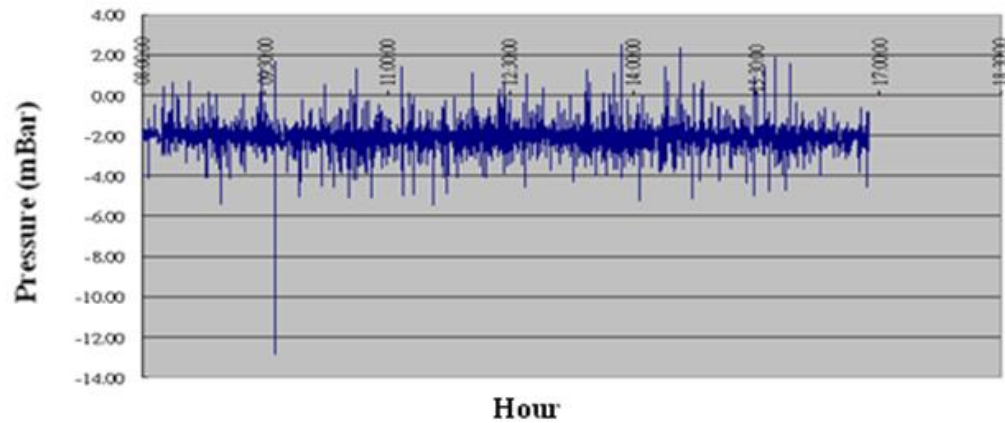


Figure 6.5 - Air pressure inside 150 stack at 6/F, Li Ka Shing Building

#### 6.1.2.3 Data collection at 12/F of LKS

Same as 6/F, 12/F is in a negative pressure zone. The average of air pressure is -2.05 mbar (with a maximum of 2.52 mbar and minimum of -12.83 mbar). There is no great variation or maxima at particular times. Air pressures in the stack at 12/F, like the 6/F, appears more stable than at the M/F.



**Figure 6.6 – Air pressure inside 150 stack at 6/F, Li Ka Shing Building**

There are approximately 20 peaks or more high positive air pressures be observed between 11:45 and 14:15. On 10 occasions, the air pressure exceeds 4.5 mBar, and 5 of these occasions even exceed 5.5 mbar. It means that a number of sanitary appliances are used simultaneously during that period and water seal of all traps including water closet are unstable in the 3/F toilets. From Table 6.1, the standard deviations of the 6/F and 12/F data are similar while the value for the M/F is much larger, indicating that the air pressure variation is much larger at M/F.

## **6.2 Remote Monitoring in Drainage System**

### **6.2.1 Communication with the Drainage System**

A network-based pipe monitoring system was installed to the above-mentioned drainage system, which facilitates remote monitoring and logging pipe pressure through Ethernet. It also generates alarm output when stack (or pipe) air pressure exceeds the pre-set value. Data log file can also be downloaded through Internet. The whole system includes HMI software, monitoring PC, network-based AD converter and the air pressure sensor.

The monitoring PC and network-based AD converter is linked by Ethernet so that all logged data can be transferred to a centralized system for analysis. The network based AD converter transfers the sensor signal to the monitoring PC through Ethernet. Other optional functions include alarm output signal transfer when the air pressure over the preset value. The monitoring PC is installed with HMI software display and log the data into Excel format obtained from Network based AD converter. In addition, FTP and remote desktop software can be installed so that the log file of the air pressure can be received by other remote

desktop for data analysis. Figure 6.7 shows the schematic diagram for the data transfer system to incorporate air pressure monitoring in drainage stack.

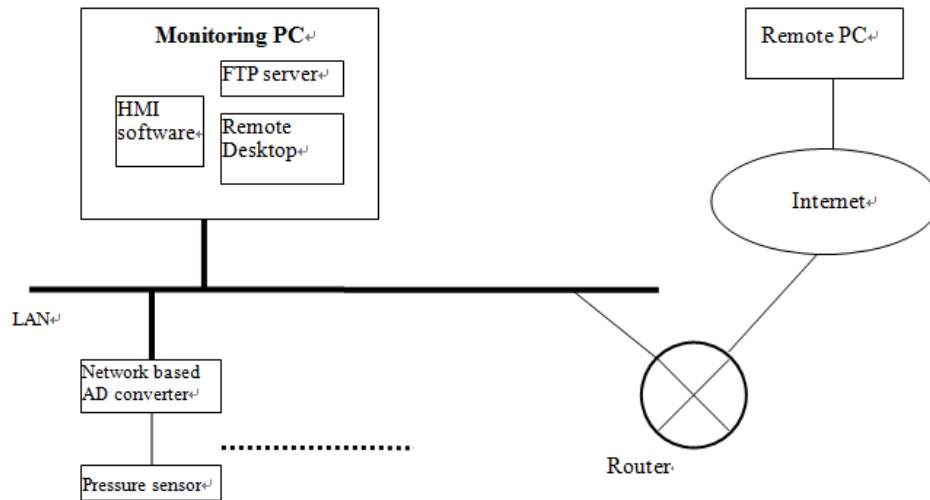


**Figure 6.7 : schematic diagram for the data transmission system**

Human Management Interface (HMI) can be easily used, which can show the details of the drainage system. The HMI software can display real-time air pressure data and alert signal of the corresponding area received from Network-based AD converter. Data can be converted to output file in MS-Excel format output by schedule.

Network based AD converter converts analog sensor signal to digital signal and transfer the signals to PC via network. The monitoring interface can also be



programmed to provide digital output signal when air pressure is detected such that the pre-set value is exceeded

Long duration logging on air pressure at 3 survey points were conducted in this research, the survey points are located on the existing main foul-water drainage stack (150mm dia.) of the building at the mezzanine (M) floor, the 6<sup>th</sup> floor and the 12<sup>th</sup> floor. The objective is to determine the air pressure distribution of the main stack and how it varies in the logging period.

When air pressure exceeds 500 Pa (5 mbar), the warning level of BDS is reached. Signal would be sent from the monitoring system to the Building Management System.

This kind of communication system should be able to communicate within different networks of the building. The monitoring PC and Network based converter are connected to building's router for internet access. Such router should have at least 1 public IP and configured the Port forward so that the monitoring PC is accessible through the Internet. In this research, the system has

some limitations. CAT 5 cables are used for networking, while this limits the maximum point to point distance to 100m. Optical cable is recommended when developing a wireless transmission.

Long duration monitoring is applied in the LKS building inside the Hong Kong Polytechnic University. Data on air pressure inside such drainage foul stack has been logged for a few years. From such a large size database record, it is identified that in weekday, highest pressure value is found to occur between 11:00 am to 3:00 pm., and after mid-night the pressure value is the smallest.

In terms of air pressure pattern within a week, peak value of air pressure is noticed on weekday but smaller value is found in weekend, which a typical phenomenon for the university's holiday. All of the data are scanned to identify the behaviour of water flushing which is possibly dependent with time, date and the usage by building occupants.

### **6.3 Air pressure fluctuation in the Drainage Stack**

A well-functioning drainage system without failure operation should be able to convey the soil and waste matter smoothly to the designated location such as a manhole or a sewer. Any blockage inside the pipework results in an increased air and water pressure. From this consideration, the degree of fluctuation of the pressure inside the piping system can be a good indicator on the smoothness of soil and waste discharge. Field measurement is necessary and the results can also be calibrated and validated by a simulation model. In addition, everyday maintenance on the drainage system can be performed more properly by initiate acupuncture study, perform signal levels analysis and establish an alarm system of the building drainage. Figure 6.8 shows the measurement station in LKS building inside the Hong Kong Polytechnic University (PolyU). The station is installed at a 150 diameter foul stack.



**Figure 6.8 shows an air pressure sensor in LKS building, the Hong Kong Polytechnic University**

An acupuncture study on drainage system helps in the selection of the representative locations for stack pressure monitoring, to identify if there is any drainage problem which includes blockage, noise, vibration, loss of water seal, and smell emission. All of them are related to the variation of air pressure transient.

### 6.3.1 Air fluctuation behaviour in the drainage system

Air pressure fluctuation behaviour in a high-rise building drainage system (HBDS) can be presented by probability density functions (Wong et al. 2011). And, statistical analysis can be applied on the measured data obtained from the drainage stack in this real-life case in year 2008. The Li Ka-Shing (LKS)

Building in PolyU has eighteen-floors. Observation points at the mezzanine (M), 6th and 12th floors are connected to record the air pressure in the primary building stack. (Configuration of LKS building measurement station is shown in Figure 6.1). Pressure sensor IP67 in the type of WIKA was used in the measurement. It has a measuring range of about  $\pm 100\text{mbar}$ , with an accuracy of about 0.25%. Calibration was done using 150mm height U tube manometer, which was connected to the pressure sensor and an air pump. The pressure sensor can detect the air pressure in the stack of the test building by providing electric current signals having unit mA, which are transferred to a set of data logger.



**Figure 6.9: PLC measurement station at 6/F, LKS building, the HK PolyU**

The logger system at 6/F is shown in Figure 6.9. The data logger has two parts: an analog input module used to convert mA signals to digital signals, and a programmable logic controller (PLC) used for signal control. The type of the

PLC is micrologix-1500. The software named as RS-logix- 500 was used for data logging in PLC. Digital signals were sent to the personal computer by using the DH485 communication port and cable. The data for the present statistical analysis was recorded in the daytime from 8:00 a.m. on 28 of April in 2008.

The measured data is stored in a personal computer with a sampling interval of 1 second. The statistical analysis revealed that the air pressure in the real-life HBDS is largely dependent with floor location. The flatness factor of the pressure fluctuation increases with the floor number, while the skewness factor has a reversed variation tendency. The value decreases from a positive one in the M floor to negative values at higher floors. Probability density functions show the pressure fluctuation behaviour is largely different from normal distributions.

The present interest of HBDS is motivated by a previously lack of interest on the air pressure data during real-life operation of the building drainage system. Considering this situation, the LKS building in Hong Kong PolyU is tested as an example. The air-pressure in the building drainage stack is measured and

analyzed to explore the pressure fluctuation behaviours which are crucial in drainage system assessment and troubleshooting.

A summary of the statistical analysis of measured air pressure in the primary stack of the test building is given in Table 6.1.

Floor	$p_m(\text{mbar})$	$s(\text{mbar})$	$C_S$	$C_F$	record number
M	1.175	0.866	0.899	3.795	38206
6th	-2.28	0.339	-0.52	8.632	38055
12th	-2.05	0.303	-1.10	75.27	32357

**Table 6.1 : Mean pressure, standard deviation, skewness and flatness factors of pressure fluctuation.**

The pressure evolutions during 8:00 to 10:00 a.m. on 28 of April of 2008 is shown in figures 6.10(a-c).

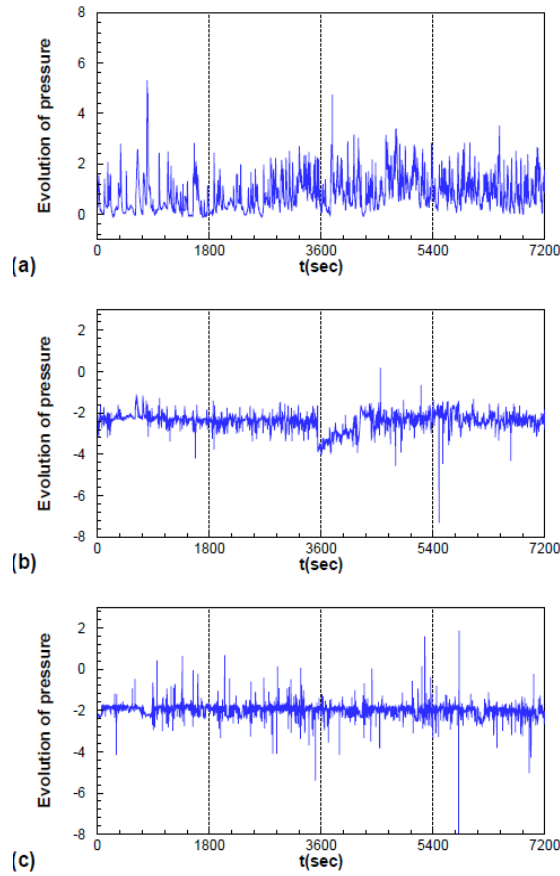


**Figure 6.10 : Evolution of air pressure (a) M floor, (b) 6th floor, (c) 12th floor.**

The result indicates that the pressure depends mainly on the floor level, as reported in our research study (Wong et al. 2008b). At the M floor, the air pressure has a positive mean value of approximately 1.2mbar, with a larger standard deviation of 0.87mbar. The pressure fluctuation at the M floor has a positive skewness factor ( $C_s$ ) of around 0.9, and a flatness factor ( $C_F$ ) of 3.8, as given in Table I.



### 6.3.2 Probability density function (PDF) in air pressure fluctuation behaviour study

A PDF is used in research of drainage air fluctuation behaviour study. It is density of a continuous random air pressure variable. It is also a function that describes the relative likelihood for this random variable to take on a given duration value (Terzaghi 1986).

The values of these statistical parameters also depend on the floor level. In particular, the mean stack pressures in the 6th and 12th floors are negative. The standard deviations are roughly third of that in the M floor, may refer that the fluctuations have lower intensities. The skewness factors  $CS$  in the 6th and 12th floors are negative, indicating that fluctuations with larger amplitude is negatively oriented, i.e. large amplitude negative pulsations are more common according to the observation on in figures 6.11(a-c).

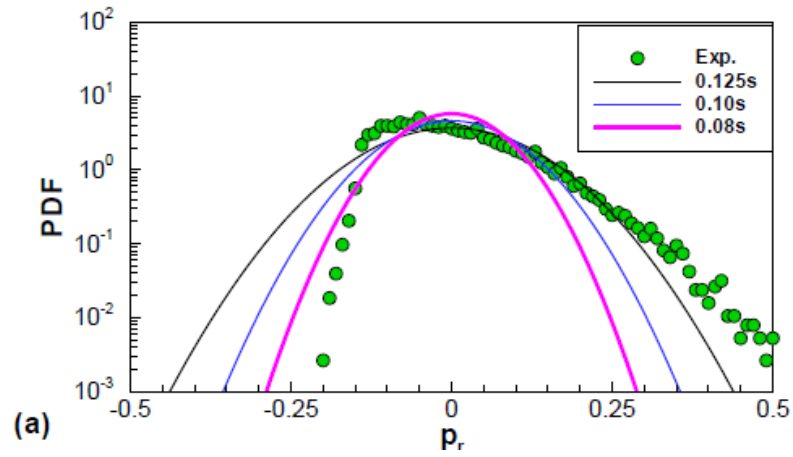


**Figure 6.11(a) PDFs of measured pressures and normal distributions with standard deviation  $C_0s$ . at M floor**

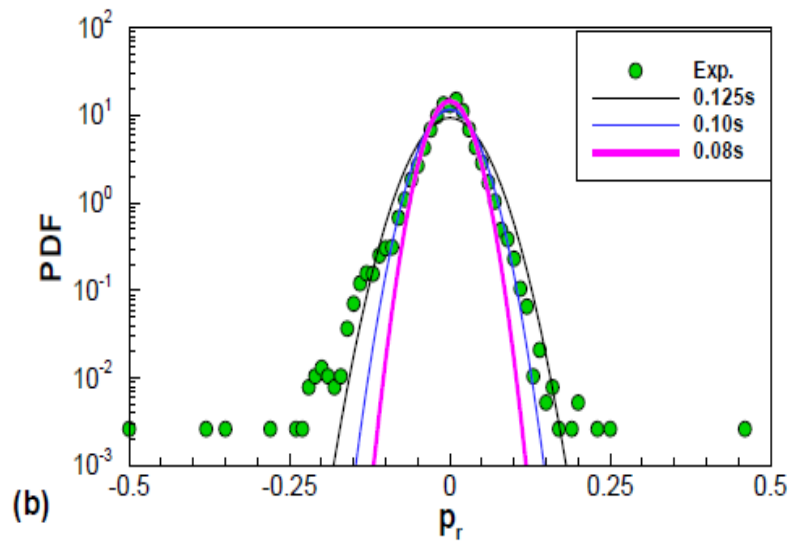


**Figure 6.11(b) PDFs of measured pressures and normal distributions with standard deviation  $C_0s$ . at 6th floor**

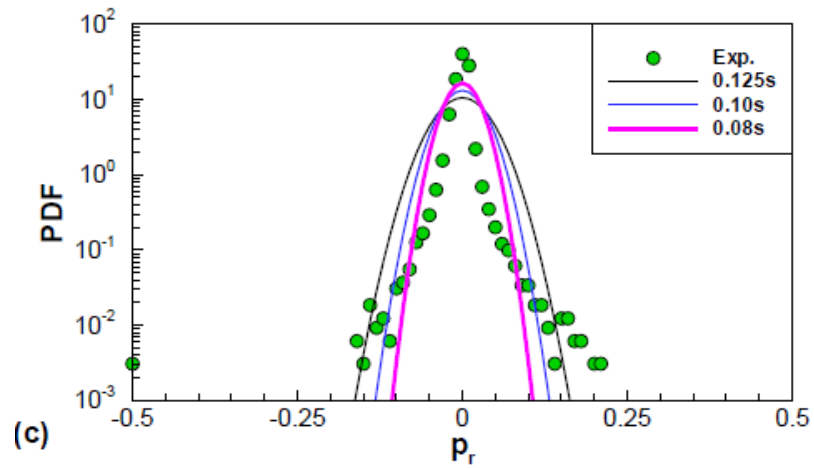


**Figure 6.11(c) PDFs of measured pressures and normal distributions with standard deviation  $C_0s$ . at 12th floor**

The  $C_s$  for the 12th floor is about twice of the  $C_s$  for the 6th floor, showing that at the 6-th floor there are more intensified and negatively oriented pulsations. The flatness factor  $C_F$  for the 12th floor is around 75. It is much higher than that of the 6th floor which is 8.6 (from table 6.1), implying the pressure distribution is particularly narrowed. As shown in figure 6.11(c), almost all the fluctuations are concentrated within the narrow range of  $p_r$  from -0.15 to 0.2. The probability density functions (PDFs) were formulated in terms of measured air pressure in the primary stack of the test building, in order to indicate the pressure fluctuation behaviours. The rescaled pressure is defined by:

$$p_r = (p - p_m)/[p] \quad (\text{eq 6.1})$$

and pressure variation range

$$[p] = \max(p) - \min(p) \quad (\text{eq 6.2})$$

Which is shifted so that the midpoint of the range has the mean value  $p_m$ . As shown in figure 6.11 (a to c), the pressure fluctuations are less similar to the PDFs ( $f_p$ ) of normal distributions with standard deviations  $C_{0s}$ ,

$$f_p = \frac{1}{\sqrt{2\pi}C_{0s}} \exp \left\{ -\frac{p_r^2}{2(C_{0s})^2} \right\} \quad (\text{eq 6.3})$$

Here the parameter of  $C_0$  (the standard deviation) was chosen as 0.125, 0.10, or 0.08 (1/mbar) for the stations at M/F, 6/F and 12/F. The shape of  $f_p$  becomes narrow with the reduction of  $C_0$ . In figure 6.11(a), it can be observed that the negative pulsations with amplitude beyond 0.25 is scarce, because the air flow driven by the drained water in the stack is stagnated at the bottom of the stack.

This fluctuation behaviour determines the standard deviation from a normal distribution PDF in relative to the measured PDF increase with the increment of

$1/C_0$ , The variation trend to be quite different from that of the pressure fluctuations observed from the 6th and 12th floors (See figure 6.12).

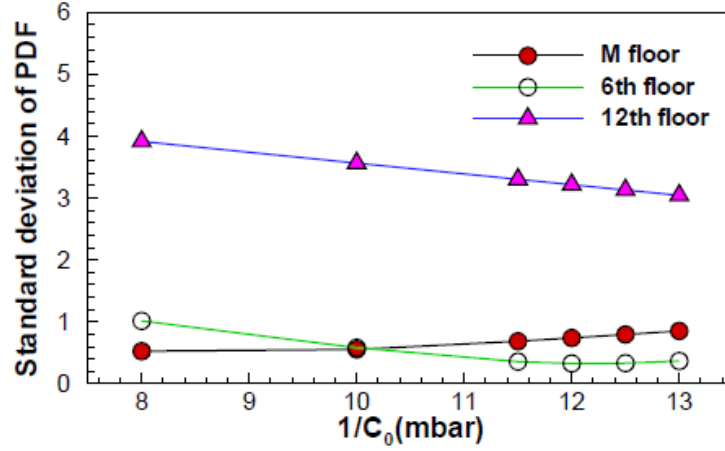


Figure 6.12 shows Standard deviation between the measured PDF and the normal distribution with standard deviation  $C_0s$ , plotted as a function of  $1/C_0$ . Here  $s$  denotes the root mean square of pressure.

In figure 6.11(b), the measured PDF generally fits a normal distribution. For small amplitude of pressure pulsations, large deviation occurs in the tails representing larger amplitude oscillations. The standard deviation from normal distribution PDF, as shown by the line connected by unfilled circles in Figure 6.12, has a minima around  $1/C_0 = 12$  mbar. In figure 6.11(c), the measured PDF cannot fit the normal distributions for  $1/C_0$  in the range from 8 to 13 mbar, because the standard deviation of PDF is almost over 3, as shown by the line linked by filled deltas as shown in figure 6.12.

In conclusion, the measurements of air pressure in the real-life LKS building shows that:

(a) The air pressure distribution does not fit with a kind of normal distribution while the distribution in the M floor appears to have the largest deviation from the normal distributions.

(b) The air pressure in the mezzanine (M) floor has a larger standard deviation that it is two to three times larger than in the 6th and 12th floors.

(c) The air pressures in the 6th and 12th floors have negative skewness factors and larger flatness factors.

### 6.3.3 Visual inspection inside the stack

The air pressure and the standard deviation at the M/F level inside the stack are considerably higher. There is a concern that whether the accumulation of soil near the bottom of the stack contributed to an increase of air pressure, since such fouling would reduce the actual cross-sectional area of the stack. The visual inspection method, introduced in chapter 3, is employed again. Figures 6.13 shows a typical case that is same as the stack around the 3/F level (1 floor above M/F is always suffering positive air pressure). There is no abnormal reduction

on cross-sectional area of the internal part of the stack, nor any sharp increase on the thickness on the internal part. Thus, the hypothesis on soil deposition (or fouling) that increases the air pressure is ruled out.

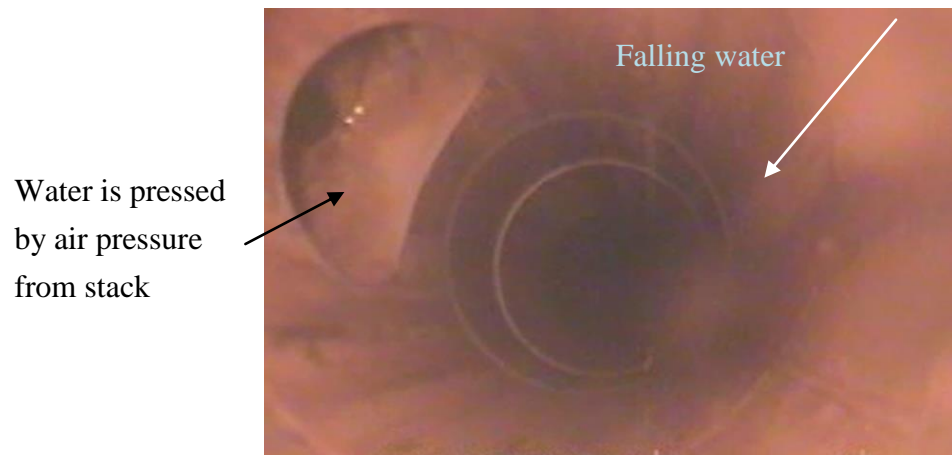


**Figure 6.13 shows positive air pressure that always exist in lower floors of building (M/F etc.)**

In this research, the objective to record and analyse the air pressure inside a real operating 150 mm diameter foul water drainage stack is achieved by means of PDF. Air fluctuation is found and it is a useful mathematic approach for this investigation. Larger deviations of data represent larger air fluctuation and this led to a recommendation that more attention should be paid within the range of stack. More air pressure sensors can be placed within this region (4/F, 5/F) and the alarm level can be set in higher resolution. In fact, complaints have been

received form 4/F females toilet with smell and overshooting from water closets

had been found before this research.

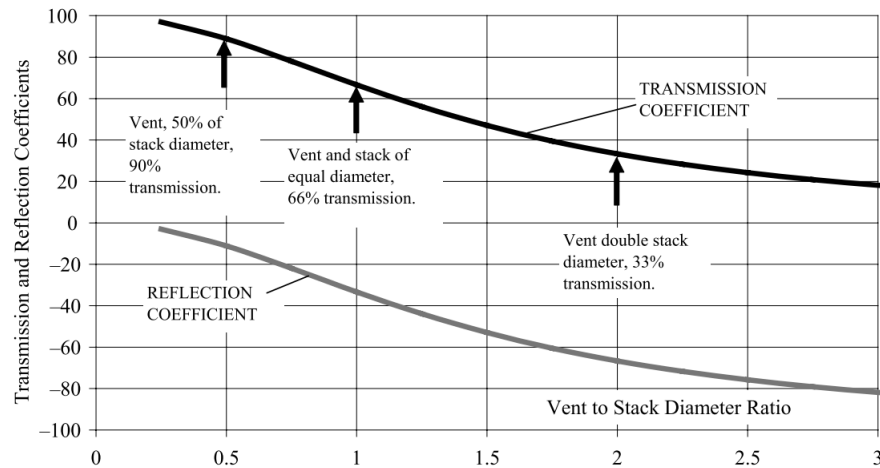


**Figure 6.14 shows relationship between Vent / Stack Dia. ratio to transmission & reflection coefficient of air pressure inside the drainage system.**

As M/F has larger air fluctuation and higher PDF, a larger size ventilation pipe is recommended if it is possible to retrofit. However solely retrofitting the ventilation pipe may not be enough to solve the problem completely because the size of ventilation pipe is just the same as drainage stack (i.e. the vent to stack diameter ratio is 1). The air pressure transmissions coefficient is just 66% as only as observed from figure 6.14 (Swaffield, 2010).



Considering that the drainage stack is installed in a narrow duct room, 8S twin stack can be installed to replace the existing stack partially. It provides a number of CVC (introduce in Chapter 5) to release excessive air pressure inside the drainage stack during discharge. At present, adding air attenuator valve unit (one unit can absorb 4L air and reduce air pressure temporary) is another way to solve the problem. The PDF results can help to optimize the sizing of stack when retrofit works is conducted.

## **Chapter 7      Conclusion**

Risk management for the drainage stack consists of a wide range of research. It covers research on strategies at various life-cycle stages so that the risk of failure or faulty operation of BDS can be reduced. The strategies are decided in the design stage. The innovative design develops system components which include: the 8S twin stack, smart trap, and also the smart connection of traps. It has also developed a monitoring system for daily operation of air pressure in the drainage system. A simulation model has been developed to predict the outcome of the newly developed system, with verification by on-site field measurement during real operation.

### **7.1      Risk Model in Drainage Stack**

In this research, a risk model which includes identification, control, communication and monitoring for BDS is covered in the various chapters in this thesis:

- BDS risk investigation is conducted in a real building, with an objective to demonstrate a protocol to trace the path of foul air transmission found in

existing systems, such that the defective part of the operation failure of BDS can be confirmed.

- One of the research foci, the mathematical model development on air pressure prediction, has been completed. The development starts with the application of Computational Fluid Dynamics (CFD) simulation to predict air pressure profile in drainage systems, and conducting tests at the PolyU drainage research rig. The simulation result generally agrees with real measurement data from the rig. However, for real building operation, the discharge point is not single and can be located at an elevated level. Before the completion of higher drainage rigs in Asia, a mathematical model is developed for predicting air pressure profile in BDS with higher height of service. The research adopts a characteristic line method. When a high-rise drainage research rig in the Asian context is available, measured data from a high-rise drainage system will become available for comparison. The mathematical model takes into account of the relationship between water discharge flow and air pressure inside the drainage stack.
- The confirmation of the effect on air pressure by increasing cross ventilation in drainage pipes leads to a further development step, to create

an innovative idea based on the balance concept, and the outcome product is the 8S twin pipe vertical stack. The idea is that air pressure caused by fall water volume downfall can be balanced by itself within the twin-pipe design. One of the twin pipes is for downfall water discharge and the other vertical pipe, is connected with a large number of cross ventilation “horizontal pipes” with very short length, providing the required ventilation. They are connected by numbers of small cross pipe so that the 8S can decrease air pressure effectively. As the ventilation pipe is already “packed” in a single stack adjacent immediately to the water downfall vertical pipe, once the 8S twin pipe vertical stack is used, there is no need to install a separated ventilation stack and related long distance horizontal cross ventilation pipe connection. It is no doubt that the new design has savings on material cost, man-hour time for installation with a neat appearance, and the ability to reduce the space allocation requirement. In this research, 8S twin pipe development employs CFD simulation to predict its function and capacity. A measurement set-up has also been successfully established in the PolyU Drainage Research Rig, with the data verification process completed. In Hong Kong, the 8S twin pipe has already entered the

commercial market. The first installation is already in progress and more field measurement data can also be obtained in the near future. This has been an achievement of this research.

At the same time, air attenuator and admittance devices are also important for existing systems, where retrofitting with the 8S twin pipe is not feasible due to various reasons. For example, limited space inside the pipe/duct area makes the demolition of old stack impossible, or very costly. The attenuator and admittance devices take an important role as remedial measure, and to minimize the risk of failure of operation due to excessive air pressure in existing installation with the traditional design.

- For monitoring and risk evaluation, this research provides a BDS monitoring systems set up as an active prevention measure. The concept is implemented in a real administrative office building in a University campus. The air pressure sensors are still sensing and logging data today. In the near future, it can prevent the system failure which is water overshooting occurred in water closets of toilets at the lower floors a few years ago. The system allows long-term monitoring and ensures that unhealthy operation of the BDS can be detected immediately when it happens. An advanced data

analysis technique, the Probability Density Function analysis was developed.

Once the financial issues for some remedial options, e.g. attenuators installation, is found to be acceptable and feasible for the site, this analysis can help facility managers to size the attenuators with better reference information.

## **7.2 Limitation**

The main research focus has been the problem of excessive air pressure in vertical stacks only. The following problems, which lead to an increase on risk of operation failure, should actually be considered in real practice, although not able to be addressed with research analysis in this thesis. These include:

- The material of stack, for example, uPVC drainage stacks are used widely in above ground drainage system. It is well known that uPVC suffers degradation under sun light, such that leakage of foul air or even foul water can occur.
- In risk identification, it is often difficult to identify the spatial location of failure, which makes such a work more tedious in real practice.
- Although traps are of vital importance in BDS, there is a lack of trap

monitoring method provided in the research field. While some preliminary work has been conducted in this research, injection sound impulse into a stack that the effect of sound reflection may help to identify any location with empty floor trap (loss of water seal), based on an analogy of playing bamboo flute (one of Chinese musical equipments). Tests are conducted at the PolyU Drainage Research Rig. However, empty traps in different locations may result in the same sound reflection pattern. This ambiguity problem limits the successful rate on true identification of emptied trap. Thus, more research work has to be done when proceeding in this direction for empty trap identification.

- The 8S does not get the interest among most of the real estate developers or owner committees. So, the application in real buildings is very limited at present. More works are needed to prove the performance and the promotion of merits are needed in order to obtain real operation experience for further improvement and enhancement on this invention.

### **7.3 Future Development**

This research on drainage risk management has intensively studied the selected aspects in an extensive coverage of life cycle stages on design and operation of drainage system. It strengthens the risk model by linking various attributes together for a holistic approach on drainage system design and, operation management is to be developed in future. The attributes are shown in figure 7.1.

#### **7.3.1 Model Enhancement**

In figure 7.1, the model can be improved by adding linkage between risk communication and risk control (linkage in brown colour). More research is needed for automation control of risk occurrence. If any invention is successfully developed in future, more sensors can serve not only on the detection of hazards, but also the control of future drainage system fitments with electronic functions. This can solve automatically the typical problems occur in drainage system. Other inventions, such as electronic drainage traps will be considered, to explore the feasibility on a better detection of empty traps in high-rise buildings.



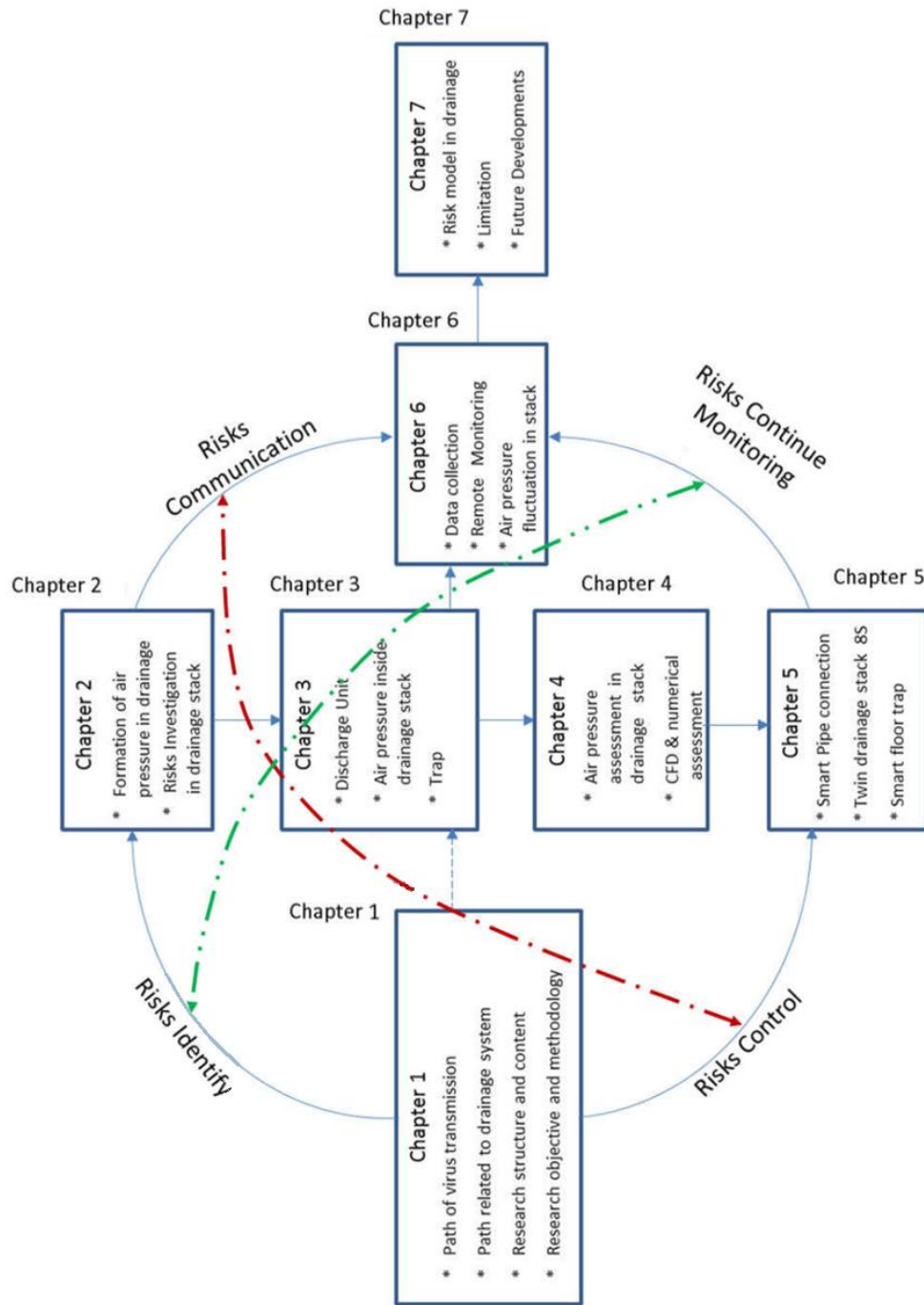


Figure 7.1: schematic diagram for the data transmission

To prevent virus or pathogen from spreading in the drainage system and entering the built environment, only passive control by blocking the entrance routes is

now feasible to reduce the risk of disease outbreak. Ideally, the traps may also function actively by introducing the mechanism that it can kill the infectious micro-organisms or reduce the infectiousness of virus and other pathogens. There is a great room to reduce the risk of disease outbreak caused by pathogen transmission via the drainage routes. More knowledge and resources for further development in this area is still required.

On the other hand, an additional connection link is the relationship between risks identification and risk monitoring (linkage in green colour in figure 7.1). The updated approach is to develop methods for automatic detection on depleted water seal in traps. This is already mentioned in section 5.4. The research has been started to provide a stepping stone for further investigation on the acoustical properties of trap in the drainage system with more complicated connections. It is hoped that these preliminary results and experience can contribute to future research. Once a protocol for the identification of those defective through an acoustics investigation is available, the model plays an important role in drainage system operation and maintenance without the need of the tedious inspection on traps one-by-one. It is not only because of the saving

on the testing and maintenance cost, but also the clear benefits in simulation techniques to facilitate the prediction and identification of defective trap seals. Hence, it can prevent the spread of pathogen in disease outbreak through the building drainage system as early as possible.

### 7.3.2 Facilities Management on Drainage System

The drainage management system and the risk model can be promoted in real building in the future. At present, the data communication protocol is applied mainly in the context of research only. Enhancement is needed such as the Graphical User Interface (GUI). In particular, the connectivity to Building Management System (BMS) is needed to for exploration so that the system would become widely accepted among facilities management organizations. With the aid from professionals with experience on operation and maintenance management, drainage coding and protocols can be further developed. Preliminary concept on developing a coding system is presented in the following section.

### 7.3.3 Code system for above ground drainage stack

The condition of drainage stack can be defined as coding. The conditions indicating defects, which include the positions of cracks, fractures, deformation, broken, dislocated joints, the presence of hole etc. All of them can be observed inside the vertical drainage stack by means of CCTV. One type of defect will have its own abbreviation for the ease of record and reporting. For example, cracks can be classified as CC (crack circumferential), CL (crack longitudinal) and CM (crack multiple). Fracture is actually similar to crack but its width is more than 0.6 mm. Drainage code is currently applied for underground drainage system only and, is rarely used for above-ground drainage. In fact, when defining the drainage code for a vertical stack, it is very difficult to define the orientations of the moving and rotating camera. Possible ways to develop the coding system is to be explored in the future.

### 7.3.4 Experiments Testing in Super High-rise Building

As mentioned in chapter 4, numerical and CFD techniques are applied to predict the air flow inside the drainage stack. It can be verified by the recorded results but more important is to get more measurement data from real buildings,

especially for high-rise drainage rigs and buildings. It is amazing that a series of drainage testing in a 123m height drainage rig in China will carry on (see figure 3.6). More collaboration and resources are needed to carry on the research.

## Reference

Abarbanel S and Gottlieb D, 1981, “Optimal time splitting for two- and three-dimensional navier-stokes equations with mixed derivatives.” *Journal of Computational Physics*, vol. 41, no. 1, pp. 1–33.

Alirol E, Getaz L, Stoll B, Chappuis F and Loutan L, 2011, “Urbanisation and infectious diseases in a globalised world”. *Lancet infectious diseases*, vol. 11, no. 2, pp. 131 – 141.

American Society of Civil Engineers, 1996, *Hydrology Handbook*. New York: The Society, 2nd ed.

Boobyer P, 1896, “Typhoid in midden towns”. *Public Health*, vol. 9, pp. 380 – 383.

British Standard Institute, 2000, *Sanitary pipework, layout and calculation*. British Standard BS EN 12056: Part 2. published by European Committee for standardization, p. 14

British Standard Institution, 2000, *Gravity drainage systems inside buildings*. British Standard BS EN 12056: Part 1 to 5. United Kingdom: British Standard Institution.

Chan DWT, Law LKC, Chan EHW, Ngao DWY and Ip KKP, 2005, “*Contemporary drainage engineering practices in Hong Kong residential buildings*”. Healthy Building – Community Health and the Built Environment, CII-HK Conference 2005, Nov. 30, 2005, Hong Kong.

Chan WT, Lau TC and Wong SW, 2008, “*Development of smart floor trap for enhanced seal protection*”, Proceedings from the CIB W062 34th International Symposium on Water Supply and Drainage for Buildings, Hong Kong, China, 8-10 September 2008, pp. 438-447.

Cheng CL, He KC and Yen CJ, 2008, “Decision-making and assessment tool for design and construction of high-rise building drainage systems”. *Automation in Construction*, vol. 17, pp. 897 – 906.

Council of Labour Affairs, 2007, “*There shall be more concern for prevention of disasters in restricted spaces*”.

[http://www.cla.gov.tw/cgi-](http://www.cla.gov.tw/cgi-bin/Message/MM_msg_control?mode=viewnews&ts=45b84e03:47ef&theme=/.theme/Msg-Eng)

[bin/Message/MM\\_msg\\_control?mode=viewnews&ts=45b84e03:47ef&theme=/.the](http://www.cla.gov.tw/cgi-bin/Message/MM_msg_control?mode=viewnews&ts=45b84e03:47ef&theme=/.theme/Msg-Eng)  
[me/Msg-Eng](http://www.cla.gov.tw/cgi-bin/Message/MM_msg_control?mode=viewnews&ts=45b84e03:47ef&theme=/.theme/Msg-Eng)

Department of Health, 2003, *Outbreak of severe acute respiratory syndrome (SARS) at Amoy Gardens, Kowloon Bay, Hong Kong: Main findings of investigation, HKSAR*. [http://www.info.gov.hk/info/sars/pdf/amoy\\_e.pdf](http://www.info.gov.hk/info/sars/pdf/amoy_e.pdf) (Assessed 10 JAN 2008)

Douglas JF, Gasiorek JM, Swaffield JA and Jack LB, 2005, *Fluid Mechanics*. Harlow, England; New York : Pearson/Prentice Hall. 5th edition.

Douglas JF, Gasiorek JM, Swaffield JA and Jack LB, 2011, *Fluid Mechanics*. Harlow, England: Prentice Hall/ Pearson Education. 6th edition.

Gormley M, Swaffield JA, Sleight PA and Noakes CJ, 2011, “An assessment of, and response to, potential cross contamination routes due to defective appliance water trap seals in building drainage systems”. *Building Services Engineering Research Technology*, published online, 9 Sept 2011, DOI: 10.1177 / 014362441141619.

Hardy A, 1993, *The Epidemic Streets – Infectious Disease and the Rise of Preventive Medicine*. Suffolk: Oxford University Press.

Hung HCK, Chan DWT, Law LKC, Chan EHW and Wong ESW, 2006, “Industrial experience and research into the causes of SARS virus transmission in a high-rise residential housing estate in Hong Kong”. *Building Services Engineering Research and Technology*, vol. 27, no. 2, pp. 91–102

Hong Kong Government, 2004, *Press Release: "Drainage Ambassador" Scheme*. <http://www.info.gov.hk/gia/general/200402/25/0225195.htm> (Assessed 16 April 2013)

Chan IK, Wong SW, Hung CK and Wong MB, 2008, “*Air leakage test of the uPVC combined stack system*”, Proceedings from the CIB W062 34th International Symposium on Water Supply and Drainage for Buildings, Hong Kong, China, 8-10 September 2008, pp. 286-289.

Institute of Plumbing, 2002, “*Plumbing Engineering Services Design Guide*”, Hornchurch, Essex: The Institute, pp. 112-113.

Jack LB, 1997, *An investigation and analysis of air pressure regime within building drainage vent system*. Ph.D. thesis, Heriot-Watt University, Edinburgh, England.

Jack LB, Swaffield JA and Filsell S, 2005, “Identification of possible cross contamination scenarios facilitated by building drainage and ventilation systems, and the contributory role of modeling positive transient pressure propagation”. *CIB W062 Symposium*. 31th International Symposium on Water Supply and Drainage for Buildings, Sept 14 – 16, 2005, Brussels, Belgian.

Jensen ME, 2010, “*Estimating evaporation from water surfaces*”, CSU/ARS Evapotranspiration Workshop, Fort Collins, 15 March 2010. Retrieved from [http://ccc.atmos.colostate.edu/ET\\_Workshop/ET\\_Jensen/ET\\_water\\_surf.pdf](http://ccc.atmos.colostate.edu/ET_Workshop/ET_Jensen/ET_water_surf.pdf)

Karniadakis GEM, Israeli M and Orszag SA, 1991, “High-order splitting methods for the incompressible Navier-Stokes equations.” *Journal of Computational Physics*, vol. 97, no. 2, pp. 414–443.

Lau JTF, Tsui H, Lau M and Yang X, 2004, “SARS Transmissions, Risk Factors and Prevention in Hong Kong”. *Emerging Infectious Diseases*, vol. 10, no.4, pp. 587 – 592.

Lee EWM, 2006, “Preliminary study on the application of computational fluid dynamics to building drainage system design”. *Surveying and Built Environment*, vol. 17, no. 1, pp. 35 – 44.

Lee SH, 2003, “The SARS Epidemic in Hong Kong”. *Journal of Epidemiology and Community Health*, vol. 57, no. 9, pp. 652 – 654.



Li, Y., Wong, E., and Zhu, Z., 2013 “Mathematical Modeling of Air Pressure in a Drainage Stack of a High-Rise Building Test Platform”, *Journal of Architectural Engineering*, (ISSN: 1076-0431) DOI:10.1061/(ASCE) AE.1943-5568.0000123.

Lim T, Cho J and Kim BS, 2010, “The Influence of Ward Ventilation on Hospital Cross Infection by Varying the Location of Supply and Exhaust Air Diffuser Using CFD”. *Journal of Asian Architecture and Building Engineering*, vol. 9, no. 1, pp. 259 – 266.

Lu An Jian Zhu, 2006, “*Plumbing system design in United State*”, published by Economic Daily Press, December 2006. page 172-212 (ISBN-10: 7801806158).

Mosses SS, 1995, “Factors in the Emergence of Infectious Diseases”. *Emerging Infectious Diseases*, vol. 1, no.1, pp. 7 – 15.

Nappa M, 2009, *Thermal Convection: Patterns, Evolution and Stability*, Oxford: Wiley-Blackwell, p. 6.

O’ Donovan M, 1997, “Risk management and the medical profession”. *Journal of Management Development*, vol. 16, no. 2, pp. 125-133.

Orhan G and Aral MM, 2004, *Surface and subsurface flow and contaminant transport modeling in lower Altamaha watershed*. Atlanta: Multimedia Environmental Simulations Laboratory, School of Civil and Environmental Engineering, Georgia Institute of Technology.

Parkes L, 1892, *Lancet*, vol. I, p. 1423.

Roe PC, 1981, “Approximate riemann solvers, parameter vectors, and difference schemes.” *Journal of Computational Physics*, vol. 43, pp. 357–372.

Rotty RM, 1962, *Introduction to Gas Dynamics*. John Wiley and Sons Pub. Co.

Sleigh PA, Gaskell PH, Berzins M, and Wright NG, 1998, “An unstructured finite-volume algorithm for predicting flow in rivers and estuaries”, *Computers and Fluids*, vol. 27, no.4, 479– 508.

Steve W and Chia HH, 2013, “*FLUENT Learning Modules*”, Cornell University, U.S.A.

<https://confluence.cornell.edu/display/SIMULATION/FLUENT+Learning+Modules>

Swaffield JA and Campbell DP, 1992a, “*Air pressure transient propagation in building drainage vent systems, an application of unsteady flow analysis.*” *Building and Environment*, vol. 27, no. 3, pp. 357–365.

Swaffield JA and Campbell DP, 1992b, “Numerical modelling of air pressure transient propagation in building drainage vent systems, including the influence of mechanical boundary conditions”. *Building and Environment*, vol. 27, no.3, pp. 455–467.

Swaffield JA and Jack LB, 2004, “*Simulation and analysis of airborne cross-contamination routes due to the operation of building drainage and vent systems*”. *Building Research and Information*, vol. 32, no. 6, pp. 451–467.

Swaffield JA, Jack LB, and Campbell DP, 2004, “*Control and suppression of air pressure transients in building drainage and vent systems.*” *Building and Environment*, vol. 39, no. 7, pp. 783–794.

Swaffield JA, 2010, “*Transient airflow in building drainage systems*”. Spon Press.

Terzaghi K, 1986, “*Terzaghi lectures, 1974-1982*”. New York: American Society of Civil Engineers, p. 317.

Wang C and Zhang Q, 2009, *Gao ceng jian zhu ji shui pai shui gong cheng = 高层建筑给水排水工程*. Chongqing, China: Chongqing University Press. [Publication in Chinese Language]

Weiss RA and McMichael AJ (2004) Social and Environmental Risk Factors in the Emergence of Infectious Diseases. *Nature Medicine*, vol. 10, supp. 12, pp. S70 – S76.

Wise AFE and Swaffield JA (2002) *Water, Sanitary and Waste Services for Buildings*. Oxford, Woburn, Mass: Butterworth-Heinemann.

Wong ESW, Chan DWT, Jones P and Law LKC, 2008a, “*Assessment of Air Pressure inside a Drainage Stack*”, Proceedings of the International Multi-conference of Engineers and Computer Scientists 2008 Vol. II IMECS 2008, Hong Kong, China, 19.-21 March 2008

Wong ESW, Lau WM and Chan WT, 2008b, “*Positive Pressure Profiles in Drainage Stacks – Full Scale Tests*”, Proceedings from the CIB W062 34th International Symposium on Water Supply and Drainage for Buildings, Hong Kong, China, 8-10 September 2008, pp. 274-285

Wong ESW, Chan DWT and Zhu Z, 2011, “Air Pressure Fluctuation Behaviours in a High-Rise Building Drainage System”, *Journal of Architectural Engineering*, vol. 17, no. 2, pp. 82-84 (ISSN: 1076-0431) **DOI: 10.1061/(ASCE) AE.1943-5568.0000029.**

Wong ESW, Li Y, and Zhu Z, 2013, “Predicting air pressure in a drainage stack of high-rise building”, *Applied Mathematics and Mechanics* (English Edition), vol. 34, no. 3, pp. 1-14 (ISSN: 0253-4827) **DOI: 10.1007/s10483-013-1675-7.**

World Health Organization, 2003, *Final Report: Amoy Gardens–WHO Environmental Investigation*. WHO Regional Office for the West Pacific. <http://www.info.gov.hk/info/sars/who-amoye.pdf>  
[Accessed 10 Jan 2008]

World Health Organization, 2006, *Health Aspect of Plumbing*. Geneva: World Health Organization & World Plumbing Council. ISBN: 92-4-156318-4

Yu ITS, Li YG, Wong TW et al., 2003, “Evidence of airborne transmission of the severe acute respiratory syndrome virus”. *New England Journal of Medicine*, v. 350, no. 17, pp. 1731 – 1739.

Yuen KK, Lee EWM, Lo SM, 2003, “The fight against SARS: A backfilling connection for the prevention of drying out of floor drains’ U-trap”. *Structural Survey*, vol. 21, no. 4, pp. 114 – 118.

Zhang L, and Chen YF, 2006, “*Experimental report on the impact features of sanitary performance in drainage stack systems, part II: Experimental Data*” (In Chinese), Report of China National Engineering Research Center for Human Settlements.

Zhang Z and Zhan L, 2012, “*Research and exploration concerning full scale simulated experiment of housing building water supply and drainage in China*” (In Chinese), Proceedings from the CIB W062 38th International Symposium on Water Supply and Drainage for Buildings, 27 - 30 August 2012 in Edinburgh, Scotland.